USING INCLINED PLANE TEST TO COMPARE TRACKING ON SILICON RUBBER UNDER HVAC AND HVDC

KHUMBULANI MAFASIGODO

211546490

IN FULFILMENT OF MASTER OF SCIENCE DEGREE IN ELECTRICAL ENGINEERING

COLLEGE OF AGRICULTURE, ENGINEERING AND SCIENCE
UNIVERSITY OF KWAZULU-NATAL

November 2018

Supervisor: Dr A. G. Swanson

Co-Supervisor: Dr A. L. L. Jarvis

As the candidate's Supervisor, l have approved this dissertation for submission.

Signed……. Date…….

Name: Dr A. G. Swanson

COLLEGE OF AGRICULTURE, ENGINEERING AND SCIENCE

DECLARATION 1 - PLAGIARISM

I, Khumbulani Mafasigodo, declare that:

1. The research reported in this thesis, except where otherwise indicated, and is my original research.

2. This thesis has not been submitted for any degree or examination at any other university.

3. This thesis does not contain other persons' data, pictures, graphs or other information, unless specifically acknowledged as being sourced from other persons.

4. This thesis does not contain other persons' writing, unless specifically acknowledged as being sourced from other researchers. Where other written sources have been quoted, then:

   A.2 Their words have been re-written but the general information attributed to them has been referenced

   B.2 Where their exact words have been used, then their writing has been placed in italics and inside quotation marks, and referenced.

5. This thesis does not contain text, graphics or tables copied and pasted from the Internet, unless specifically acknowledged, and the source being detailed in the thesis and in the References sections.

Signed

……Date……

ACKNOWLEDGEMENTS

I appreciate deeply the continuous support of my supervisor Dr A. G. Swanson and co-supervisor Dr A. L. L. Jarvis; their guidance, suggestions, and advice throughout my research are highly valued. Working under their supervision has been a delight.

I would like to thank the HVDC SMART GRID RESEARCH CENTRE department for funding the research work. I also would like to thank UKZN Westville Microscopy Unit and Chemistry Department technical staff for their assistance with the various equipment.

Lastly, I would love to thank my family for believing in me and motivating me to go the extra mile, I am forever grateful for their love.

ABSTRACT

This dissertation presents research work conducted on high-temperature vulcanised (HTV) silicon rubber electrical tracking and erosion performances under HVDC and HVAC. The aim was to evaluate the performance under outdoor environmental conditions. Failure of polymer insulators is an area that has not been researched thoroughly in the past decade. The aging mechanism of insulators is of paramount importance in manufacturing and design. Outdoor conditions like humidity, moisture, pollution affect the durability of most insulators. Silicon rubber is widely used in power distribution and transmission insulation networks. It is also being used in power devices such as metal oxide surge arresters as the electrical insulation. Its advantages are that it is lightweight, low cost, easily processed, has good dielectric and hydrophobicity properties and has better pollution performance in outdoor insulation systems.

The first part of this research looks at the procedure for testing following the normative recommendations as per IEC 60587: 2007 standard. Constant tracking voltage method was implemented in the inclined plane test for electrical tracking and erosion. A voltage of 4.5 kV was applied for all +DC, -DC and AC testing. The failure criteria as per IEC-60587 were followed. The most monitored criteria were that the leakage current magnitude should be below 60 mA. An increase in leakage current magnitude and duration of discharges were observed under +DC test conditions. The tracking time was recorded to be less under –DC than in +DC. The average current under +DC increases with the voltage application duration, however under AC the current does not increase. Under –DC voltage the current flow was observed to be less intermittent. Sample surface degradation mechanism was seen to be different in +DC, -DC and AC. A data logger monitored the leakage current measurements. An average leakage current of 9.40 mA was found under +DC. An average leakage current under –DC was measured to be 8.92 mA. Under AC voltage an average current of 11.90 mA was recorded.

The second part of the study looked at the quantitative analysis techniques of silicon rubber. Silicon rubber test samples were carried out using scanning electron microscope (SEM) with Energy Dispersive Spectroscope (EDS), Fourier transform infrared microscope (FTIR) and transmission electron microscope (TEM). These physiochemical tests results were comparable for both DC and AC, it was concluded that the insulator deterioration was due to surface tracking and dry-band arcing discharges which resulted in the erosion of the test samples. The work reveals that +DC is more aggressive for the test samples tested. It was concluded that under +DC conditions tracking is more severe as compared to –DC and AC.

Keywords: HTV Silicone rubber, Tracking, Erosion, IEC 60587, Inclined Plane Test

TABLE OF CONTENTS

LIST OF FIGURES

LIST OF TABLES

LIST OF SYMBOLS AND ABBREVIATIONS

AC	Alternating Current
ATH	Alumina Trihydrate, Aluminium Hydroxide
CTV	Constant Tracking Voltage
DC	Direct Current
EPDM	Ethylene Propylene Diene Monomer
EDS	Energy Dispersive Spectroscope
FRP	Fibre Reinforced Plastic
FTIR	Fourier Transform Infrared
HTV	High-Temperature Vulcanizing
HV	High Voltage
HVAC	High Voltage Alternating Current
HVDC	High Voltage Direct Current
HTV	High Temperature Vulcanising
LTV	Low Temperature Vulcanising
IEC	International Electro-technical Commission
IR	Infrared
ITV	Initial - Tracking Voltage
LC	Leakage Current
LMW	Low - Molecular Weight
RMS	Root Mean Square
RTV	Room Temperature Vulcanized
HTV	High Temperature Vulcanized
SEM	Scanning Electron Microscope
SIR	Silicone Rubber
TGA	Thermo-Gravimetric Analysis
TEM	Transmission Electron Microscope

CHAPTER 1: INTRODUCTION

1.1 Background

Insulators are one of the key components affecting reliability of outdoor HVDC power transmission network. The biggest challenge of polymeric insulators is that of tracking and erosion degradation under contaminated conditions. The outdoor high voltage insulators should be able to maintain a high dielectric strength under all surface environmental conditions. Silicone rubber (SIR) is considered reliable because of its hydrophobic properties, hence it has been widely used.

A well-known technique to further study the performance of silicone rubber insulation material was employed. The inclined plane test (IPT) IEC 60587 [1] standard was used to evaluate the electrical tracking and erosion resistance of outdoor silicone rubber material. They are two different methods of investigating the aging performance of SIR material, time to track and constant voltage methods. The constant voltage IPT method at 4.5 kV of +DC, -DC and AC (RMS) was implemented. The inclined plane test attempts to simulate the tracking behaviour on silicone rubber composite insulators in a controlled manner so that comparisons between the different test voltages are extracted. The erosion depth, area and eroded mass of the polymeric insulator material such as silicone rubber can determine the severity of surface discharges (corona discharges or surface leakage current flow). The lifetime of any composite insulator material depends on surface degradation. The surface degradation also depends on dry-band arcing. Dry-band arcing occurs through heat absorption in wet and polluted environments resulting in insulation deterioration. Dry-band arcing results from water droplets that form on the insulator surface, when there is leakage current flow. The heat generated cause the water to evaporate forming a dry band on the surface. A voltage gradient appears due to the disruption of current flow because of a dry band. The width of the dry band widens with time because of the electrostatic stress exerted by the voltage gradient across the surface. This results in minor arcing and flashover [2]. Hence, a clear understanding of electrical tracking and erosion of polymeric materials is of paramount importance.

The testing methodology proposed in this research is to evaluate a high temperature vulcanised silicon rubber based on the electrical tracking and erosion test as described in the IEC 60587. A quantitative material analysis looking at the severity of damage and chemical changes of the silicone rubber is further performed, Scanning Electron Microscopy (SEM) together with Energy Dispersive Spectroscopy (EDS), Transmission Electron Microscopy (TEM) and Fourier Transform infrared (FTIR) methods. The methods explored the arrangement and dispersion of microstructure of silicon rubber after +DC, -DC and AC IPT tests [3]. This dissertation focused on an inclined plane test to study the accelerated aging behaviour of silicone rubber composite insulation under HVDC and HVAC.

1.2 Research Motivation

The aim is to compare and contrast tracking on silicon rubber insulator under HVDC and HVAC. The tracking performance of polymeric insulation materials is evaluated by an inclined plane test. The parameters compared and contrasted are leakage current, visual observation of the arcing activity, quantitative analysis (FTIR, SEM, EDS and TEM imaging) and material weight analysis. The research questions are; whether ±DC and AC voltages have different tracking performances and whether leakage current is different under these voltage types.

The research proposes an evaluation of a high vulcanised temperature silicon rubber based on the electrical tracking and erosion test described in the IEC 60587 standard. After building the inclined plane test, SIR materials are tested under +DC, -DC and AC. During these different tests, a conducting carbonaceous path emerges because of the sparking and arcing on insulating components which are called a track. Tracking is triggered by regions on the material with high electric field strength, dampness, and pollutants that cause surface discharges. The tracking and erosion of polymeric insulators due to dry band arcing is the main problem which is not yet addressed. According to IEC 60587 standard, inclined plane test method is used to evaluate the performance of aging SIR composite insulation samples.

The main purpose of the inclined plane test is to evaluate the tracking and erosion performance of silicon rubber housing material. If the material has inherent hydrophobicity, this property is destroyed when using a wetting agent, which then simulates the 'late aged phase' of the material from the tests. The results can vary considerably depending on certain test parameters such as; leakage current and root temperature of the arc, the mobility of the discharge (influenced by electrode roughness or contour), impedance and 'stiffness' of the voltage source, the physical structure of damage path. In the case of DC voltage stress, other test parameters also influence results, including; polarity, the chemical composition of the electrode material, and ripple shape of voltage.

1.3 Hypothesis

It was hypothesized that the severity of surface damage by +DC voltage will be more than the corresponding –DC and AC voltages. Insulator materials breakdown totally because of surface tracking. Outdoor SIR insulators must withstand factors like surface arcs, discharges, moisture, solar UV, pollution and electric fields which are the primary cause of deterioration. The test samples are characterized in terms of the charge accumulation and decay characteristics. It is also hypothesized that unless there is erosion, tracking does not alter the physical and chemical composition of an aging sample.

1.4 Key Objectives of the Research

The objective of the dissertation is to evaluate and analyse the relative performance of polymeric SIR insulator material under HVDC and HVAC. A range of studies have compared the performance of SIR insulation materials using IPT under AC and DC tests, but some of the published results are controversial. Consequently, the focus of this work is primarily on the thermal stability of the silicon rubber material, an important issue for outdoor insulation housing applications. The work focus on whether +DC, -DC and AC have different tracking performances and leakage current. Consequently,

this investigation considers the evaluation of aspects such as leakage current, arcing activity, quantitative analysis and material weight analysis. It also focuses on improving the dry band arcing erosion resistance, with the objective of increasing the service life of polymer insulator SIR in polluted outdoor service environments. The main objectives of this thesis in the field of composites materials for outdoor insulation are listed below:

- A better understanding of the dry band arcing mechanism in silicone rubber materials.
- An evaluation of the eroded mass and thermal characteristics of silicone rubber materials.
- The development of a new surface treatment method to obtain high erosion resistance composites for outdoor insulation.

1.5 Problem statement and Research question

The research proposed an evaluation of a high-temperature vulcanised silicon rubber based on the electrical tracking and erosion test as described in the IEC 60587 [1] standard. Therefore, it is the intention of this research to contribute knowledge on whether +DC, -DC and AC tests have different tracking and erosion performances on silicon rubber insulator material. Also to find out whether tests under +DC, -DC and AC have different leakage currents and material degradation on silicon rubber. The research focuses on the accelerated aging of silicon rubber when subjected to DC and AC stress. The test results of this work will be compared and contrasted with similar tests as published in the literature, looking at parameters such as leakage current, visual observations of the arcing activity, quantitative analysis (FTIR, SEM, EDS and TEM imaging) and material weight analysis.

1.6 Contributions of the Research Work

The main contributions of the study to industry:

a) The proposed testing and criteria in +DC, -DC and AC applied for electrical tracking and erosion test.

b) Comparative analysis for tracking performance.

c) Investigating the accelerated aging behaviour of SIR composite insulation under +DC, -DC and AC.

d) A more advanced physiochemical analysis looking at the erosion of the material based on the weight loss.

1.7 Outline of the dissertation

This section presents an overview of chapters. The scientific contribution of the dissertation is as follows:

Chapter 1 introduces the subject matter and objectives of this dissertation. The major problems caused by the outdoor insulation are addressed, different techniques used to evaluate the materials are introduced, and the proposed method used in this research, as well as the objectives of this dissertation, are discussed.

Chapter 2 introduces a review of insulators materials, different types based on materials (ceramic, metal, polymer), alternative solutions for testing the materials that have been investigated through different works. It outlines the results of the different evaluations of insulators prepared to seek improvements in their electrical and mechanical properties, as well as their resistance to arcing erosion The previous work done on evaluating silicon rubber insulating material are also presented in this chapter. The chapter provides a general review of the literature.

Chapter 3 presents the design and experimental setup of the IPT. The experimental setups for evaluation and the modelling of the physiochemical properties of silicon rubber insulator are presented.

Chapter 4 presents the analysis of the tests carried out, the results and discussion of the work.

Chapter 5 concludes the thesis, offers recommendations and future study alternatives.

CHAPTER 2: LITERATURE REVIEW

2.1 Introduction

This chapter focuses on a brief overview of high-temperature vulcanised (HTV) silicon rubber tracking and erosion performances with special emphasis on the comparison of HVDC and HVAC applications. In the previous chapter aims and objectives of this thesis were outlined, hence in this chapter relevant literature will be reviewed to understand the principles behind inclined plane test. Different insulators types are going to be addressed, ceramic and polymeric insulators. The chapter goes on to briefly cover the various standards and justify the use of those standards for material testing. Other insulator testing methods other than inclined plane test are discussed. The chapter continues with an overview on silicon rubber stability in outdoor insulation housing application. The material composition of silicon rubber composite is also discussed in subsequent paragraphs. Furthermore, the chapter discusses the methodology and how the investigation can help in understanding the degradation and failure mechanism in silicon rubber.

2.2 Outdoor Insulation

Overhead lines are vital in transmission and distribution of electricity; hence insulation is necessary to protect against environmental conditions. Performance of outdoor insulators exposed to various types of stresses like ice, snow, pollution or their mixture on the surface is of great concern to utilities. These various factors will eventually lead to insulator flashovers during their services. Incidents of power outages have been reported from various countries in the past and resulting in the loss of billions of dollars [4]. Hence, most efforts have been focused on modification of insulator surface properties.

There are a variety of insulators that are currently being used; which are: ceramic and polymeric insulators. For the past decade, silicon rubber has been manufactured as the commonly used insulator for high voltage applications. Ceramic insulators such as shed glass and porcelain have completely dominated as insulation materials for a long period of time. They are still being used in low medium voltage utilities showing great performances in those moderate conditions. However, modern outdoor insulation has concentrated on polymer composite material. High temperature vulcanised silicon rubber has been the ideal insulator for many electrical utilities usage.

Due to the increasing use of electric power in this modern society, a reliable power transmission is of paramount importance. Polymeric insulators such as silicon rubber used in outdoor applications have increased in the past decade. The properties of most polymeric insulators are what determines the service life, its durability over harsh environmental conditions. Overall, polymeric insulators are light in weight as compared to ceramic and metal ones, which gives them an advantage that it is easy to handle and install. Under wet and contaminated environments silicon rubber insulators show good electrical performances [5]. Silicon rubber insulator endures high-temperature conditions. They do have some downside characteristics such as their tracking resistance and chemical properties. They are other polymeric insulators with some superior properties such as ethylene propylene diene monomer rubber (EPDM), ethylene propylene rubber (EPR), and epoxy. Looking at EPDM for instance, its resistance to harsh weather conditions, recovering its hydrophobicity quickly can be used to categorize these insulators accordingly. These outdoor insulators material have no base polymer

material that has all the required properties. Hence, to improve the electrical performance of polymeric insulators fillers are added.

2.2.1 Composite Insulators

A typical composite insulator consists of a central rod made of fibre reinforced plastic (FRP) and an outer weather-shed made of silicone rubber or EPDM. It has a fibre rod structure covered with weather resistant rubbers, fillers and fitted with end fittings. These fibres reinforced plastics are mechanically very strong but are not able to bear the outdoor environmental effects. The presence of dirt and moisture in combination with electrical stress causes the material to degrade by tracking and erosion. So, the rod is covered by a coating that protects it from outside stresses such as rain, salt, fog and pollution. This coating is referred to as housing. A composite insulator can be easily transported and assembled because of its low weight. It allows construction of lighter towers [6]. The early types of housing material had an epoxy bonded glass fibre core covered with a thin room temperature vulcanized (RTV) silicon rubber housing. The early housing material was replaced with ATH- filled high temperature vulcanized (HTV) silicon rubber because of changing production technology [7]. Composite insulators have a wide range of applications in overhead transmission lines. Figure 2-1 shows a polluted and wet silicon rubber insulator under high voltage conditions. It can be seen that there is discharge activity on the surface of the insulator near the end fitting.

Figure 2-1: Composite insulator, HV Lab (HC) UKZN

2.2.2 High-Temperature Vulcanized (HTV) Silicone Rubber

Silicone rubber has an important characteristic of hydrophobicity which makes it a unique polymeric material. Hydrophobicity is treated as the resistance to formation of conducting water tracks that increase leakage current, chances of flashover, and other deterioration effects. Figure 2-2 shows the hydrophobic nature of silicon rubber arising from organic non-water soluble functional groups $[\mathrm{R_2SiO}]_\mathrm{n}$, which are light and thus silicone has a low molecular weight [8] . This results in the insulating surface that prevents water filming on a hydrophobic surface instead discrete water droplets are formed. The primary reasons for the loss of hydrophobicity of silicone rubber are electrical activity and aging of the material. Aging is caused by multiple phenomena such as UV, temperature, pollutants, and moisture [9]. Hydrophobicity may be lost naturally due to the rain or artificially by washing the insulating surface.

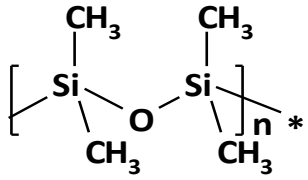

Figure 2-2: Chemical formula and structure of the repeating unit of silicon rubber

The hydrophobicity is recovered after a few hours at normal temperatures through the migration of the low molecular weight fluid to the surface [9]. The amount of leakage current through the insulator surface determines its performance. The insulator capabilities to withstand damage wears off over time because of erosion. A higher magnitude of leakage current accelerates the conditions which then leads to failure. Hydrophobicity properties are affected by environmental conditions mostly moisture in the form of fog, rain, dew, contaminants from sea and chemicals from industries [2].

Chandrasekar et al. [10] showed that silicone rubber insulators are more suitable for polluted environments because they perform better than ceramic insulators in highly polluted conditions with or without preventive maintenance. Moreover, high-temperature vulcanizing (HTV) silicone coatings are applied on apparatus bushings, surge arresters, and porcelain station posts as an alternative. The main advantage of silicone rubber insulation is its low life cycle cost. Not only are the purchase and installation costs being lower, but also the maintenance costs over the life of the insulators are also lower. Most electrical utilities have preferred the installation of silicone rubber polymeric insulators in sea coastal areas and industrial areas, even though tracking and erosion degradation has been observed in some extremely polluted environments. These insulators have also been used in desert areas and in regions with a high incidence of vandalism. The reduced number of metallic parts in this kind of insulator makes it suitable for saline areas, where the corrosion of the hardware is a significant problem, insulation is often damaged by the corrosion of the metallic parts.

In addition, outdoor insulation housing materials are subjected to ultraviolet radiation. Hence, with all these characteristics of silicon rubber, it is of great importance to investigate its reliability under high voltage applications. Zhou et al. [11], pointed out that adding alumina ($\mathrm{AI_2O_3}$), SiC in silicon rubber improved the thermal conductivity, thermal stability and the resistance to dry band arcing. The contact is formed between fillers which improve the properties of the silicon rubber material. The fillers inhibit the degradation of the insulation either by tracking or erosion. They slow down the

processes of failure of a material over time. When the SIR material surfaces age it creates favourable conditions for high leakage current, which can lead to an insulator complete failure.

2.2.3 Ceramic insulators

Ceramic insulators are usually composed of inorganic materials such clay, glass and porcelain. Ceramic insulators have properties such as mechanical strength, poor heat and electrical conductivity. In areas such as industrial or coastal, ceramics are ideal insulators. Porcelain insulators are made up of plastic kaolin, feslpar and quartz. The tensile strength is about 70 000 kg/cm^2 and 500 kg/cm^2 and the dielectric strength is about 60 kV/cm of its thickness. Glass insulator material are also used over porcelain because of low co-efficient thermal expansion and because it is easy to detect cracks or impurities as it is transparent. It has a high dielectric strength of about 140 kV/cm of its thickness and a high resistivity [12]. Whereas in polluted areas these ceramic performances are poor because pollutants can easily form conductive layers which causes great leakage currents. Figure 2-3 shows a picture of a ceramic insulator and a glass insulator.

Figure 2-3: Ceramic (left) and Glass Cap and Pin (right) insulators, HV Lab (HC) UKZN

2.2.4 Performance of different insulators

Danikas et al. [13] conducted aging studies of glass, porcelain, and polymeric insulators and reported better performance of EPDM and silicone rubber insulators than glass and porcelain based one. He also reported comparatively better hydrophobicity and lower leakage current activity in silicone than EPDM. Tracking and erosion of these non-ceramic insulators determine long-term pollution performance and aging of the insulator. It was highlighted earlier that the flow of leakage current normally happens when the hydrophobicity is lost; automatically aging starts which then trigger the dry-band arcing process. After some time under silicone rubber, test flashover is seen because of the bridging of high voltage electrode and ground electrode hence deteriorating the polymeric material.

That is why an extensive research in designing outdoor insulation is necessary because of this significant aspect of contamination flashover. The flashovers are caused by the formation of conductive layers which result in partially developing arcs. Dry band arcing concentrate more on the ground electrode, which leads to flashover. Danikas et al. also emphasized that conditions like humidity, temperature, and operating voltage affect both the contamination levels and the leakage current. A salt fog test was used to evaluate the performance of silicon rubber and EPDM rubber [13].

Ehsani et al. [14] reported a study about weather-shed materials and housing properties looking at the electrical, thermal and mechanical characteristics from EPDM/Silicone blend for outdoor polymeric insulators. EPDM blend improves the thermal degradation of silicon rubber by suppressing the process as revealed by the results of Thermo-Gravimetric Analysis (TGA) experimental measurements. There is good breakdown voltage strength with blends of silicone – EPDM relative to silicon rubber material. Improvement in surface and volume resistance of silicone rubber by incorporation of EPDM content was further reported. Silicon rubber leakage currents were lower than those of EPDM. The paper highlighted the relationship between dry band arcing and flashover voltage. In silicone insulators, the flashover voltage was found to be higher than similar manufacturers in EPDM.

In theory, a material that hinders the flow of electric charge and does not respond to an electric field is considered a perfect insulator. They should not allow a flow of current between conductors. Properties such as high dielectric strength define a material as an insulator, especially dielectric materials. The free charge does not have any mobility in a dielectric as is seen in a conductor. The resistivity and relative permittivity play an important role in determining the effectiveness of an insulator. A high voltage insulator is described as a good insulator when it passes tests such as exposure to contamination, moisture, electric stress etc. When a polymeric insulator withstands such outdoor weathering stresses they are fewer chances of failure due to development of leakage current and flashover.

2.3 Material Testing for Outdoor insulation

There are different standards and tests that have been used to evaluate electrical tracking and erosion of insulators or insulating materials. These standards are listed below.

ASTM D2303 – Standard Test Methods for Liquid-Contaminant, Inclined-Plane Tracking and Erosion of Insulating Materials [15] and **IEC 60587** – Electrical insulating materials used under severe ambient conditions – Test methods for evaluating resistance to tracking and erosion [1] The standards were introduced as material test methods for evaluating erosion and tracking resistance under prolonged exposure to a contaminant where the hydrophobicity of the insulator is removed. The currents are generally in the mA range.

ASTM 495 – Standard Test Method for High-Voltage, Low-Current, Dry Arc Resistance of Solid Electrical Insulation and **IEC 61621** – Dry, Solid Insulating Materials - Resistance Test to High-Voltage, Low-Current Arc Discharges. These standards evaluate the resistance of the material under clean, dry laboratory conditions with currents in the mA range.

ASTM D3638 – Standard Test Method for Comparative Tracking Index of Electrical Insulating Materials, which is performed at low voltage with a current of 1 A. The test is also performed with an electrolytic solution.

IEC 61302 – Electrical Insulating Materials - Method to Evaluate the Resistance to Tracking and Erosion - Rotating Wheel Dip Test, which tests the performance of insulators themselves.

IEC 62217 – Polymeric HV insulators for indoor and outdoor use – General definitions, test methods and acceptance criteria, provides details of the 1000 hour tracking and erosion test which is also performed on insulators themselves.

A number of these test have been used to test insulators and materials under HVDC, but the most commonly tested are ASTM D2303 and IEC 60587 as they appear to be the most comprehensive tests for tracking and erosion of insulating materials.

A short review of the other tests under HVDC is provided, followed by a review of the inclined plane test.

2.3.1 Material Tests

Kühnel et al. [16] performed the arc resistance test on silicone elastomer materials investigating the DC and AC stress according to the high voltage (HV) arc-test IEC 61621 standard. The test looked at the arc dynamic and thermal energy release on the insulation surface. A higher mobility of the arc was found at the cathode at low current. DC stress showed higher temperature measurements as compared to AC. The DC test results had a lower arc-withstand time compared to AC tests, which is in line with results from inclined plane tests. They identified a correlation between DC tracking and erosion classification and DC arc-withstand time. The insulation tested materials with a low tracking and erosion will also be assigned having a low arc-withstand time and vice-versa. The HV arc-test proved to be a very effective material screening under DC-stress.

2.3.2 Salt Fog Chamber Test and Rotating Wheel Dip Test

Gorur et al. [17] evaluated polymeric insulators energized under AC and DC voltages using a salt fog chamber test. Cylindrical rod samples of high temperature vulcanised (HTV) silicone rubber and ethylene propylene diene monomer (EPDM) were investigated. The supplied test voltage, surface electric stress, water conductivity, contaminant flow rate, temperature and electrode types are some of the parameters that were considered for this salt fog test. The leakage current, cumulative charge, time to failure, contamination flashover voltage are some of the quantities that were monitored and measured during the test. In both low and high conductivity fog, the time to failure with AC and DC was similar. A comparison of the material performance was made, which showed that silicone rubber performed better than EPDM samples.

Gorur et al also concluded that under positive DC the test samples were severely damaged compared to ones tested under negative DC and AC. In AC test showed a slight reduction in tracking and erosion resistance. The degree of material degradation was reported to be determined by leakage current magnitude and the time to track, formation of dry bands on a particular surface region. The experiment was conducted for a period of 8 hours for the aging of the test samples. The samples

regained their hydrophobicity when they were put to rest. The surface roughness, cracks, and porosity were revealed by scanning electron microscope (SEM) analysis. On the silicon rubber surface, there were electrical discharges and they influenced also the hydrophobicity property of the silicon rubber which later results in material deterioration. The literature state that the hydrophobicity loss was high due to the charge accumulation and moisture on the test sample surface. This accelerated aging test allowed different high voltage outdoor insulators to be evaluated, some materials suffered severe deterioration whilst some passed the test. A significant difference was observed in the surface deterioration between AC and DC insulators [17].

The rotating wheel dip test (RWDT) is another electrical tracking and erosion testing method used to evaluate the performance of polymeric insulators. Insulators are rotated through a contaminant while voltage is applied across them. Limbo designed and performed the RWDT for a number of polymeric insulators under AC and DC voltages [18]. The aim was to compare the performance of different materials and to study the effect of the type of voltage energization. A total of six samples were tested. The samples included HTV silicone rubber and EPDM composite insulators, RTV silicone rubber coated porcelain insulator and uncoated porcelain insulator. He measured the leakage current and compared the tracking and erosion visually as well as compared the hydrophobicity before and after the test. The main conclusion was the DC voltages caused more damage to the insulators than the AC voltage, in particular positive DC.

In the report on the feasibility study for a DC tracking and erosion test produced by Cigre working group D1.27 [19], it was reported that Yin et al. [20] found negative DC voltage to be more severe than positive DC stress in RWDT test. The hydrophobicity of the composite insulator surface controlled the leakage currents. The development of erosion and tracking processes were triggered by the non-uniform electric field distribution on the insulator surface. Furthermore Kurogayi et al. [21] reported that they carried out investigations on silicone rubber using the RWDT They studied on surface degradation and leakage current characteristics of silicone rubber under positive DC and AC. They concluded that DC samples experienced severe surface degradation as compared to AC test samples and that weight loss was about twice as high.

Salama et al. [22] performed a low speed rotating wheel spray on a number of low tracking resistance insulator polymers. The materials tested included cross-linked polyethylene (XLPE), epoxy resin with glass filler and Bakelite covered with one layer of silicone rubber tape. They reported that the insulation failure due to tracking is subject to variables such as; discharge inception voltage, carbon formation, carbon path propagation, energy content of the discharge, type of electrolyte, geometry and composition of electrodes, applied voltage and environmental conditions. It was concluded that that the time required for tracking to develop was found to increase with the wheel speed. Gazzola [23] reported a study on DC polymeric insulators tracking using a wheel test. He used the same voltage level to understand DC energization by compared AC and HVDC systems. He concluded that all types of insulators are much more liable to flashover under DC than AC voltages.

2.4 Inclined Plane Testing Method

The inclined plane test method, outlined in the IEC 60587 [1] standard, is used to evaluate the resistance of polymeric housing insulators to tracking and erosion under AC voltage. The inclined plane test schematic is shown in figure 2-4 with a sample having a dimension of 118 x 50 x 6 mm. The sample is suspended at an angle of 45°. This was done to allow ammonium chloride liquid contaminant to flow from the filter paper compartment on the high voltage electrode down to the lower ground electrode. A gap of 50 mm should be measured between the electrodes. The applied voltages have corresponding rates of contaminant flow. The flow rate must maintain a continuous spark of light on the surface of the sample. This helps to suppress interchange cycles of wetting and sparks on hydrophobic surfaces. Tracking of a material usually starts at the lower ground electrode due to the continuous sparks and progresses towards the high voltage electrode. Erosion usually follows on a defined area on the sample surface. The leakage current will flow on the contaminant path, causing discharges and with time, after 6 hours, failure of the material may happen due to tracking and erosion [1].

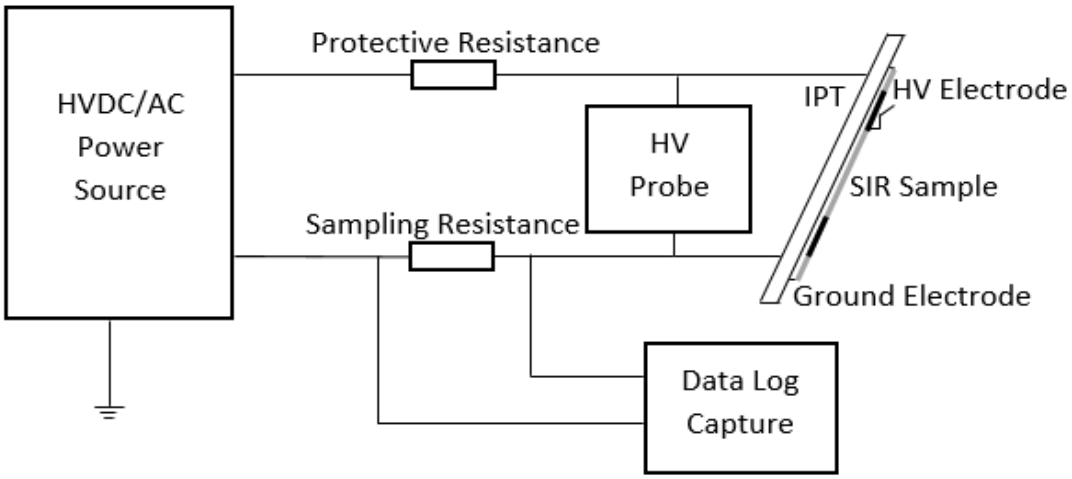

Figure 2-4: Layout of IPT Test [14]

The electrical testing methodology is divided into two tracking tests in the IEC 60587 [1] standard, constant tracking voltage (CTV) and stepwise tracking methods (ITV). If both the contaminant flow rate and applied voltage are constant during the test, it is called constant tracking voltage. The second method, the applied voltage is incremented every hour by 250 V for 6 hours or until the material under test failure is reached, this method is called stepwise tracking method. The samples are ranked according to the highest voltage withstood. The failure criteria for both these methods are the same. As stated in the IEC 60587 standard, when the material leakage current exceeds 60 mA for 2 to 3 seconds and the distance measured from the bottom electrode reaches 25 mm on the surface track then the material would have failed. However, the test is completely stopped if a hole develops due to excessive erosions or if the sample catches fire.

2.4.1 Inclined Plane Test Literature Review

Buontempo et al. [5] investigated HTV silicon rubber samples for a voltage level of 6 kV. They subjected the samples to AC and DC testing, where they used negative DC testing as they stated that it would be more conservative. The ratings of their testing circuits were not stated, of particular interest was the value of capacitance of the half-wave rectifier used for the DC supply. They performed the stepwise tracking voltage test and constant tracking voltage tests with 5 samples per test. The voltages used were up 6 kV rms and 6 kV DC. They presented the quantification of erosion through weight loss and presented images of their samples afterwards. There was significantly more erosion for the AC test samples than for the DC test samples for the stepwise tracking voltage test. For the constant tracking voltage test they showed that the weight loss due to erosion was similar for the AC and the DC test samples.

In the 2015 report on the feasibility study for a DC tracking and erosion test produced by Cigre working group D1.27 [19], the round robin test results for polymeric samples subjected to the IPT were presented. Five samples were tested under constant DC test voltage of 4.5 kV. They reported a higher severity of electrode erosion due to electrolysis, hence for each test run new samples and new electrodes were used. The dissolved metals ions increased the electrolyte conductivity, which impacted the leakage current level and surface arcs. The work reported that, for a long term performance of polymeric insulating material, the ability to minimize leakage current is crucial such that electrical discharge that cause degradation and flashover are eliminated. The resistance to tracking and erosion initiated by sustained electrical discharge activity on the surface was also a factor that was considered. In these tests however, they do not provide enough information on the leakage current suppression capability. It is found that DC stressed samples showed higher leakage current and exhibited larger surface degradation compared to samples exposed to AC voltage. The round robin tests concluded that there is an increased severity of DC over AC stress on silicone rubber based polymeric insulator materials [19].

Bruce et al [24] reported that the aging of a composite insulator was determined by electrical stresses and environmental conditions. They investigated silicon rubber performance in DC tracking tests using inclined plane test. The tracking and erosion tests were carried out according to IEC 60587 standard. The samples were all subjected to a constant voltage tracking test. The samples were tested under three voltage levels (2.3, 2.7 and 3.2 kV) for positive DC and negative DC. They observed that a higher surface degradation was under +DC voltage. The average and peak leakage currents were presented, and were highest under positive DC. A higher level of erosion was reported under 2.7 and 3.2 kV positive DC tests. Quantitative analysis of a material such as FTIR and SEM with EDS were employed to investigate the mechanical and chemical properties change after the long 6-hour tests. They found that the heat generated during dry band arcing is because of silicone fluid forming on the exposed surface of the material and under +DC voltage heat generated is higher. FTIR analysis also found that an interchange of silicone bonds, hydrolysis, and oxidation due to the heat caused a decrease in the hydrophobicity during the dry band phase. The conclusion was that the surface degradation is dependent on polarity, +DC tests have higher leakage current and produce deep erosion and greater sample mass loss as compared to –DC test.

Ghunem et al [25] studied the resistance of silicone rubber to electrical tracking and erosion using inclined plane test. They used ASTM D2303 and IEC 60587 as the guideline to carry out the

investigation. The constant tracking voltage and stepwise tracking method were employed for both DC polarity tests. They looked at the correlation between dry-band arcing energy with tracking and erosion, and found that the rate of absorption of energy determines material failure during inclined plane test. They also found that inorganic fillers inhibit track formation in silicon rubber samples. The silicone rubber with ATH filler, performed better under +DC voltage application. Under –DC stress, the erosion resistance was better in filled silicone rubber than in unfilled. The role of fillers in silicon rubber material is in improving the chemical and mechanical properties. It depends on the type and quantity of filler that is applied. For the past decade, application of fillers has changed the technology behind the manufacturing of outdoor insulation.

Izadi et al. [26] studied the voltage and electric field distribution on outdoor polymer insulator. A HTV silicone rubber was considered for the investigation. The magnitude of the leakage current was monitored, periodically observing the changes like weight loss, surface appearance and tracking. They concluded that erosion was severe under +DC voltage due to high temperature arcing. Partial discharges were noticed on the ground electrode under AC. The results made it possible for long-term use of polymeric insulators in overhead lines applications. The research study was concerned only with the silicon rubber housing material and its ability to perform in polluted environments.

An issue with DC voltage is the corrosion of the electrodes. Bruce et al. [27] showed that electrodes can become significantly eroded under the DC tracking tests. They reported that the corrosion was due to oxidation of the stainless steel electrodes as a result of high temperature arcing. The erosion process is due to electrolysis. They showed that the mass of electrode liberated is proportional to the total charge passed, by calculating the cumulative charge. In +DC tests, the top positive electrode was found to be more eroded, whereas in –DC tests the bottom ground electrode was more eroded. Both the eroded electrodes showed an increase in mass and formation of a solid dark layer was observed. They also found that upon bridging the high voltage electrode and the lower voltage electrode of a sample in incline plane testing, joule heating and conduction of the contaminant starts instantaneously [27]. This then result in the surface temperature to increase slowly. The continuous spark discharges produce rapid localized heating. This non-uniform heating causes dry-band to form in the sample area with a highest leakage current activity. The area with a high resistivity dry band cause breakdown of air above it and ultimately forming a carbonized track. Leakage current fluctuations results in changing the current waveforms and varying different harmonic contents of the tested sample. The material probably fails due to the chemical reactions initiated by the discharge activity, which leads to deterioration of the electrical and mechanical properties of the material. They concluded that tracking is more severe under +DC conditions than AC because of an increase in magnitude and duration of discharges under +DC. The tracking time was less under –DC as compared to +DC because the magnitude of leakage current flow for –DC was higher than +DC.

Vas et al. [28] tested nanocomposite silicone rubber materials under DC voltage using inclined plane test. ASTM D2303 standard procedure was employed to investigate the tracking and erosion performance of silicone rubber samples filled with micron sized alumina trihydrate (ATH) and nano sized alumina fillers. A quantitative analysis was conducted using scanning electron microscopy (SEM) together with energy dispersive spectroscopy (EDS) on both nanocomposite and micro-composites samples. They looked at the changes in surface morphology and filler dispersion of the tested samples. The results suggested that under ±DC stress, nanocomposites performed better than micro-composites. They concluded that the tracking and erosion performance was better under –DC as

compared to +DC voltage. They showed that electrodes under DC voltage corrode heavily. They explained this phenomenon being caused by the migration of conductive ions from the electrodes and from the pollutant. The erosion was high on the positive electrode due to the gradual removal of the HV electrode surface into the solution as suggested by Bruce et al [27] because of electrolysis.

Knauel et al. [29] developed a modified IPT for the investigation of electrical tracking and erosion behaviour under DC stress. The insulation material was a HTV silicone rubber of which five samples were tested at the same time. They used modified electrodes, laser cut stainless steel and inert carbon. Both those modified electrodes do not participate in the electrochemical processes at the anode or cathode. There was a lower degree of corrosive degradation of the test electrodes because of metal ion concentration, which was later reported caused dry-band arcing. They also showed presence of iron (Fe^{2+}) ions on the sample surface after cleaning. A microscopic image was shown of reddish-brown coating on the surface. These electrolytic contaminants were reported to influence the degree of material damage, the mass loss and erosion depth. The +DC voltage show larger loss of material as compared to –DC stress due to corrosion. They focused on the behaviour of low energy surface discharges. The study suggested the use of new electrodes after every voltage tests to avoid erroneous results.

Heger et al. [30] investigated the performance of RTV silicone rubber coated porcelain, HTV silicone rubber and EPDM insulation materials using the IPT method. The samples were subjected to high voltage DC and AC surface discharges. They employed a constant voltage method, using test voltages of 2.5, 3.5 and 4.5 kV. The test apparatus were configured as prescribed by IEC 60587 standard. They monitored and recorded leakage current using an on-line leakage current (OLCA) data logger. A total of eighteen samples were tested from each insulator type; six for each of the three test voltages ± DC and AC. The visual test showed that the lowest arcing intensity was with AC excitation, followed by –DC excitation and then by +DC voltage. HTV silicone rubber in particular had the highest erosion severity under +DC voltage but exhibited a minimal erosion to AC test voltage. The rms leakage currents were found higher under +DC voltage than AC. The application for –DC test voltage had the lowest rms leakage current measurement in all the materials. They also carried out hydrophobicity test on the aged samples using the spray method. They concluded that all the materials experienced the highest hydrophobicity loss during the – DC tests, followed by +DC and then by the AC tests. FTIR and EDS chemical analysis was employed which focused on the loss of ATH filler, loss of methyl groups and oxidization through the formation of carbonyl groups. They showed a correlation between the chemical analysis and erosion severity, in particular HTV silicone rubber had a formation of carbonyl groups and loss of ATH material which indicated material damage. A greater loss of methyl groups on the test samples showed an increased loss of surface hydrophobicity. The HTV silicone rubber was severely eroded by surface discharges under +DC voltage.

Khaaiye et al. [31] [32] studied HTV silicone rubber insulation material using IPT method. They compared electrical tracking and erosion under AC and DC voltage. They adhered to the IEC 60587 standards guidelines for testing insulator materials. The intravenous (IV) system was employed as the pollutant supply. A constant tracking voltage method was chosen because of its simplicity. Test voltages of 3.5 and 4.5 kV for both AC and +DC voltage were supplied. The results showed that 4.5 kV +DC test samples for silicone rubber were heavily eroded as compared to 3.5 kV test voltage. AC test voltage showed an extensive erosion on the insulator samples. The erosion severity under +DC voltage correlated with the leakage current results that were found. The +DC leakage current was three times

bigger than that under AC for the same equivalent voltages. DC test voltage showed more electrode corrosion than AC. They reported that was because of the electrolytic erosion by-products of the anode which modified the pollutant conductivity and enhanced the degradation severity. FTIR analysis was carried out, which compared the aged and unaged spectra for all the samples under AC and DC. The aged samples showed a decrease of functional groups such as OH, Si-OH and C-H. There were distinctive absorption peaks. These physiochemical changes of aged samples were attributed to the tracking and erosion generated under both types of voltages. EDS analysis showed atomic concentrations of elements found in the aged samples. The iron content among other elements was found to be high under +DC voltage, from the electrolytic corrosion of the metallic electrodes. The SEM analysis was also carried out, it showed the material structural changes on the surface of the aged samples. The micrographs showed the material damage of aged samples looking at edges and depth of erosion on the surface. DC test voltage had the high material deterioration. They concluded that the degree of insulation surface erosion due to tracking is directly proportional to the leakage current magnitude.

Mahatho et al. [33] did an investigation almost similar to Khaaiye et al. [31] on accelerated ageing of HTV silicone rubber when subjected to DC stress. The AC IPT method was used, as per IEC 60587 standard, and an equivalent modified DC test was implemented. A constant tracking voltage method was used for 4.5 and 6.3 kV. The samples that were subjected under DC stress were reported to fail quicker than AC samples as suggested by Khaaiye et al. The erosion was severe under +DC. A hole developed after 95 minutes on the silicone rubber surface near the ground electrode which led to the test being stopped under +DC. They found higher levels of leakage currents under +DC test voltage than – DC voltage. The – 6.3 kV DC test had the minimal erosion. A post aging quantitative analyses using SEM, FTIR and EDS were also conducted. They examined the surface morphology of damaged and undamaged samples as expected. It was concluded that excessive erosion was found to occur under +DC stress.

Ashitha et al. [34] studied the effect of UV radiations on HTV silicone rubber insulators under polluted conditions using IPT tracking and erosion test as per IEC 60587. A constant tracking voltage of 4.5 kV was applied for 6 hours. The UV source used was a UV lamp with 300 W power. They found that the presence of UV radiations reduced the erosion on the insulator sample while tracking was found to increase. The silicone rubber matrix have high resistance against UV radiations as the photons that impinge on the insulator surface does not have sufficient energy to break the covalent Si-O bonds. They reported the erratic pattern of leakage current attributed by the loss in hydrophobicity of the samples, which led to formations of intermittent dry band arcing under UV radiations thereby causing severe tracking. Biswas et al. [35] looked at tracking of UV aged samples and reported similar results, a reduction in the erosion and dominance of tracking. The physiochemical analysis, FTIR was carried out to show the chain scission of Si-CH_3 side chain and carbonization of free radicals attributed by UV radiation which caused tracking. The study provided a better assessment on silicone rubber tracking and erosion performance.

Heo et al. [36] performed another investigation on HTV silicone rubber comparing AC and DC surface discharges. They incorporated a constant tracking method with 4.5 kV voltage application as per IEC 60587 standard. They looked at the changing aspects of silicone rubber samples and electrodes due to surface discharges. An infrared radiation camera measured temperatures as high as 130 °C for both AC and DC. However, at tracking breakdown they reported that the average temperature of ± DC is

higher than that of AC. In tracking test, +DC test voltage showed a higher degree of erosion followed by –DC and then AC test voltage. The occurrence of discharges increased the leakage current for the formation of dry band. The visual test showed the appearances of electrodes after test, they confirmed that AC has little change but DC has electrical corrosion as suggested by Bruce et al [27]. The electrodes are lost because the anode is eroded due to metal ionization from oxidation. The silicone rubber samples under DC test voltage had larger erosion depth and mass loss than AC voltage. They concluded that AC voltage showed occasional discharges with short discharging time, less erosion, and that DC voltage showed constant minor flame discharge and arc with high surface erosion.

A summary of an assessment of different electrical tracking and erosion test methods is described in the literature is shown in Table 2-1. The table assess the quality of silicon rubber materials by looking at certain parameters such as mass loss, time to track and most importantly leakage current. The work that is done before on tracking and erosion do not really explain conclusively whether the silicon rubber sample failed or passed the test. Normally the results are expected to be presented in absolute quantitative values, not using words like better or lower/higher when concluding. Most researchers conclude that silicone rubber material performs better under AC voltage followed by – DC and +DC voltage [28]. The leakage current was not clearly explained. Furthermore, the work concluded that material loss was higher due to tracking and the arc was fixed more on the ground electrode. In most instances the leakage current and mass loss are not given. Upon comparison on the performance, the discharge activity is stable for +DC as compared to –DC and that the tracking resistance is much lower for –DC. There isn't a systematic consistent methodology for inclined plane test.

Table 2-1: Summary of the electrical tracking and erosion test methods

Reference and Year	Voltage Magnitude and Type	Material	Testing Method	Leakage Current (mA)			Mass Loss (g)			Time to Track (minutes)		
				AC	+DC	-DC	AC	+DC	-DC	AC	+DC	-DC
Gorur et al. [37], 1996	5.4 kV AC for RWDT, 60-80 V/mm for Salt Fog	RTV SiR coatings	RRT, RWDT, Salt Fog	>10	15	8	0.1	2.4	0.1	-	-	-
Sarathi et al. [10], 2004	4 kV AC & ± 4 kV DC	High Density Polyethylene (HDPE) material	CTV (IPT)	20	30	40	-	-	-	353	353	225
Bruce et al. [24], 2010	2.5 & 3.5 kV AC, ± 2.25 & 3.15 kV DC	HTV SiR	CTV (IPT)	-	14.1	7.2	-	1.3	0.2	-	-	-
Heger et al. [30], 2010	2.5, 3.5 and 4.5 kV AC ± 2.5, 3.5 and 4.5 kV DC	HTV & RTV SiR, EPDM	CTV (IPT)	10	12	7	0.1	3.1	0.3	-	-	-
Ghunem et al. [2], 2012	3.25 kV AC, + 2 kV DC & -2.5 kV DC	HTV & RTV SiR, EPDM	ITV (IPT)	4.7	6.7	4	-	-	-	-	-	-
Heo et al. [36], 2012	4.5 kV AC & ± 4.5 kV DC	HTV SiR	CTV (IPT)	-	-	-	0.3	2.9	1.4	360	45	76
Vas et al. [28], 2012	± 2.5 kV DC	Nanocomposites	CTV (IPT)	-	8	4.3	-	0.6	0.1	-	-	-

Reference and Year	Voltage Magnitude and Type	Material	Testing Method	Leakage Current (mA)			Mass Loss (g)			Time to Track (minutes)		
				AC	+DC	-DC	AC	+DC	-DC	AC	+DC	-DC
Mahatho et al. [33], 2013	4.5 kV AC, ± 4.5 ± 6.3 kV DC	HTV SiR	CTV (IPT)	-	48	27	-	-	-	-	-	
Buontempo et al. [5], 2016	+1.0 kV ITV , 6 kV AC, 6 kV DC CTV	6 kV HTV SiR	ITV (IPT) CTV (IPT)	-	-	-	0.1	0.2	0.08	-	-	-
Khaayie et al. [31], 2017	+3.5 kV DC, 3.5 kV AC +4.5 kV DC, 4.5 kV AC	HTV SiR	CTV (IPT)	14 22	25 30	- -	- -	- -	- -	360 240	60 30	- -
Arshad et al. [4], 2017	+2 & -2.5 kV DC for ITV, +3.5 kV DC for CTV	Super hydrophobic coating on HTV SiR	RWDT & CTV/ITV (IPT)	-	40	10	-	0.3	0.1	-	-	-
Summary	Modified test voltages were incorporated by these authors that were not specified in the IEC 60587 standard. The positive DC leakage current is highest, followed by negative DC and then AC. The AC mass loss is lower than DC. The positive DC has a higher mass loss than negative DC. The table also show that AC has the longest time to track than DC. The inclined plane test, constant tracking voltage method (CTV) is the common test method that was used.											

2.5 Post-aging characterisation techniques

The physiochemical analysis used for the post-aging analysis of the samples include Fourier Transform Infrared (FTIR), Transmission Electron Microscope (TEM) and Scanning Electron Microscope (SEM) with Energy Dispersive Spectroscopy (EDS).

2.5.1 Scanning Electron Microscopy (SEM)

SEM creates a high-resolution image by scanning a focused high energy electron beam over a surface. Electron sample interactions produce a variety of signals because of the energy that is dissipated by high accelerated electrons carrying significant amounts of kinetic energy. These signals contain information about the samples surface structure and composition [38]. The SEM image shows the sample before and after the treatment, where the structure of the silicone rubber is eroded from the electrical tracking and erosion [39].

2.5.2 Energy Dispersive X-Ray Spectroscopy (EDS)

EDS is an analytical technique used for the elemental analysis or chemical characterization of a sample. It is used as background for analysis on the SEM. It allows one to identify what those particular elements are and their respective proportions. SEM and EDS analysis has been use to obtain the images and the elemental composition of the aged samples [40]. The EDS shows that the eroded sample has new peaks i.e. chlorine due to the contaminant used for the tracking test, the count of Al in the eroded sample increased because of excessive burning which caused the aluminium from ATH to be liberated and iron (Fe^{2+}) count increased due to corrosion of electrodes [39].

2.5.3 Fourier Transform Infrared Spectroscopy (FTIR)

FTIR is a standard technique used in the identification of a particular organic material chemical composition or bonding present in an unknown molecule. The technique measures the absorption of IR with respect to the wavelength of radiation of a sample. It provides a graphical representation of structural information about the presence of certain functional groups that are present in a sample [41]. The FTIR spectra results can then be used to characterize or identify a particular material. The spectrum shows the fresh sample has more prominent functional groups, for silicone rubber in particular i.e. Si-C bands and that the eroded samples have diminished.

2.5.4 Transmission Electron Microscopy (TEM)

TEM is a powerful tool for directly imaging nanomaterials to determine particle size and shape. It characterizes the size of the particle present in a particular composite material by using the same principles as a light microscope and it uses electrons instead of light [42]. Overall, it is a quantitative measure of particle or grain size, size distribution, and morphology of a particular material. It produces a high-resolution image with a magnification of 1 Nano-meter (nm). The material characterization shows the aggregated form, morphology and internal structure. This material analysis provides vast valuable information about its composition. The TEM shows the characterization dispersion of

particles within a polymeric insulation sample. The micrographs show large agglomerates, suggesting that the tested sample eroded immensely. The morphology of particles changes with time. This analysis also reveal the particles size [43].

2.6 Conclusion

Following the literature review, insulators need to be tested to check the reliability in outdoor HVDC and HVAC electricity transmission and distribution lines. Polymeric composite insulators are preferred over the traditional ceramic and glass insulators because they have better hydrophobicity, improved resistance to tracking and erosion, lower weight and better impact resistance. Several studies have been carried out by various researchers to improve the characteristics of composites insulators, particularly silicone rubber. IEC 60587 standard inclined plane test (IPT) method was found to be the appropriate method of testing. It describes two test methods, namely constant tracking voltage and step tracking voltage. The DC performance was an issue because the DC stressed samples showed higher leakage currents and more severe degradation, compared to the samples exposed to AC voltage. The physiochemical analysis using SEM, EDS and FTIR show the material structural changes on the surface of the samples and elemental compositions after the tests, which helps to compare different works. The aim of the research described in this paper is therefore to evaluate the performance, especially the resistance to tracking and erosion, of HTV silicone rubber insulator materials under +DC, - DC and AC voltages during inclined plane testing.

CHAPTER 3: EXPERIMENTAL SETUP

3.1 Introduction

An inclined plane test setup was designed and implemented as per the IEC 60587 [1] standard. The inclined plane test outlined in IEC 60587 standard is a well-known test for evaluating the resistance to tracking and erosion of insulating materials. The objective of the research was to identify the durability or aging of the insulation material under AC, +DC and -DC applied voltages. Tracking and erosion, leakage current, weight loss and physiochemical analysis of the samples were the main parameters evaluated. This chapter provides details of the test setup.

3.2 Power Supply

3.2.1 AC Supply

The inclined plane test (IPT) was carried out from an AC power voltage source with fundamental frequency of 50 Hz [5]. For this work, the constant tracking voltage (CTV) method was used. IEC 60587 specifies that the supply must be able to provide 100 mA for each sample tested and that the output voltage must be stabilized to 5%.

Chrzan et al. [44] evaluated the effect of the transformer source power for the inclined plane test. He used a variable transformer with a power 2 kVA, an isolating transformer (with no ratings), a low-pass filter (with no ratings) and a high voltage transformer with a voltage rating of 10 kV and power rating of 20 kVA. He noted the effect of a weak supply on the degradation of the insulation samples as the degradation decreased as he increased the number of samples simultaneously tested. He also noted that the 2 kVA variable transformer was too small to supply the required current and that the voltage was below the requirements of the standard. The additional components (isolation transformer and filter) would also have played a part. Mahatho et al. [33] used a 230 V /12 kV transformer to test 5 samples at a time, but there were no indications of the rating. It is probable the transformer was a SWER 16 kVA transformer. Khaaiye et al. [45] used a transformer of 5 kVA, 220 V/ 50 kV connected to a 30 A 220 V autotransformer. They connected 5 samples and noted large voltage drops of up to 20%. Although the transformer was rated at 0.5 A, the power ratings of the source and the impedance of the system need to be accounted for. They ultimately tested with one sample to ensure the correct performance.

The AC supply for the IPT is illustrated in Figure 3-1, where a variable autotransformer rated 250 V, 25 A 3-phase is connected to the primary winding of the power transformer rated 32 kVA, 230 V / 19 kV in order to deliver 4.5 kV at the secondary winding. The ratings of the components and the reasoning for the sizing are capture in Table 3-1. Figure 3-2 and Figure 3-3 show the variac and the transformer respectively. A 100 mA fast blown fuse is inserted between the ground electrode and the common ground.

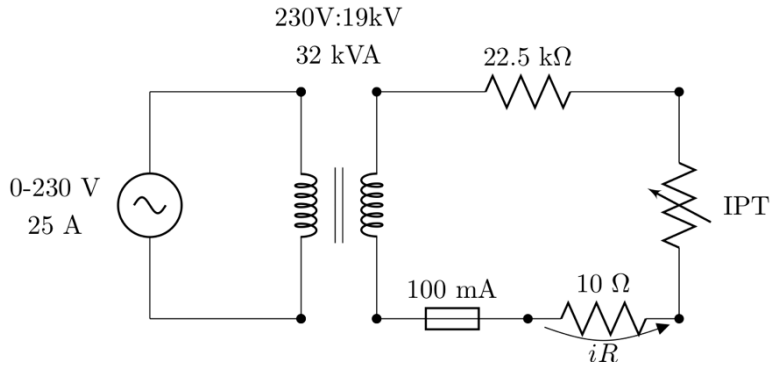

Figure 3-1: AC Supply Circuit

Table 3-1: List of equipment for the AC supply

Item	Voltage Rating	Current Rating	Power Rating	Comment
Variac	250 V	25 A	20 kVA	Sufficiently sized to supply transformer. Overload protection of 25 A.
Transformer	230 V/ 19 kV	139 A/ 1.68 A	32 kVA	100 mA is 6% of the rated current. There would be no significant change in the voltage required for IPT.
Current limiting resistor	>230 V		50 W	22.5 kΩ, 25 W additionally mounted on heat sink to improve power rating
Fuse		100 mA		Fast blow fuse.

Figure 3-2: Autotransformer

Figure 3-3: HV Transformer

3.2.2 DC Supply

The DC supply was developed to ensure that 100 mA was available for the sample and that the voltage drop due to the leakage current was minimal.

Mahatho et al. [33] conducted an IPT using five samples simultaneously. A Spellman 50 kV, 80 mA DC generator was used to charge a 66 µF capacitor for the +DC tests. A half wave rectifier circuit was constructed for the -DC test. The diode had a rating of 80 kV, 500 mA and was connected in series with a 100 Ω resistor to charge the 66 µF capacitor. The large capacitor ensured that there were no large voltage drops. Khaaiye et al. [45] similarly used a Spellman 50kV, 80 mA DC generator, but without a capacitor, and had issues when they connected 5 samples. The voltage dropped by up to 20% and the arc eventually extinguished. The required current could not be supplied and as such they opted to test one sample at a time.

The DC supply for the inclined plane test was developed for one sample at a time. A half-wave DC rectifier was placed at the secondary of the power transformer, represented by a single high voltage diode rated 80 kV. The diode was put in series with limiting resistors. The diode is reversed to change the polarity of the DC. A smoothing capacitor rated 34.7 µF is connected in parallel to control the excessive ripple voltages on the output test voltage and to ensure a stiff supply.

The DC supply circuit is shown in Figure 3-4 and the ratings and commentary about each component is shown in Table 3-2.

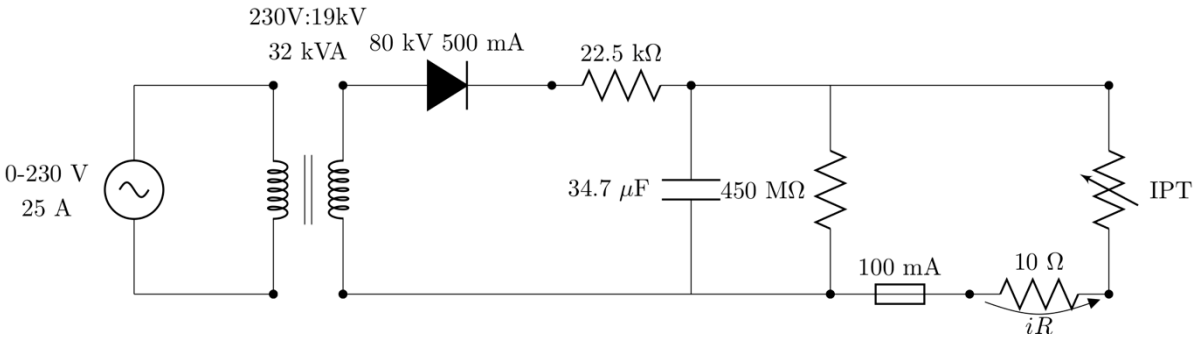

Figure 3-4: The Test Setup Equivalent Circuit

Table 3-2: List of equipment for the DC supply

Item	Value	Voltage Rating	Current Rating	Power Rating	Comment
Diode	-	80 kV	500 mA	-	Rectifying a voltage, turning AC into DC voltages.
Current limiting resistor	22.5 kΩ	>230 V	-	37.5 W	Sized to limit the current below the 500 mA rating of the diode. Sized so that 200 mA can be supplied to the circuit. 100 mA to charge the capacitor and 100 mA to be supplied to the inclined plane circuit.
Capacitor	37.4 µF	10 kV	-	-	Capacitor has to be large enough so that the voltage drop for the incline plane is not greater than 5%. Voltage drop of 28 V.

Parallel discharge resistor	450 MΩ	20 kV	-	-	Combination of 2 x 220 M Ω resistors. The resistor is connected in parallel with the output of a high-voltage power supply circuit for the purpose of discharging the electric charge stored in the power supply's filter capacitors when the equipment is turned off, for safety reasons.
Grounding stick and discharge resistor	200 kΩ	20 kV	-	-	Grounding stick was not directly connected to ground as this would have caused large discharge of current. The discharge resistor limited this and allowed the capacitor to discharge at a fast enough rate between tests.

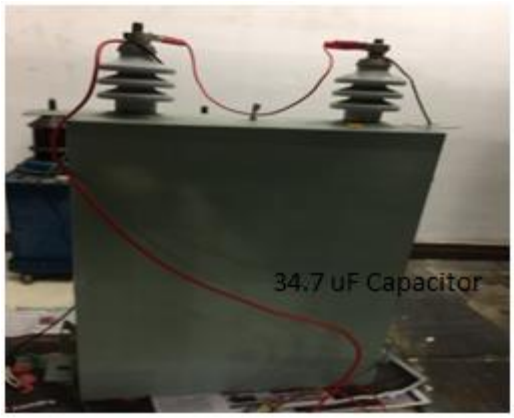

Figure 3-5: Capacitor

3.1 Overall Inclined Plane Test Setup

Figure 3-6 shows the practical setup that was used in the high voltage laboratory.

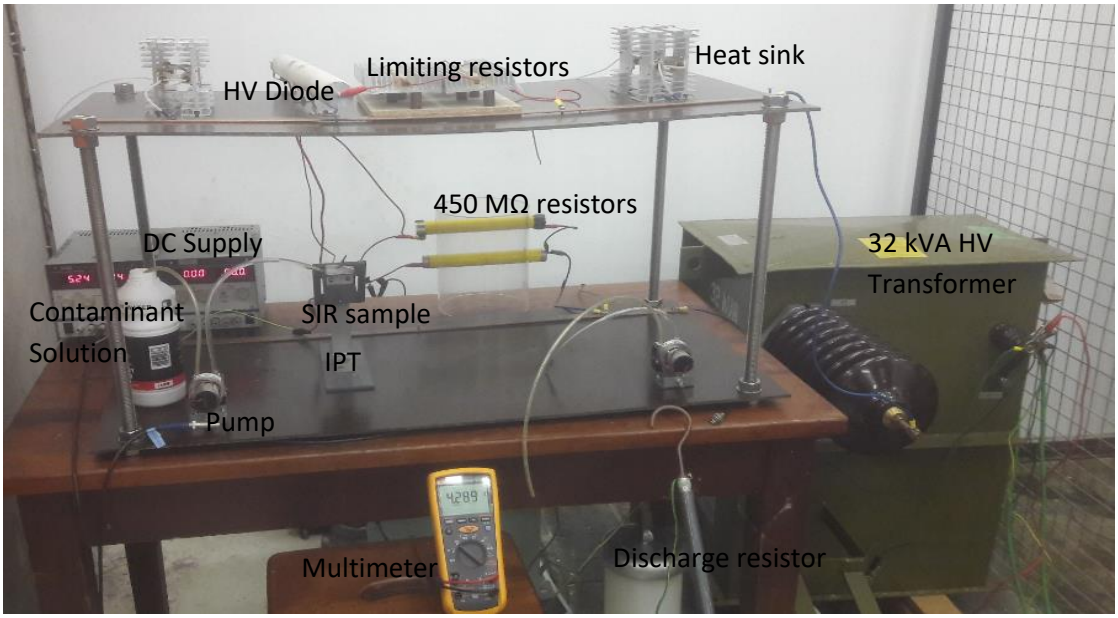

Figure 3-6: The overall IPT setup, HV Lab (HC) UKZN

3.2 Measurement System

3.2.1 Voltage Measurement System

The applied voltage was measured using a 1:1000 AC/DC high voltage probe connected to a True RMS multimeter (Digital Multimeter - Fluke 117 - True RMS multimeter).

Figure 3-7: Voltage Probe 1:1000

The voltage drop was measured using a 1:1000 wideband high voltage probe (Tektronix P6015) connected to a digital oscilloscope (Rigol D51052E 50 MHz 1 GSa/s) was used.

3.2.2 Current Measurement System

The current measurement system consisted of:

- 10 Ω measurement resistor with associated protection,
- Digital Oscilloscope - Rigol D51052E 50 MHz 1 GSa/s,
- Pico-log CM3 current data logger,
- Personal Computer, and
- Digital Multimeter - Fluke 117 - True RMS multimeter.

The Pico-log CM3 logs data onto a PC and had the following specifications [46]:

- Number of channels: 3,
- Range (voltage input): 0 to 1 V AC RMS,
- Accuracy (voltage input): ±1 % (to 200 mV) ±2.5 % (to 1 V),
- Overload protection: ±30 V DC, and
- Voltage input: 1 V RMS 20 Hz to 1 kHz.

The Pico-log CM3 is normally used with a current clamp to measure an AC waveform and not normally used to measure intermittent AC and DC signals. It takes a number of samples from the input signal and converts this to an AC root mean square value, this is not the true root mean square value as it does not contain the DC component of the signal. Note: The sampling rate (e.g. 100 ms) refers to the rate of the rms value of the signal transmitted to the PC.

The voltage input of the Pico-log is 1 V RMS. In the case of failure of the insulation sample, it could be an overvoltage across the terminals. The terminals are protected by using Zener diodes with a forward voltage of 1.2 V in parallel with the resistor. The circuit is protected from any contaminant by enclosing it.

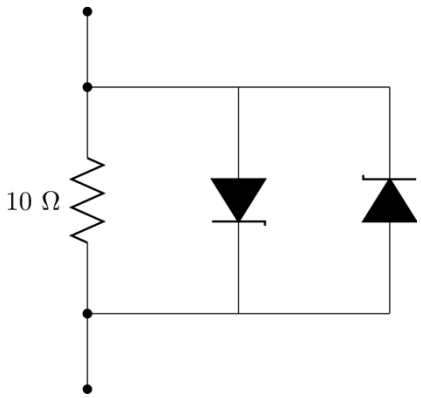

Figure 3-8: Leakage current measuring circuit

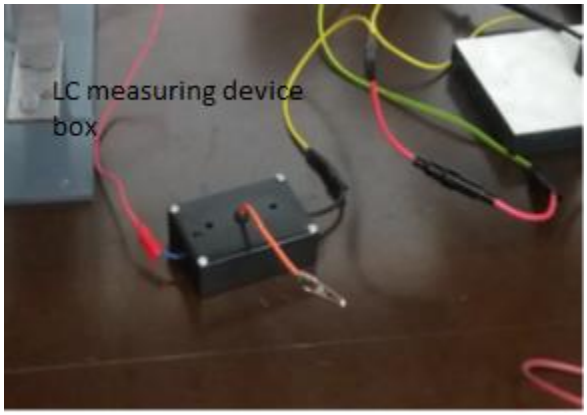

Figure 3-9: Leakage current measuring device

3.3 Inclined Plane Test Setup

3.3.1 Insulation Samples

High temperature vulcanized (HTV) silicon rubber test samples were used for the experiments. The approximate dimensions of a samples were 118 x 50 x 6 mm and weighed approximately 56.00 g. The weight for the samples were measured using an accurate weighing balance (Mettler Toledo). Three SIR samples were selected for the test of each voltage type. In total 9 samples were tested for the AC and DC tests, a number of these samples were used in setting up the tests and were not included in the analysis.


Figure 3-10: HTV Silicone Rubber Sample HV Lab (HC) UKZN

3.3.2 Contaminant System

An electric peristaltic pump was used for the contaminant supply in the IPT setup in order to achieve desired controllable flow rates. Figure 3-10 show the peristaltic pump system. The motor pump was rated at 5000 RPM; 24 V. A DC supply of 5.24 V was used to provide the required contaminant flow rate of up to 0.6 ml/min. The peristaltic pump accommodated testing of one sample.

The liquid contaminant comprises of de-ionized water, ammonium chloride and a non-ionic wetting agent mixed proportionally. The conductivity of the contaminant solution is measured and maintained at 2.5 mS/cm. The sample is inclined at an angle of 45°, the contaminant flows from the high voltage top electrode along the test sample surface towards the ground electrode.

Ammonium chloride(NH_4CL) 0.1 % ± 0,002 % by mass was used as contaminant. The contaminant had a conductivity of 2.5 mS/cm and resistivity of 3.95 Ωm ± 0.05 Ωm at 23 °C as per IEC-60587 standard. The conductivity was measured with the Hanna instruments conductivity meter.

Figure 3-11: DC supply for Peristaltic Motor Pump

3.3.3 Mounting Support and Electrodes

As per the IEC 60587 standard, a distance of 50 mm should separate the ground and high voltage electrodes. The electrodes are made from stainless steel and are attached to the surface of the flat rectangular silicon rubber insulator. Two kinds of stainless steel were selected as electrode materials namely austenitic steel (widely used steel) and AISI 316L austenitic steel type (used in the design because of its anti-pitting characteristics) [47]. The test surface faces downwards as the sample was mounted at an angle of 45° to the horizontal plane in accordance with the standard. The mounting support was built as per the standard. Initially PVC insulation material was used to build the support system. It is heat resistant and it's electrically insulation properties make it a suitable material. The mounting support system and a silicon rubber insulator already mounted are shown in figure 3-11. The material was later changed to Nylon before the testing as there was tracking on surface of the PVC material.

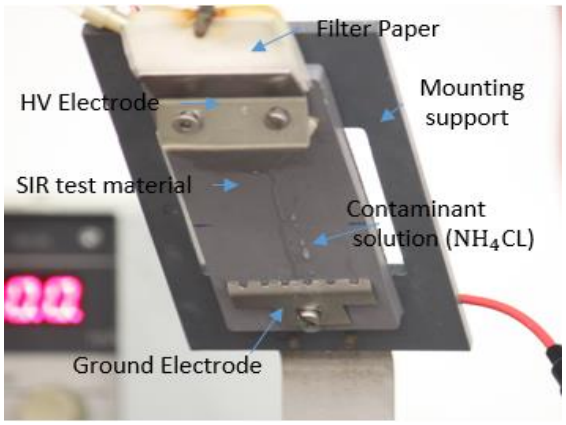

Figure 3-12: Electrode configuration according to IEC-60587

Eight layers of filter paper were clamped between the top electrode and the sample to maintain a steady flow of the liquid contaminant solution. The electrodes were replaced for each test.

3.3.4 Failure Criteria

HTV silicon rubber sometimes forms a layered char due to overheating. Underneath this layer dry band arcing occur which cause deep erosion between the test electrodes rather than creating tracking paths. According to IEC-60587 standard, there are a number of failure criteria for samples under IPT, including:

- A test sample sometimes catches fire, when this happens the whole test is stopped immediately.
- A test sample develops a deep erosion hole.
- The leakage current is 60 mA for 2 to 3s.
- The tracking length is longer than 25 mm.

If a test sample catches fire, it is an indication of premature failure. A high leakage current level above 60 mA induces dry band arcing which results in flashovers on the sample.

3.3.5 Test Procedure

The testing took place in the High Voltage Laboratory at Howard College at the University of KwaZulu-Natal.

An ambient temperature of 23 °C ± 2 °C is recommended at the time of carrying out the test, however the IEC 60587 standard does not specify the humidity or the altitude of the test location. The high voltage lab is temperature controlled and meets the requirements.

The test voltage chosen for the tests was 4.5 kV (RMS) or 4.5 kV (DC) continuous tracking voltage (CTV) which required a contaminant flow rate of 0.6 ml/min for the duration of the 6-hour test. One sample was tested at a time.

Nitrile powder-free latex gloves were used in handling the samples before and after testing so that the samples would be free from any external contamination. The liquid contaminant was prepared and mixed thoroughly prior to each test.

3.3.5.1 **The testing procedure was as follows:**

- Weight measurement of the sample was done prior to the test,
- The sample was cleaned with dielectric cleaning fluid detergent and allowed to dry,
- The sample was mounted on the bracket and connected to the circuit,
- The contaminant system was started,
- The contaminant was allowed to fully wet the filter paper uniformly and reach the ground electrode,
- Ground stick removed,
- Voltage was applied and increased until 4.5 kV (+DC, -DC, or AC RMS) at the appropriate rate,
- Current measurement logger was started,
- The test was run for 6 hours,
- Images were taken using a digital camera (Canon 500D) and an infrared thermal camera (FLIR),
- Voltage turned off,
- System grounded,
- Contaminant system turned off,
- Samples removed,
- Weight measurement of the samples was done after the testing, and
- Sample stored away from external contamination for post experiment physiochemical analysis.

3.3.5.2 **Post-test sample analysis**

The material analyses on the samples were conducted using equipment such as SEM, EDS, TEM and FTIR. The post aging analysis was carried out in UKZN Westville Microscopy Unit and Chemistry Department.

CHAPTER 4: RESULTS AND DISCUSSION

4.1 Introduction

The results for each series of tests are presented and discussed in this chapter. Three voltage types under consideration were +DC, - DC and AC. The objective of the work was to evaluate and analyse the relative performance of HTV SIR under IPT. A single sample test was incorporated such that comprehensive data would be gathered and a comparative analysis of the effect of voltage types would be done.

A number of other samples were used in setting up and testing the system but are not presented in this dissertation. Three test specimen were tested per each voltage type +DC, -DC and AC for credibility. A total of six samples were selected that were successfully tested. Samples 2-4 were selected for the post aging processing. Sample 5 was used as the control sample for the FTIR in the post aging analysis. Sample 6 was tested under negative DC.

The tests were done as follows:

- Sample 1 – Visual observation of +DC IPT over 6 hours,
- Sample 2 – Repeat of +DC IPT with the leakage current measurement over 6 hours,
- Sample 3 – - DC IPT with leakage current measurement over 6 hours,
- Sample 4 – AC IPT with leakage current measurement over 6 hours,
- Sample 5 – Control Sample, and
- Sample 6 - - DC IPT over 6 hours.

The section is structured with visual observations first, followed by leakage current measurement and analysis and finally the post testing analysis of FTIR, SEM, EDS, and TEM.

4.2 Visual Observations

Visual observations and physical appearances of the test sample under ± DC and AC voltages were monitored during the entire 6 hour tests. The photographs were taken by a high resolution camera and by the infrared (FLIR) camera. The contaminant was allowed to flow for 10 minutes, to ensure steady flow on the sample. Figure 4-1 shows the contaminant wetting the surface before energisation.

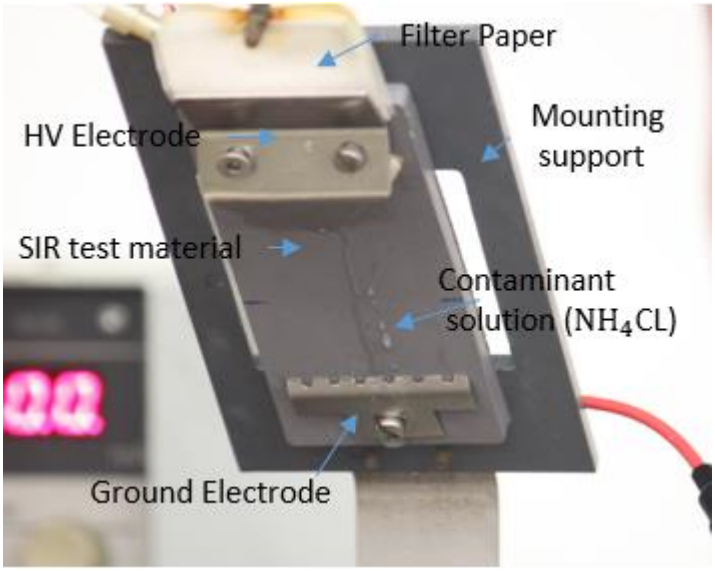

Figure 4-1: SIR sample prior to energisation

4.2.1 Positive DC test 4.5 kV

Sample 1 was weighed to be 55.86 g before testing. Scintillations began immediately upon application of high voltage.

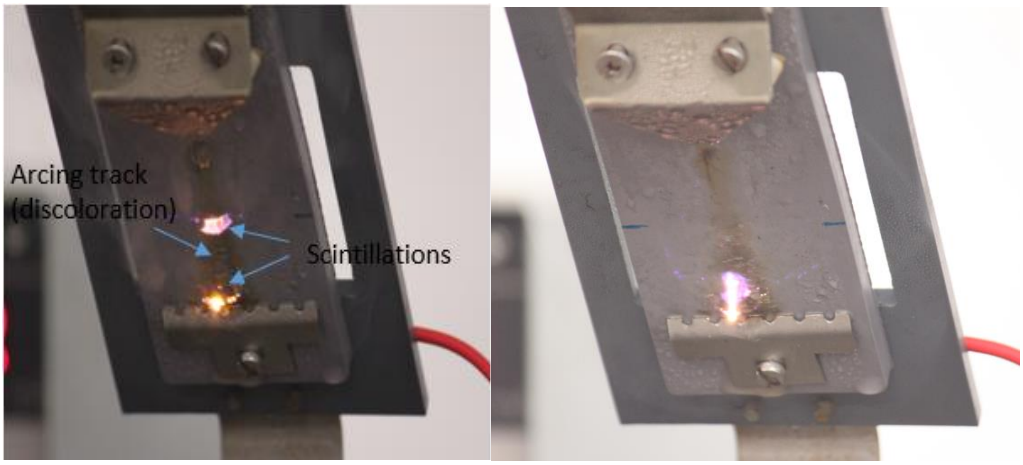

Figure 4-2: Positive DC test – Sample after 30 minutes exposure time

After 30 minutes scintillations were observed to be more vigorous and frequent as shown in figure 4-2. The arc started from the ground electrode where a yellow arc can be seen and then moved towards the high voltage electrode with a violet colour. The intermittent discharges caused the contaminant stream to spread into a delta shape that appeared to be thick at the top and thin at the bottom of the

electrodes. Tracking marks began to develop on the sample surface. A discolouration was visible along the entire length of the contaminant path from the high voltage electrode to the ground electrode. Khaaiye et al. [45] reported a similar arcing pattern, however there appeared to be less discolouration along the length of the sample in this test [32]. The arc appeared to be similar for Mahatho for an applied voltage of 4.5 kV, however he had significant erosion after 40 minutes and stopped the test after 60 minutes [33].

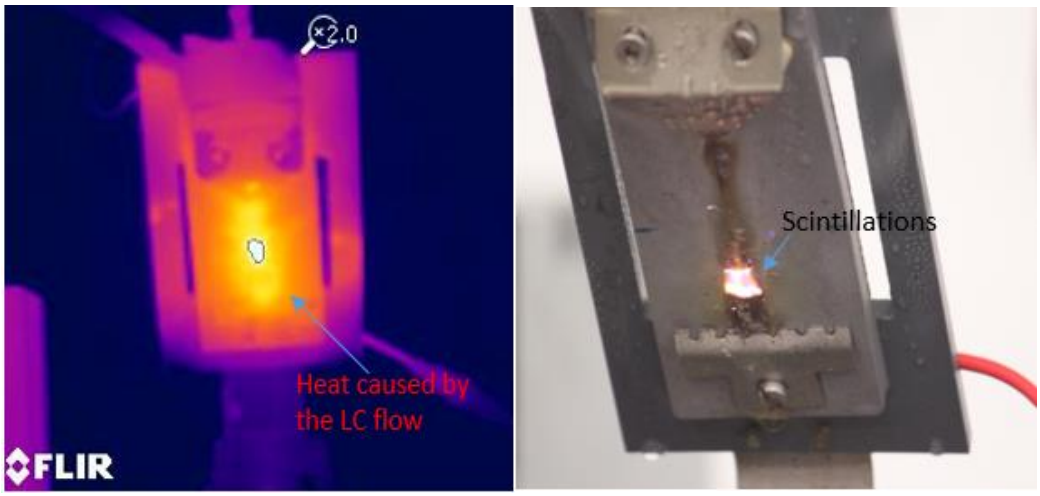

Figure 4-3: Positive DC test – Sample after 2 hours exposure time and IR image

After 2 hours the high intensity sparking at the ground electrode continued as shown in figure 4-3. The infrared camera monitored the discharge activity. An infrared image of heating caused by the arcing and current flow can be seen. Temperatures of more than 235 ± 2°C were recorded by FLIR camera. The arc followed a well-defined path that bridged the gap between the high voltage electrode and ground electrode. It can also be observed that the DC arc was more intensive and covered a larger area, especially towards the ground electrode.

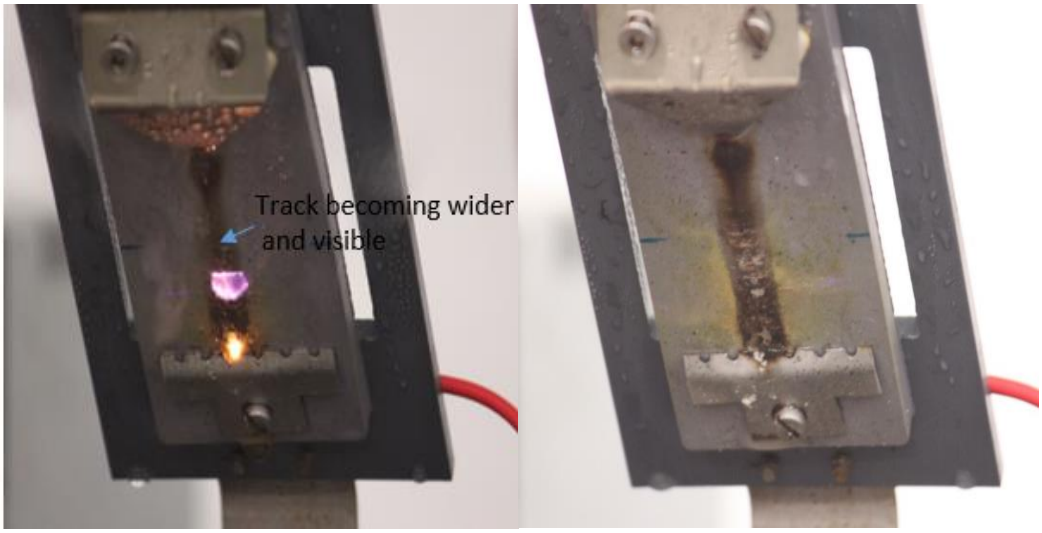

Figure 4-4: Positive DC test – Sample after 4 hours exposure time

After 4 hour arcing and erosion intensified as can be shown in figure 4-4. The scintillations were observed to be more vigorous and the DC arcing track becomes wider and visible along the entire length from the high voltage electrode to the ground electrode. The tracking and erosion on test sample continue to progress vigorously between the electrodes.

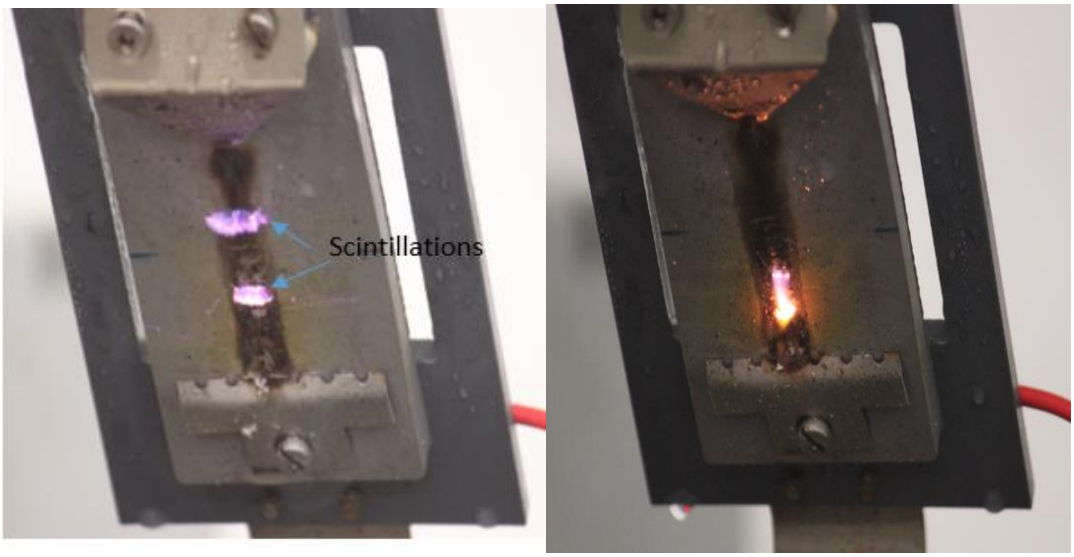

Figure 4-5: Positive DC test – Sample after 5 hours exposure time

After 5 hours the DC arcs seem to be more vigorous, longer and much brighter; erosion was clearly visible at the ground electrode as can be seen in figure 4-5. The liquid contaminant was forced off the surface because of electrostatic forces and excessive boiling. These scintillations occurred intermittently and erratically.

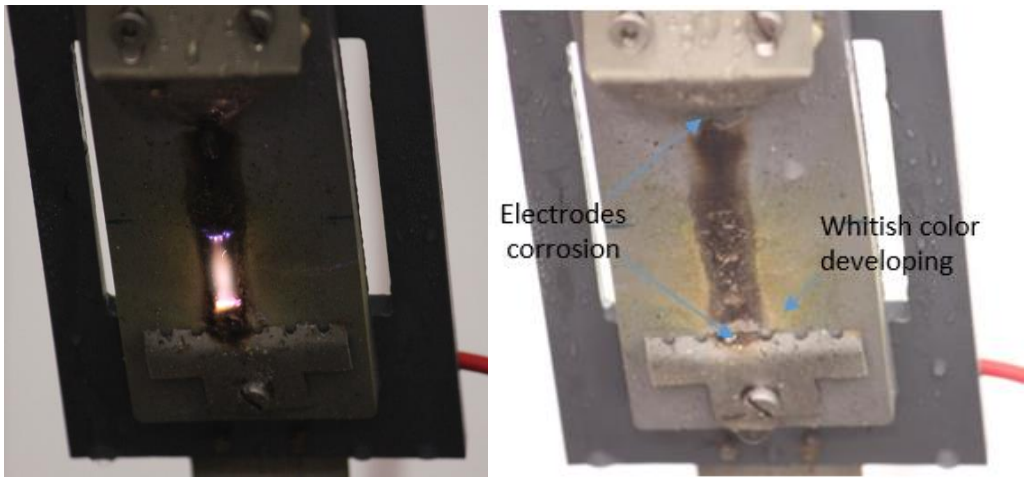

Figure 4-6: Positive DC test – Sample after 6 hours exposure time

After 6 hours it can be seen from figure 4-6 that the sample developed an eroded area of whitish colour that removed the conducting channels just above the ground electrode. The formation of a carbonized tracking path near the ground electrode stopped the arcing. Khaaiye et al. had a similar formation of a whitish substance after 1.5 hours, which stopped their tracking [45] [32].

The top and bottom electrodes are seen to be worn in Figure 4-7. Khaaiye had worn electrodes after 6 hours at 3.5 kV, the damage in this research appears to be less than that of Khaaiye [32]. The material of electrode and the contaminant solution is an important consideration for testing materials under DC for the IPT.

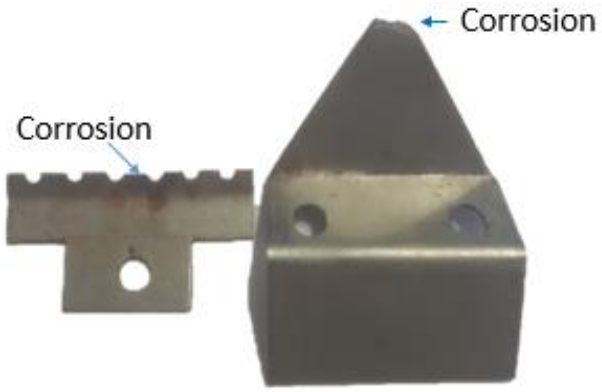

Figure 4-7: Positive DC test – Electrodes at the end of the test

Ghunem et al. [48] employed chisel-shaped platinum electrodes, which gave reproducible results and could be applicable over a wider voltage range. The intent was to use electrodes that withstand corrosion. Bruce et al [24] incorporated stainless steel electrodes for the IPT. Similarly to their work, the electrode in the +DC test was found to be more eroded, whereas in -DC tests the bottom grounded was also more eroded. The erosion process is due to electrolysis, oxidation of the stainless steel electrodes as a result of high temperature arcing. Vas et al [28] also found a brownish material deposition on the surface of the grounded electrode as seen in figure 4-7. The erosion was high on the high voltage top electrode due to electrolysis.

The contaminant NH_4CL, was used as the electrolyte because it did not build up between the electrodes and interfere with the progress of the tests.

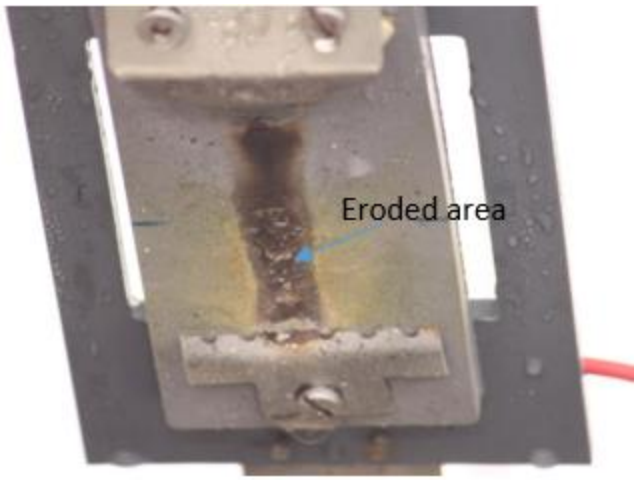

Figure 4-8: Positive DC test – Sample at the end of the test

Figure 4-8 shows that the sample passed all the failure criteria for the tracking length which was approximately 16 mm.

The sample weight at the end of the test was measured to be 55.02 g. The sample had a weight loss of 3.24 %.

4.2.2 Mounting support system

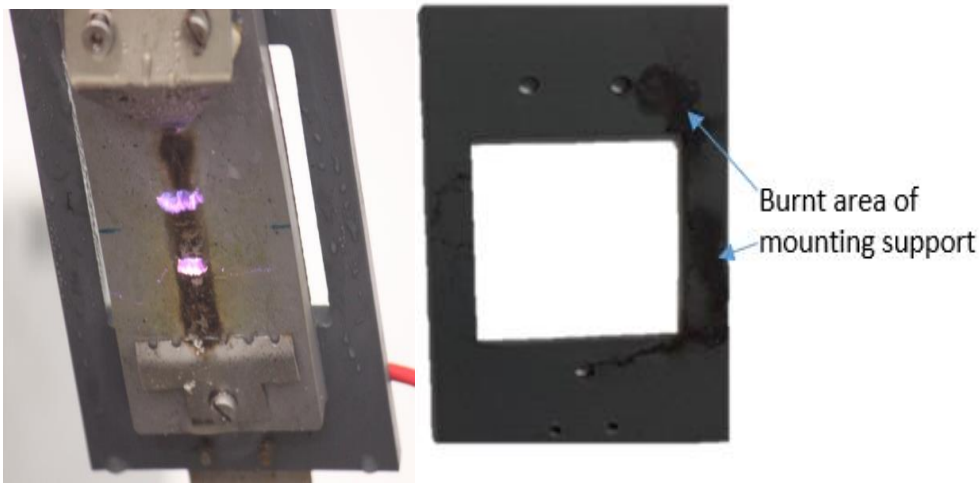

Figure 4-9: Polyvinyl chloride (PVC) showing burnt part

The mounting support in figure 4-9 was burnt after the initial +DC test. The PVC tracked easily when there was contaminant leakage in the setup. As per IEC 60587 [1] standard, the mounting support shall be such that the heat dissipation from the back of the sample is not hindered and the material shall be heat resistant and electrically insulating. Nylon was a more suitable material with higher heat resistance and a better insulating performance and was used for the succeeding tests as shown in figure 4-10.

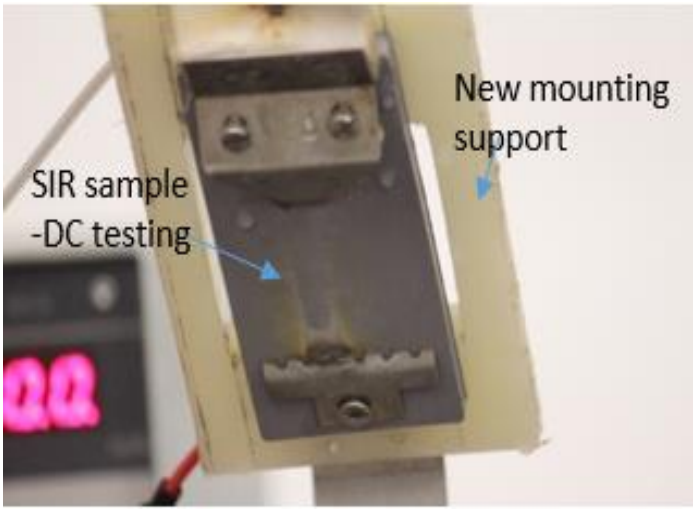

Figure 4-10: Nylon mounting support system

4.2.3 Negative DC test at 4.5 kV

Sample 3 was weighed to be 55.86 g before testing.

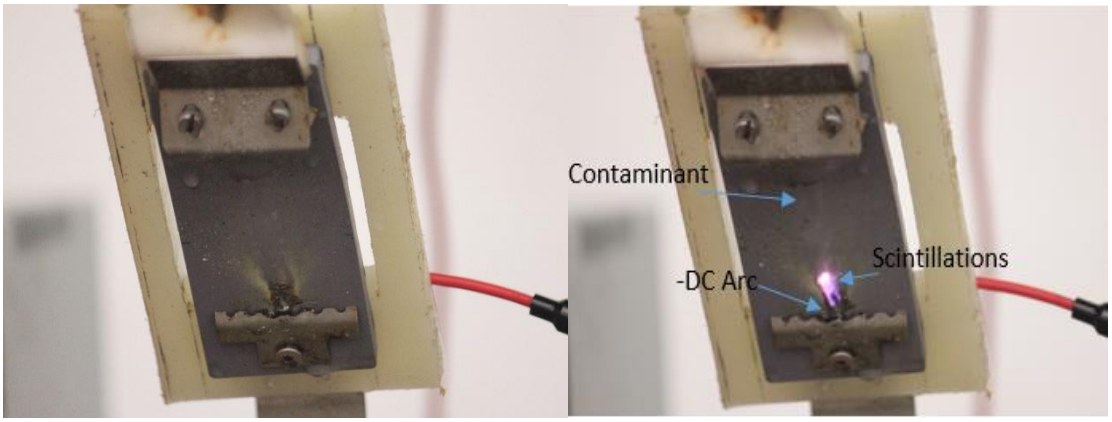

Figure 4-11: Negative DC test – Sample after 5 minutes exposure time.

After 5 minutes it was noted that scintillations appeared across the surface as seen in figure 4-11. An arc root was formed and aggressive erosion began instantly. It was observed that the contaminant was evaporated almost instantaneously as soon as it approached the ground electrode. The initial negative energization seemed to have more surface discharges as compared to the positive case. The negative DC arc was thinner and it started near the ground electrode.

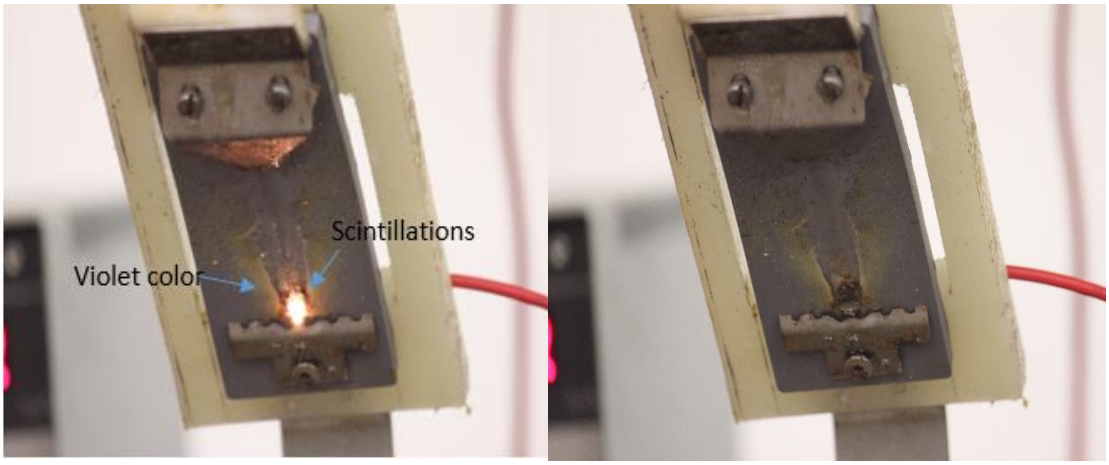

Figure 4-12: Negative DC test – Sample after 1 hour exposure time.

After 1 hour the arcing had caused erosion near the ground electrode as shown in Figure 4-12. The arc followed a consistent straight path from the ground electrode to the high voltage electrode. The colour of the arc was yellow/red near the electrode and blue as it moved towards the high voltage electrode. A track that bridged between the electrodes was formed, however, it was not nearly as visible as in the sample under +DC. Mahatho observed arcing, tracking and erosion from the ground electrode to the high voltage electrode after approximately 42 minutes [33], he stopped the test after 112 minutes as the samples were significantly damaged and burnt.

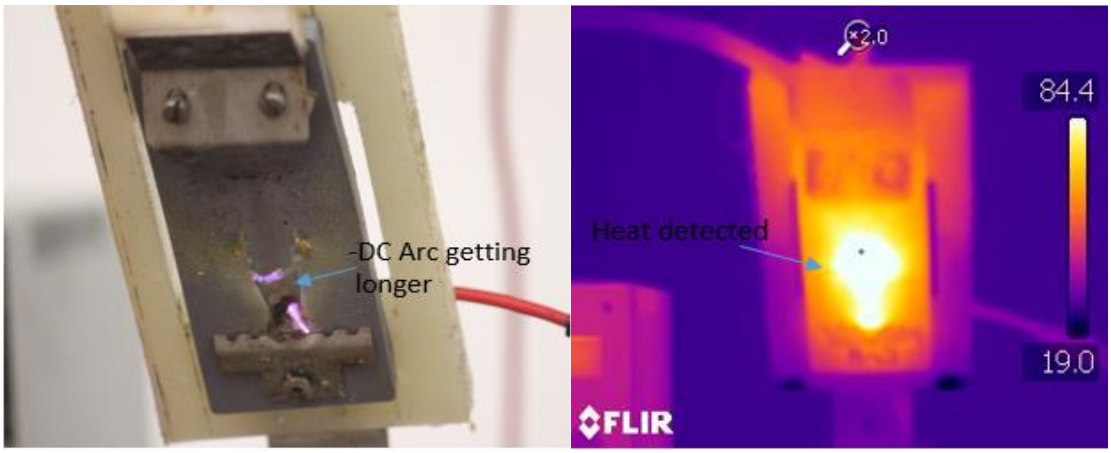

Figure 4-13: Negative DC test – Sample after 3 hours exposure time and IR image

After 3 hours' aggressive erosion continued to build up as shown in figure 4-13. The -DC arc was shorter and followed a well-defined path with a longer arcing period. The ground electrode of the -DC sample had started to look corroded. It was observed that the discharges were being evenly elongated towards the high voltage electrode and become more randomly scattered, distributed as was observed in the +DC electrical test. The maximum temperature was measured to be more than 250 °C using the infrared (FLIR) camera.

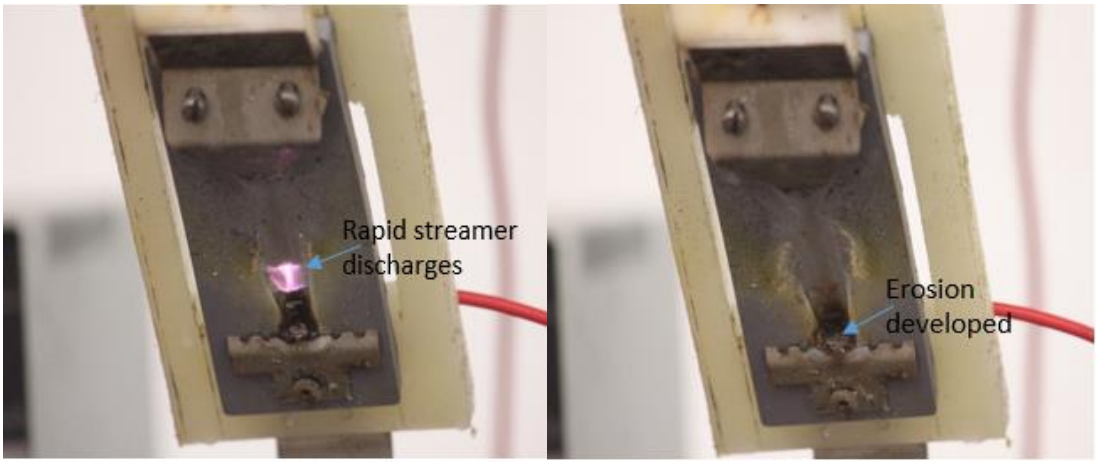

Figure 4-14: Negative DC test – Sample after 5 hours exposure time

After 5 hours Figure 4-14 show that intense discharges near the ground electrode. Aggressive and rapid streamer discharges spread along the surface of the silicon rubber test sample towards the ground electrode. The scintillations were more focused on the ground electrode side. It can be seen that the tracking and erosion was significantly less than in the +DC test.

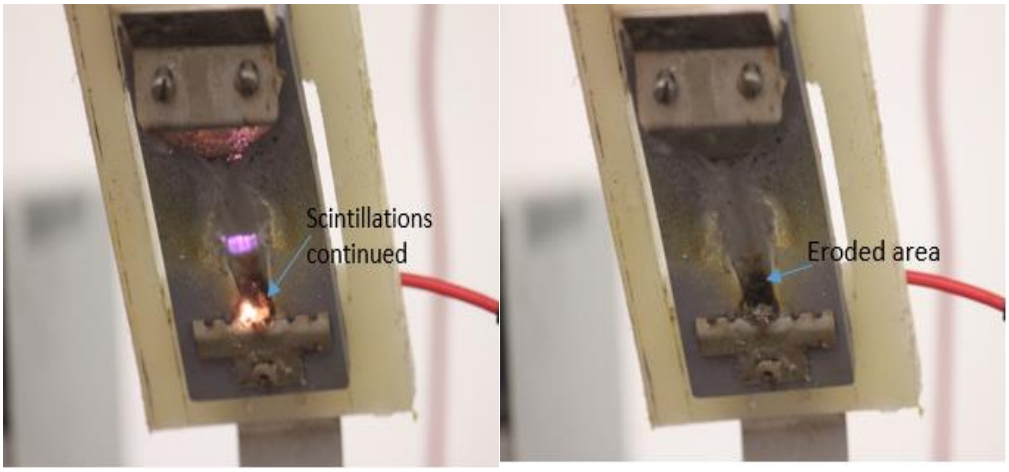

Figure 4-15: Negative DC test – Sample after 6 hours exposure time

After 6 hours it was noted that there was minimal erosion of the test sample as shown in figure 4-15. The sample passed the failure criteria test as the tracking length was approximately 16 mm long. In comparison to the sample for the +DC experiment, there was significantly less erosion and tracking. The electrodes were also far less corroded than for the +DC test.

The sample weight after the test was measured to be 55.24 g. The weight loss was calculated to be 1.11 %.

4.2.4 AC Test Experiment

Sample 4 was weighed to be 55.86 g before testing.

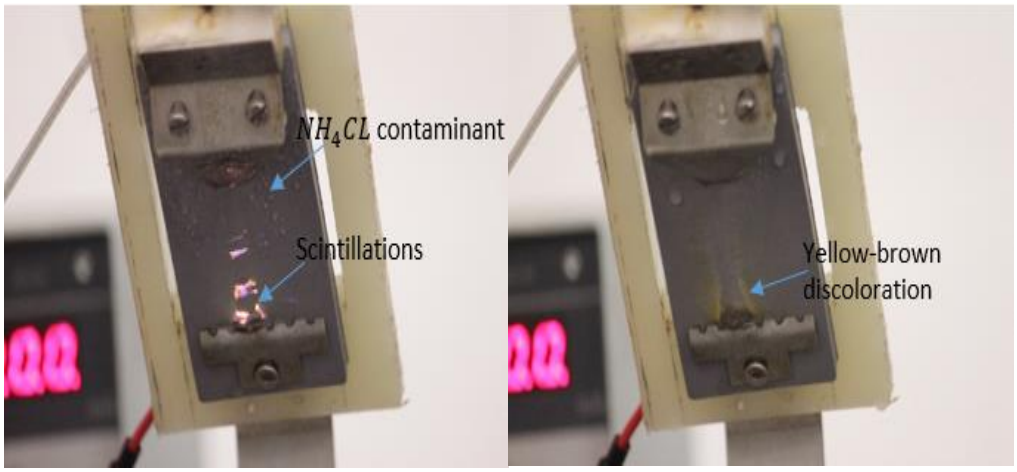

Figure 4-16: AC test – Sample after 10 minutes exposure time

After 10 minutes scintillations and discharge activity were noted as seen in figure 4-16. It was also noted that the AC arc seemed more intense when it started and that it remained at the ground electrode. The arcing was audible and frequent. A yellow-brown discolouration of the material surface started to develop. A noticeable transition in the flow of contaminant, at the start of the test a thin-tailed drop was seen which abruptly changed into an intermittent stream of contaminant. Heo et al [34] mentioned that this resulted in discharges at a higher magnitude of leakage current and higher average current per minute as was seen.

Bruce et al. [24] found a similar intermittent stream of contaminant which resulted in continuous discharges at high magnitude of leakage currents.

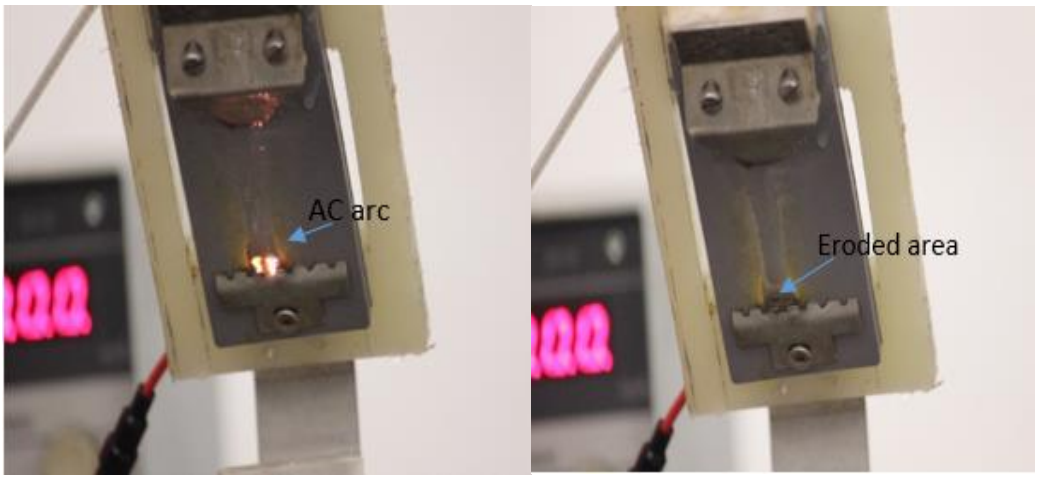

Figure 4-17: AC test – Sample after 30 minutes exposure time

After 30 minutes the AC arc root in figure 4-17 grew immensely fast and frequent, showed two parallel paths that started from the top electrode and bridged at the ground electrode. The track marks were clearly visible on the surface of the samples, along with the contamination flow path. Similar observations were made by Khaaiye et al. [45] [32] who noted that the arcing was scattered and often had more than one path. In comparison to the +DC test the tracking was less and the arc was smaller, in comparison to the –DC test there was a smaller eroded area after 1 hour.

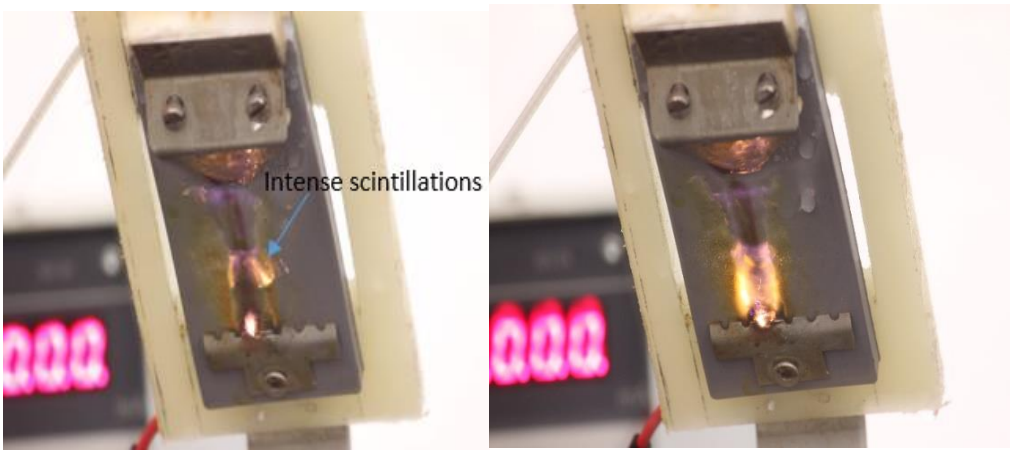

Figure 4-18: AC test – Sample after 1 hour exposure time

After 1 hour the development of arc roots with scintillations can be seen in Figure 4-18. A rapid and aggressive process of degradation follows immediately after this transition caused by higher current discharges. The AC arcing had formed a path from the lower electrode to the upper HV electrode. The AC arc was primarily concentrated at the ground electrode. A violet colour of the AC arc was observed and was scattered. In comparison to the +DC test the path formed was less intense and the shape was different. In comparison to the –DC test, the path was longer, but the eroded area appeared less. Khaaiye et al. and Mahatho et al. [45] [32] showed a similar discharge pattern for their samples, where the AC arc tended to form a couple of paths.

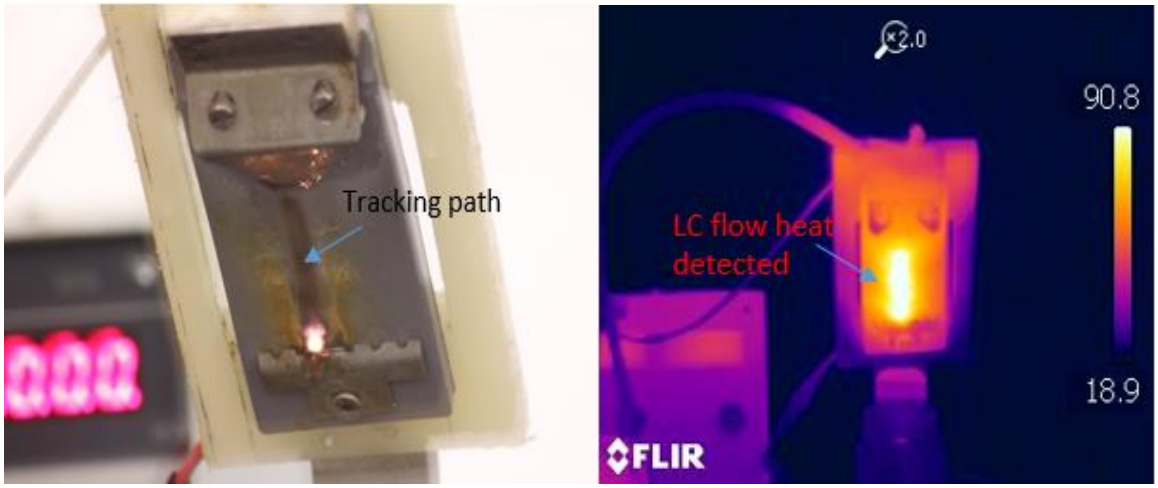

Figure 4-19: AC test – Samples after 3 hours exposure time and IR image

After 3 hours the AC arc appeared to be faint and weak and was observed to be focussed towards the ground electrode. The discharge activity was monitored with an FLIR camera, showing more clearly the areas of heat as shown in figure 4-19. The erosion of the insulation material concentrated at one region near the ground electrode. At the ground electrode, dry bands were formed. After some time, they were bridged by discharges causing deep erosion. A maximum temperature of 230 ± 2 °C was measured by the infrared (FLIR) camera. In the +DC test, the arcing and the erosion appeared to be extending further across the insulator, whereas in the –DC test and AC test the erosion seemed to localised around ground electrode.

Figure 4-20: AC test – Sample after 5 hours exposure time

After 5 hours the AC arc was faint, scattered and the tracking did not have a well-defined path as shown in figure 4-20. In the +DC test, the arc was observed to be more vigorous, longer and much brighter; the tracking path was clearly visible, whereas in –DC test the arc was shorter and followed a well-defined path with a longer arcing period.

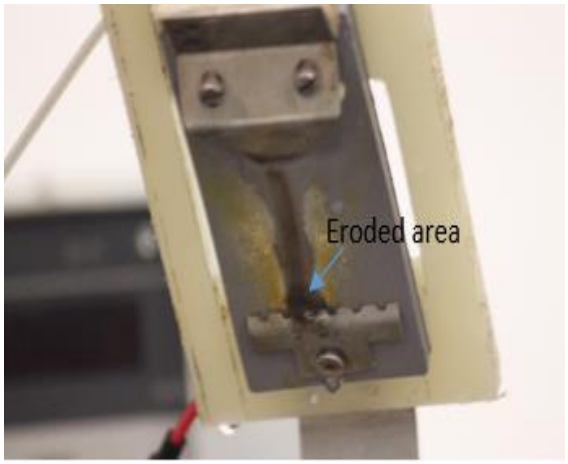

Figure 4-21: AC test - Sample at the end of the test

After 6 hours figure 4-21 shows that AC arc was getting weaker over time, faint and scattered. The electrodes showed no to minimal signs of corrosion. Khaaiye et al. [45] also found similar results for the AC test samples with no material damage at the end of the tests, though showing more frequent arcing. It was observed that the arc under AC voltage was transparent due to the surface contaminant burning off, whereas the arc under DC voltage was solid. In the +DC test, the arcing was stopped because of the formation of a carbonized tracking path near the ground electrode, comparatively in –DC test intense discharges continued to spread along the test sample surface towards ground electrode at the end of the test. The erosion under –DC is less as compared to +DC. The decolourisation on the surface of the samples under ±DC is different as mentioned by Vas et al. [24].

The sample weight after the test was measured to be 55.41 g. The weight loss was calculated to be 0.81 %.

4.2.5 Comparison between Applied Voltages

A comparison of the visual observations of the samples under +DC, -DC and AC are captured in Table 4-1.

Table 4-1 : Summary of Visual Observations

Time	+DC	-DC	AC
30 minutes	Intense scintillations, arc from ground electrode to HV electrode, tracking developed, discolouration was visible – a yellow arc.	Intense surface discharges, arc was thinner and started near the ground electrode, erosion began.	Scintillations, arc root grew immensely fast and frequent, arcing was audible, a yellow-brown discolouration developed, track marks were clearly visible.
1 hour	High intensity sparking at the ground electrode, arc followed a well-defined path, arc covered a larger area.	Arcing had caused erosion, arc followed a consistent straight path, the colour of the arc was yellow/ reddish, and the track bridged the electrodes.	Development of arc roots continued, arcing formed a path from the ground electrode to the upper HV electrode.
3 hour	Arcing and erosion intensified, DC arcing track became wider and visible.	Erosion continued to build up, arc was shorter, longer arcing period, discharges randomly scattered.	Arc appeared to be faint and weak, erosion localised around ground electrode.
5 hour	DC arc was vigorous, longer and much brighter. Erosion was visible at the ground electrode.	Scintillations more focused on the ground electrode, rapid streamer discharges spread along the surface.	Arc was faint, scattered and the tracking did not have a well-defined path.
6 hours	A whitish colour developed, carbonised tracking path stopped the arcing, severe erosion.	The erosion was significantly less than in the +DC test.	Arc was getting weaker over time, no visible tracking beyond the ground electrode, no to minimal erosion on the sample.
Overall	Scintillations were observed to be more vigorous and frequent. DC arcing track become wider and visible. A higher material damage. Passed the test after 6 hours.	No erosion took place after 30 minutes. -DC arc was short and followed a well-defined path with longer arcing period. The material damage under – DC is less compared to +DC. Passed the test after 6 hours.	AC arc appeared to be faint and weak. The arc was primarily concentrated at the ground electrode. No material damage. Passed the test after 6 hours.

Table 4-2: Summary of Sample Weight Loss

Applied Voltage	Weight before testing (g)	Weight after testing (g)	Mass loss (g)	Mass loss (%)
+DC	55.86	55.02	0.84	3.24
-DC	55.86	55.24	0.62	1.11
AC	55.86	55.41	0.45	0.81

The +DC test appeared to have caused the most damage, followed by – DC and AC. This trend is in line with work by Khaaiye et al. [45] [37] who showed that the +DC test was the most aggressive, in terms of arcing and material damage. Dry bands formed on the insulator surface as a result of DC arcing. The white patch formed afterwards later stopped the arc. AC test showed a much lesser material damage which is consistent with the investigation. Similarly Mahatho [33] showed that samples under +DC test displayed severe erosion and that AC test showed minimal erosion. The – DC test developed severe erosion but was less than the positive case.

Ghunem [48] reported that the highest erosion was under +DC voltage caused by electrolytic decomposition products from the positive electrode. Furthermore Heger et al. [30] noted that at higher electrical stress the surface degradation was severe under +DC voltage. Bruce et al. [27] also noted that +DC test seemed to produce deeper erosion than - DC tests and AC test the erosion was less severe. Gorur et al, Vas et al, Chandrasekar et al [17] [24] [30] also reported the same phenomenon, that aggressive erosion was noticed under +DC voltage followed by – DC test voltage and least AC voltage.

4.3 Leakage Current Measurement

4.3.1 Leakage Current Analysis

The leakage currents were measured through an oscilloscope for Samples 2-4 to:

- Identify any major differences in the DC and currents,
- Check that the voltage drop was within the 5% for the DC test,
- Understand the measurement of the RMS or average of the currents, and
- Whether the energy could be quantified.

The positive DC current and voltage drop measurements are shown in Figures 4-22 to Figures 4-24. The current peaks between 40 and 80 mA with voltage drops between 70 and 130 V, demonstrating the required stiffness of supply for the IPT. It was noted that the voltage drops correspond to the drops in voltage in the time domain. It was noted that there appeared to be a reverse current in the measurement after the main positive peak in the current measurement. This was unexpected and not fully understood. The interval between successive discharges appeared to be random.

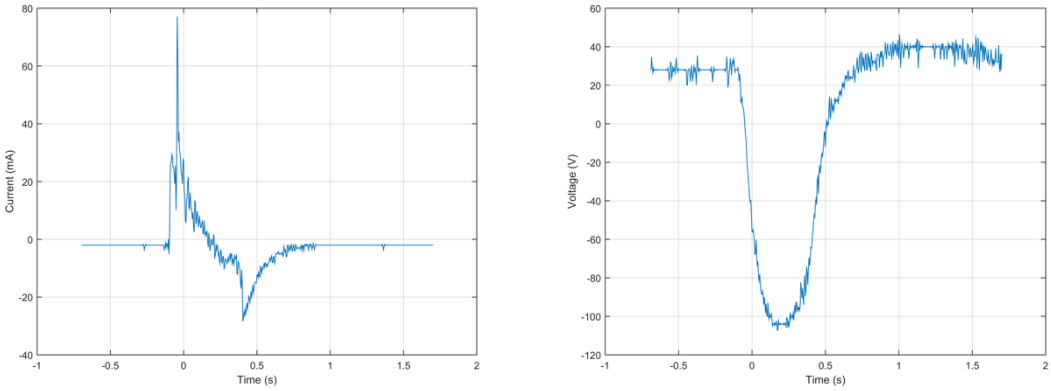

Figure 4-22: Positive DC1 current and voltage drop

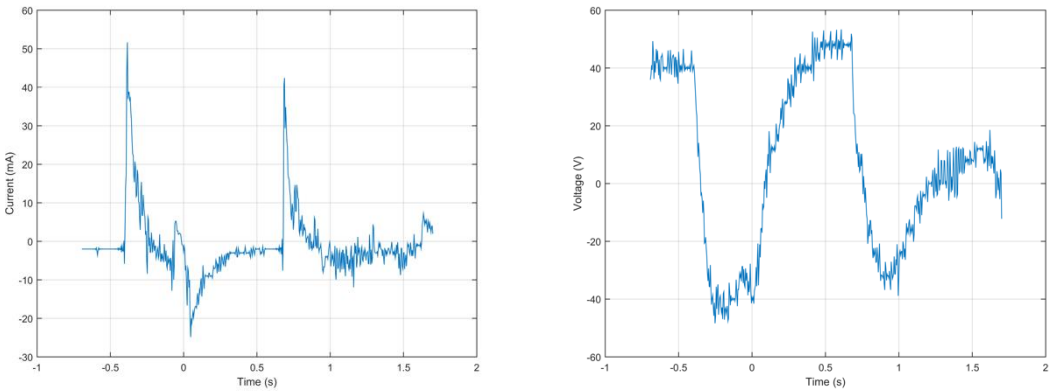

Figure 4-23: Positive DC2 current and voltage drop

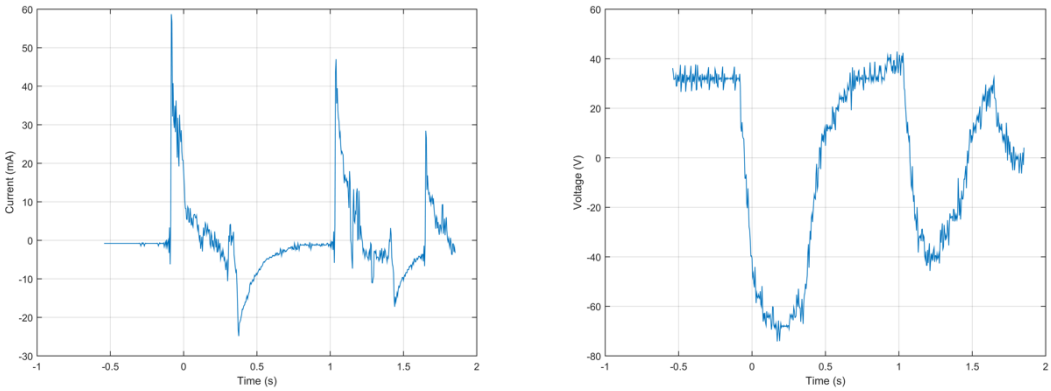

Figure 4-24: Positive DC3 current and voltage drop

The negative DC current and corresponding voltage drop are shown in Figures 4-25 to 4-28. The peak currents were between -15 and -40 mA with corresponding voltage drops between 20 and 110 V, demonstrating the required stiffness of supply for the IPT. The negative current did not have the reverse currents as were seen with the positive current. It performed as expected. It was noted that the interval between discharges was random. Also that the duration of the negative current pulses is much longer than that of the positive pulses.

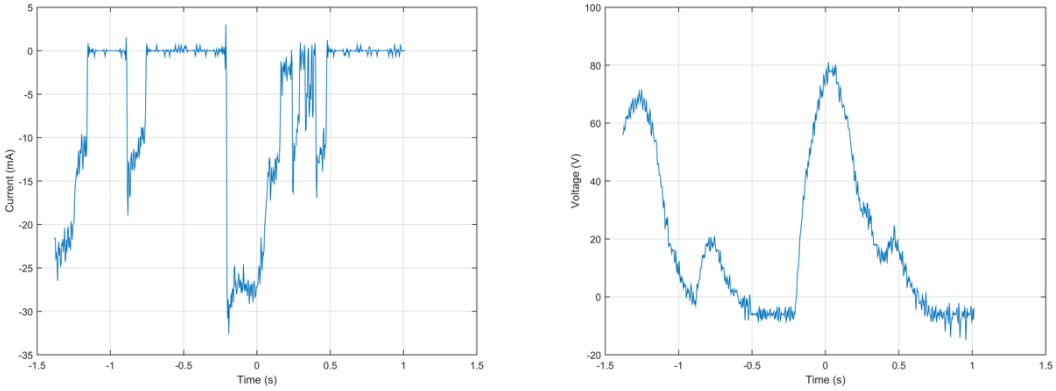

Figure 4-25: Negative DC1 current and voltage drop

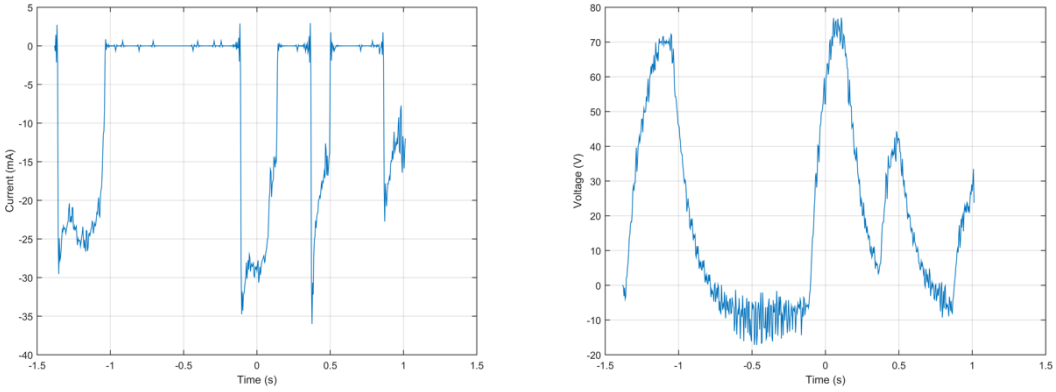

Figure 4-26: Negative DC2 current and voltage drop

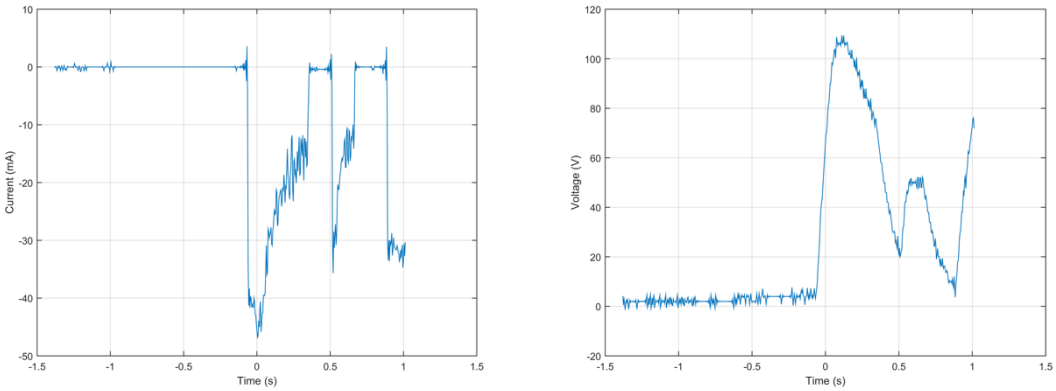

Figure 4-27: Negative DC3 current and voltage drop

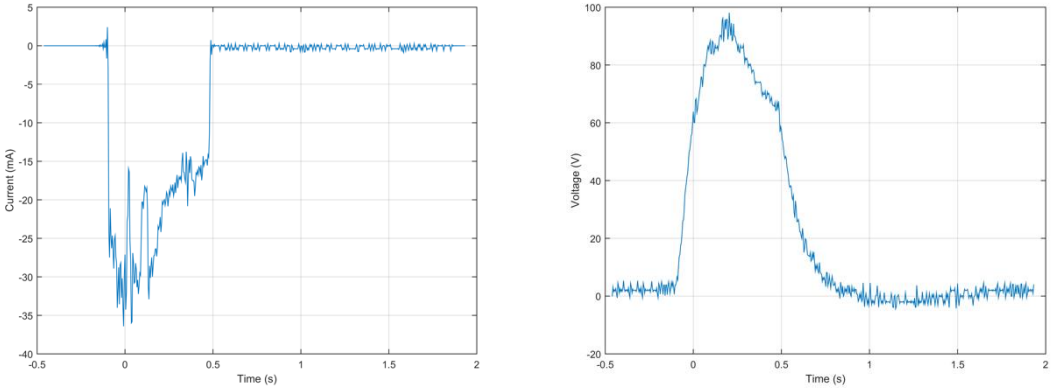

Figure 4-28: Negative DC4 current and voltage drop

The AC currents are shown in Figures 4-29 to 4-32. The peak currents varied between 40 and 70 mA. The shape of the current waveform and peaks appeared to differ between recordings. The interval between successive discharges appeared to be random at the start of the test and somewhat more consistent as the test progressed.

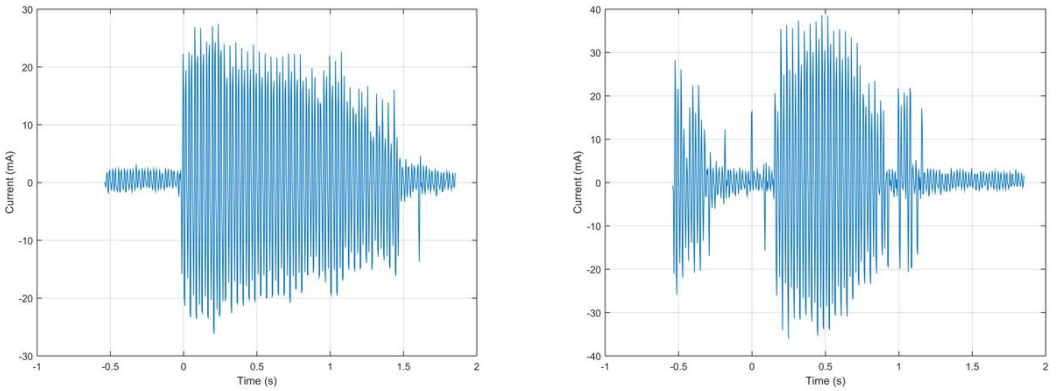

Figure 4-29: AC1 current and AC2 current

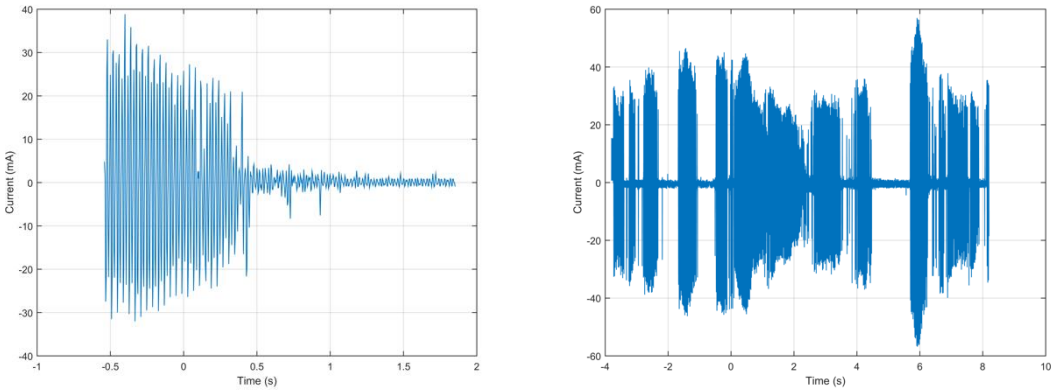

Figure 4-30: AC3 and AC sample after 0 minutes

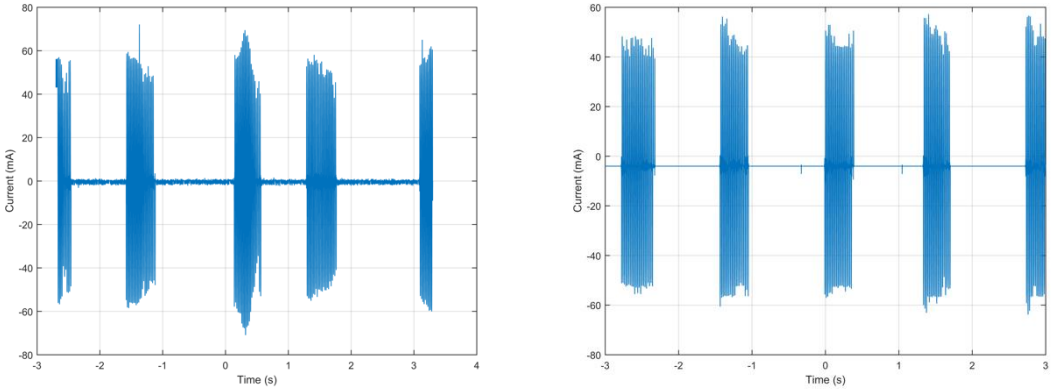

Figure 4-31: AC sample after 30 minutes and 60 minutes

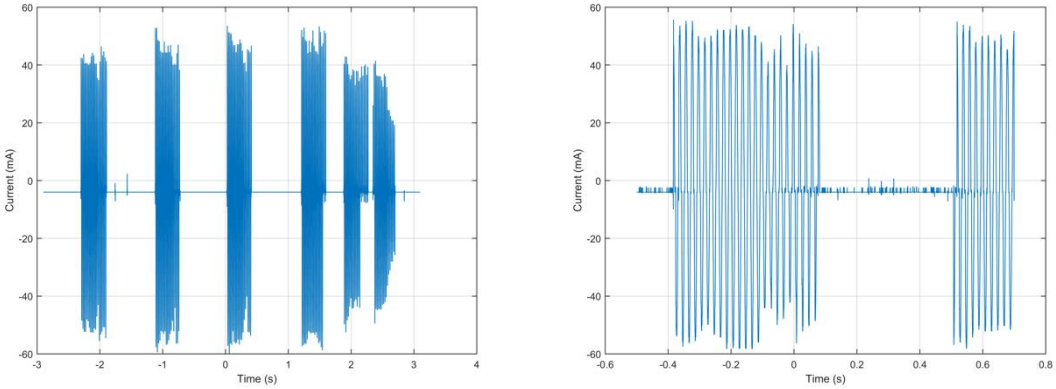

Figure 4-32: AC sample after 100 minutes and AC 100 minutes

It is evident that it is difficult to quantify the current measurement by peak current and repetition rate.

A summary of the analysis of the measured currents is shown in Table 4-3. The table presents:

- True rms current,
- AC rms current (the RMS with the average DC component removed), and
- Average DC current.

This was done as the current logger was only recording the AC rms current and the error of the results in the following section needed to be quantified. For the positive DC the reverse current made the average DC almost negligible, while the true RMS and the AC rms currents were similar. The negative DC current had a definite average DC component, with a difference in the true RMS and the AC RMS value of approximately 20%. For the AC current the true RMS and the AC RMS matched.

The current logger was deemed to track the performance of the sample over time, but not to compare with other published leakage currents.

The energy (I^2t) was considered as a possible method to compare the currents, and it can be seen in the table that where the recorded current impulses had similar recorded durations that the energies were somewhat comparable, however the average current selected was used.

Table 4-3 : Summary of Analysis of Current

Current	Ipeak (mA)	Pulse width (ms)	Irms (mA)	Iac (mA)	Idc (mA)	Vdrop (V)	Energy (J)
Positive DC1	40	250	8.9	8.8	1.8	120.00	190
Positive DC2	40	250	8.7	8.6	0.1	80.00	180
Positive DC3	40	250	10.2	10.2	0.2	90.00	240
Negative DC1	30	250	11.80	9.70	6.70	80.00	330
Negative DC2	35	250	13.50	11.10	7.80	80.00	440
Negative DC3	45	350	14.90	12.90	7.50	110.00	540
Negative DC4	30	650	11.40	10.00	5.50	95.00	310
AC1	27	1500	11.71	11.71	0	-	330
AC2	37	750	13.55	13.55	0	-	440
AC3	37	1000	11.66	11.66	0	-	330
AC after 0 minutes	57	2000	17.3	17.3	0	-	3600
AC after 30 minutes	70	300	19.9	19.9	0	-	2400
AC after 60 minutes	60	300	19.1	19.1	0	-	2200
AC after 100 minutes1	57	300	18.6	18.6	0	-	2100
AC after 100 minutes2	57	400	25.4	25.4	0	-	800

4.3.2 Leakage Current Over Duration of Test

The leakage current was recorded for Samples 2-4 through the use of the Pico-log. The sampling rate was set to 100 ms and recorded for the duration of the test.

Note: The DC currents were inaccurate as the Pico-log CM3 uses a calculation that removes the DC component of the signal. i.e. AC rms. It does not measure true RMS and as such only the trend between the currents can be compared. The actual value would be in the range 10% to 40% higher. The following graphs showed the results of the captured current waveforms throughout the duration of each test.

4.3.2.1 **Positive DC Current**

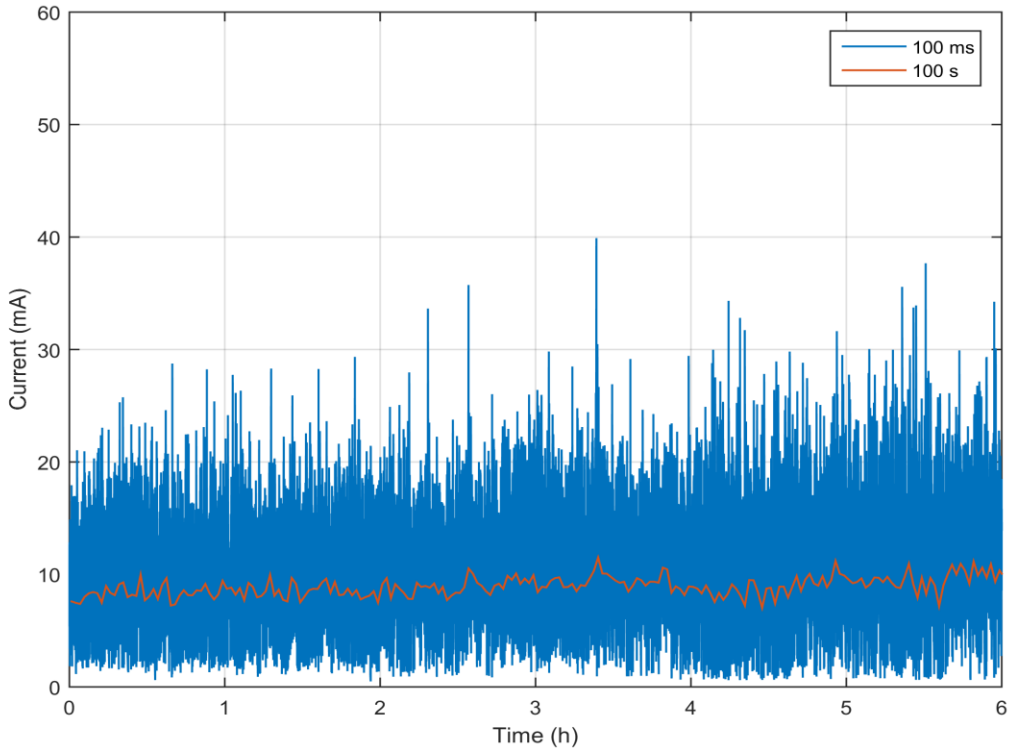

Figure 4-33: Leakage current for Positive DC test

Figure 4-33 shows the current pulse captured by the pico-log during the discharges under 4.5 kV +DC voltage. The leakage current of 4.5 kV was recorded for the entire 6-hours of the test. The maximum leakage current recorded was approximately 41.32 mA before the arcing and tracking completely stopped. The average current was measured to be 9.40 mA. The current pattern is more consistent that is less random variation signals. An intensive arcing near the ground electrode caused an erosion of the insulation and subsequently stopped the flow of the leakage current by making the DC circuit open. Before arcing stopped, however, the leakage current of the 4.5 kV +DC sample caused a consistent tracking that bridged the gap between the electrodes. The short times can be seen, where there was no discharge activity, peak leakage currents are noticed. The tracking was only visible near the ground electrode with the rest of the gap between the electrodes showing only some discoloration. The DC arcing does not alter the surface resistance of silicon rubber insulator since the current does not show an increasing trend.

4.3.2.2 **Negative DC Current**

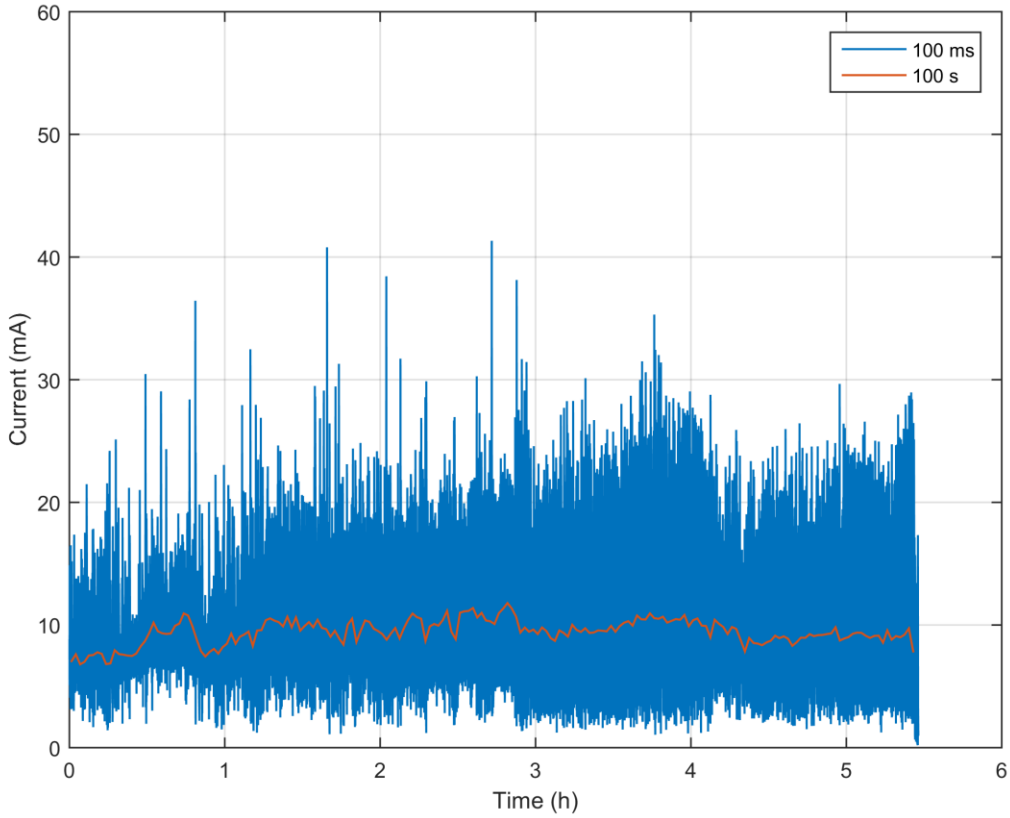

Figure 4-34: Leakage current for Negative DC test

The leakage current of 4.5 kV -DC was recorded for 5.5 hours duration of the test, but the experiment ran for 6 hours. It can be observed in figure 4-34, that the - DC leakage current does show a notable gradual increase for a period of time and slightly decrease and increase trend for the entire electrical test. The maximum leakage current recorded was approximately 10.90 mA before the arcing and tracking of the silicone rubber insulator test sample completely stopped and the average current was 8.92 mA. Figure 4-34 shows the discharge activity captured by the pico-log with current peaks as high as approximately 38.47 mA and 39.00 mA.

4.3.2.3 **AC Current**

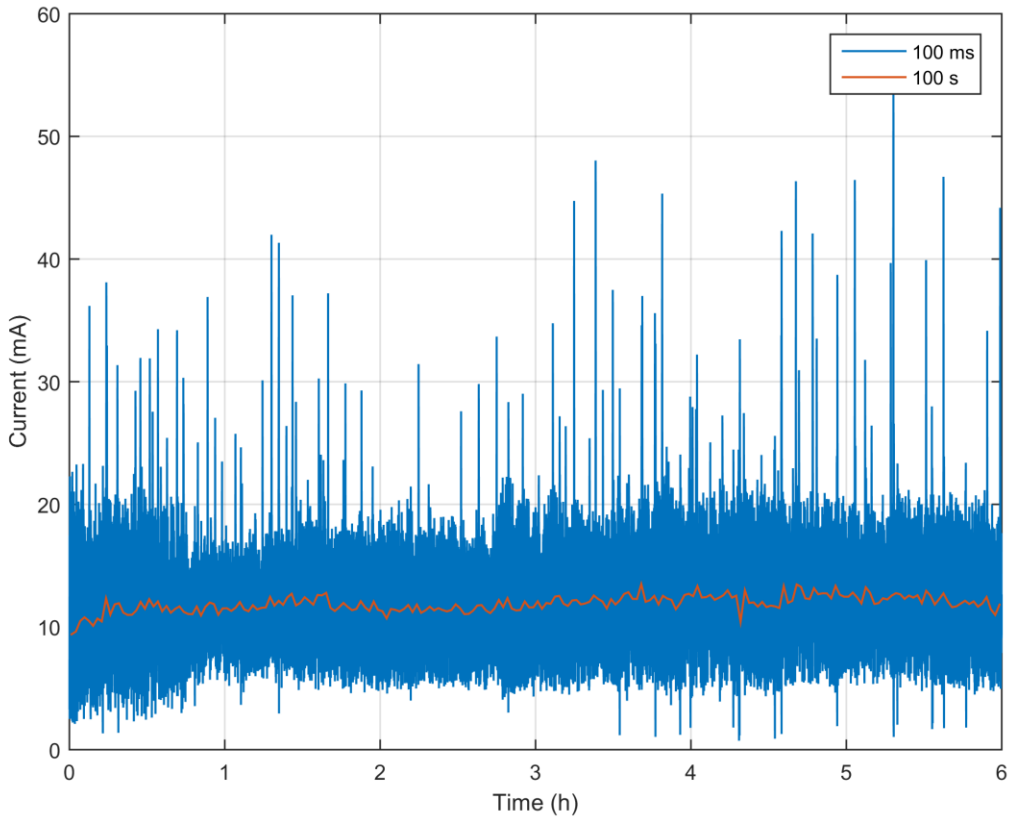

Figure 4-35: Leakage current for AC test

The leakage current of 4.5 kV AC was recorded for the entire 6-hours of the test. As can be seen in figure 4-35 the AC leakage current does not show any notable increasing or decreasing trend during the electrical test. The current shows a series of short time peaks separated by longer intervals and did not show any noticeable physical deterioration on the surface of the insulator. The erosion and tracking length depends on the stability of the leakage current over a prolonged time, which was in the range of 11.9 mA with the highest peak leakage current recorded as approximately 57.00 mA. The discharge activity could reach approximately 38.05 mA.

The discharge activity does not necessarily affect the leakage current. The leakage current is caused by the conduction through the liquid ammonium chloride contaminant and surface material. It is also observed that there was also a gradual increase of the average AC leakage current, an indication that the surface resistance of the insulator was decreasing. It is reasonable to assume that the AC leakage current would continue to increase until the gap is permanently made a short circuit between high voltage electrode and the ground electrode. According to the study by Khaaiye et al [31] pointed out that the leakage currents that cause aggressive erosion and tracking are in the range of 20 - 25 mA because of the effectiveness of current pulses.

4.3.2.4 **Summary**

From table 4-4 an average leakage current of 10 ± 2 mA was recorded for both +DC, -DC and AC test. The magnitude of the +DC leakage current was lower than that of the AC and showed a consistently steady trend for the 6-hour duration of the test. The +DC test would be expected to have a higher leakage current, however the configuration of the measurement system used removed the DC component of the current. The AC test showed the highest average value of leakage current. The leakage current under –DC is less as compared to +DC.

Table 4-4: Leakage currents results

Voltage type	I_{ave}(mA)	I_{max}(mA)
+DC	9.40	41.32
-DC	8.92	39.9
AC	11.9	57.03

Heger et al. [30] reported that under +DC the average hourly rms leakage current where higher compared to AC voltage, which was the case in this investigation. In addition, the –DC application resulted in the lowest leakage current measurements for all the test samples, which was similar to this work. Bruce et al. [24] also found similar results, the +DC tests gave higher peak leakage current and greater material damage and eroded mass than –DC at the same voltage magnitude. Results of the studies by Vas et al. [28] compared the currents under +DC and –DC, it was found that the leakage current for +DC is much higher than that under –DC. These results have shown a correlation between the rms leakage current and material degradation of the insulator material. An increased leakage current would lead to higher surface heating, higher temperature and hence a higher erosion for the same surface profile as suggested by Vas et al.

4.4 Post Testing – Material Analysis

The extent of erosion and tracking of SIR composite insulator was further analysed by looking at different techniques that study the surface degradation of polymer occurring during aging. It is known that tracking and erosion induced by high electrical stresses reduce the lifetime of SIR insulator [49].

A quantitative approach to how SIR reacts to high voltage application is of paramount importance. Surface electrical discharging on SIR composite insulator ultimately results from the build-up of leakage current. In this situation, the polymer material can undergo various chemical reactions leading to deterioration of mechanical and electrical properties. One method of degradation is the formation of a carbonaceous conducting path on the surface of the insulation, due to heat generated by discharges.

Looking at the chemical composition of SIR, silicones are polymers constructed from inorganic and organic monomers. The chemical formula for silicones is $[R_2SiO]_n$, where R is an organic group such as an alkyl (methyl, ethyl) or phenyl group. The organic side groups can be used to link two or more of these –Si-O- backbones together. The most common silicone is polydimethylsiloxane (PDMS), contains two methyl groups (CH_3) for every silicone. The dry band arcing on the surface causes very largely, temperature increase on the surface of SIR sample, and the heat generated can cause degradation reactions at the surface [49]. Figure 4-36 shows the chemical reaction when silicone reacts with a high voltage supply.

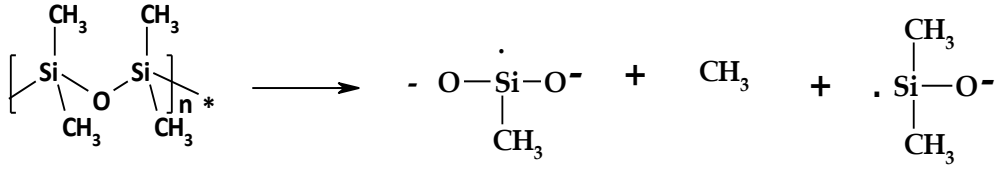

Figure 4-36 : Silicone reaction with a HV supply [49]

The chemical reactions include:

- Chain scission,
- Oxidation of hydrocarbon groups,
- Hydrolysis of siloxane bonds and hydrocarbon groups,
- Crosslinking of siloxane bonds, and
- Interchange of the chain.

The heat can cause scission of CH3 groups from Si in PDMS chain and polymer backbone of PDMS and produces free radicals (.Si, .O and CH_3). These radicals can react together from the effect of the heat from dry band arcing to form short chain backbone polymer (particles/residues). Residues carbon atoms are a source of carbonaceous tracks. Si-OH groups and H_2O produce ionic conduction paths that caused tracking. The physiochemical analysis that has been used for the post-aging analysis of the samples included Fourier Transform Infrared (FTIR), Transmission Electron Microscope (TEM) and Scanning Electron Microscope (SEM) with Energy Dispersive Spectroscopy (EDS).

4.4.1 Fourier Transform Infrared spectroscopy (FTIR) Analysis

FTIR is a standard technique used in the identification of a particular organic material chemical composition or bonding present. Residues were fractured off the test samples. These were centrifuged to concentrate them.

The typical characteristics of IR absorptions bands for high-temperature vulcanized silicon rubber are shown in Table 4-5, where the wave numbers for corresponding bonds are given.

Table 4-5: Characteristics IR absorption bands in silicones [50]

Wave numbers ($\mathbf{cm^{-1}}$)	**Bond**
3700 – 3200	OH
2962 – 2960	CH in CH_3
1440 – 1390	CH_3 in Si-CH_3
1280 – 1240	Si-CH_3
1100 – 1000	Si-O-Si
870 – 850	Si$(CH_3)_3$
840 – 790	Si$(CH_3)_2$
700	Si$(CH_3)_3$

Figure 4-37 shows a spectra of virgin (unaged sample), referred to as the control sample. The infrared waveform depicts the absorption bands that illustrates the identity of the molecular components and structures. The spectra for silicon rubber sample is in the range from 400 - 4000 cm^{-1}. The peak at 3400 – 3600 cm^{-1} indicates the presence of OH groups. It is known that O-H bonds in the infrared band are the by-products of aging and are formed instead of CH_3 groups. These hydroxyl groups absorb moisture near the surface of the surrounding and cause reduction in hydrophobicity of the polymeric materials [8]. The control sample show different characteristic absorption bands. The control sample is showing the characteristic of O-H stretching peaks between 3200 and 3600 wavenumbers (w/n), C-H stretching below 3200 and Si-C stretching between 1400 and 1000 wavenumbers (w/n).

A clear depiction of the regions that were damaged and burnt during the 6-hour test is highlighted in the FTIR results in figure 4-38 under -DC. Peaks in the range of 400 to 3200 wave number range attenuation are seen. The attenuation degree of –OH bonds is greater for the +DC test sample because of the severity of leakage current and discharge activity which cause depletion of filler material. Some degree of damage is observed in the –DC and AC test samples.

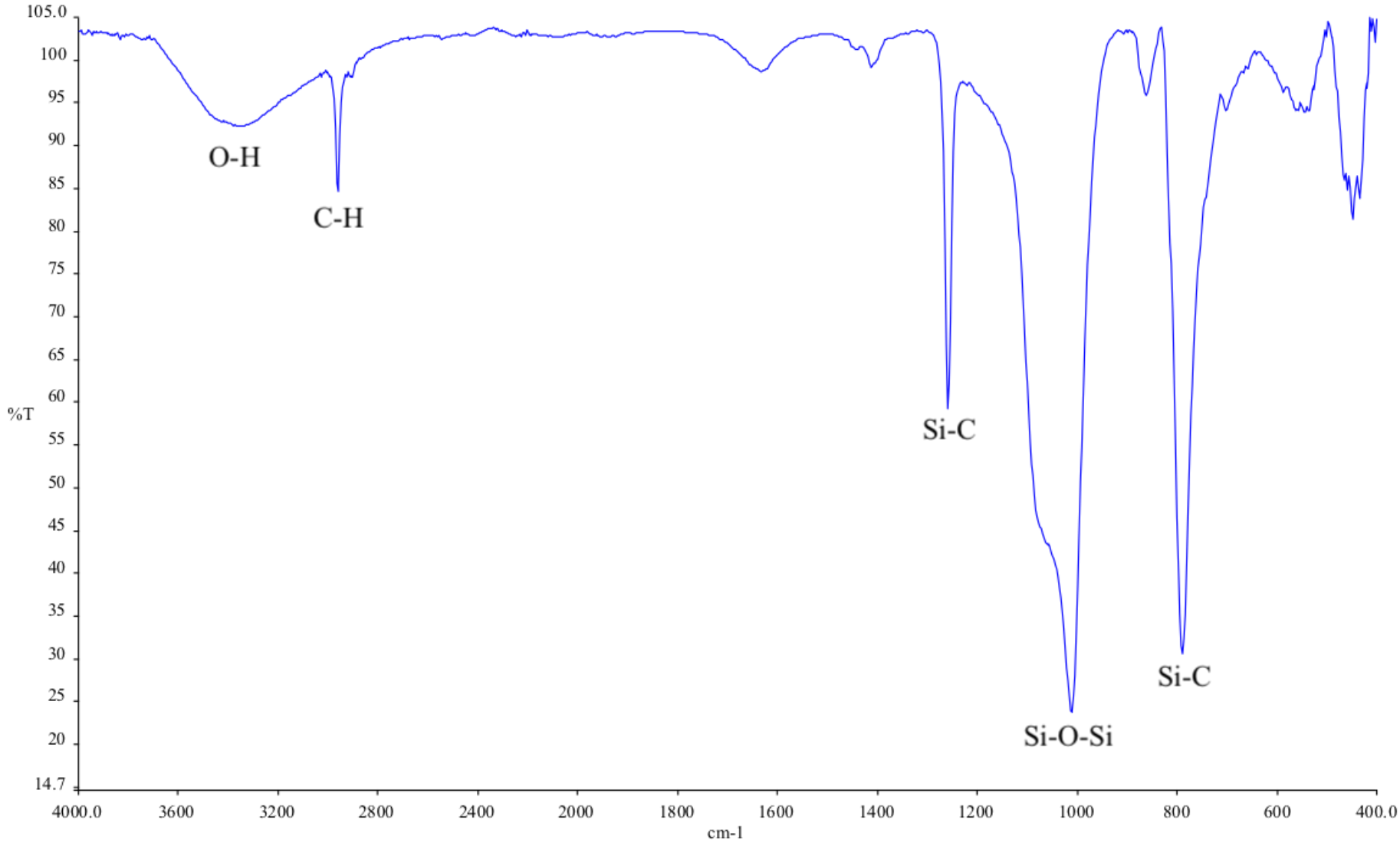

Figure 4-37: FTIR – control sample

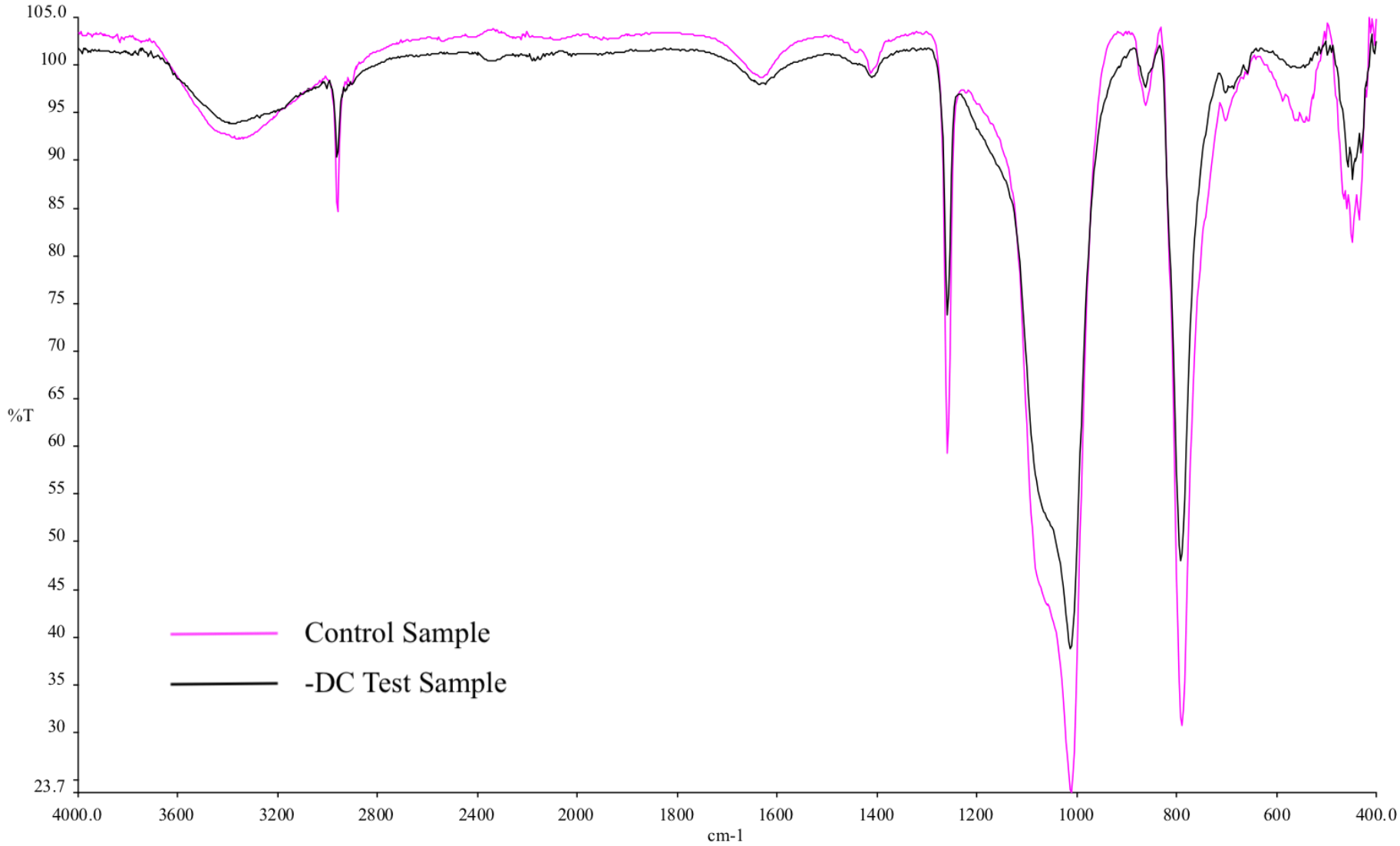

Figure 4-38: FTIR – Control sample and Negative DC test sample

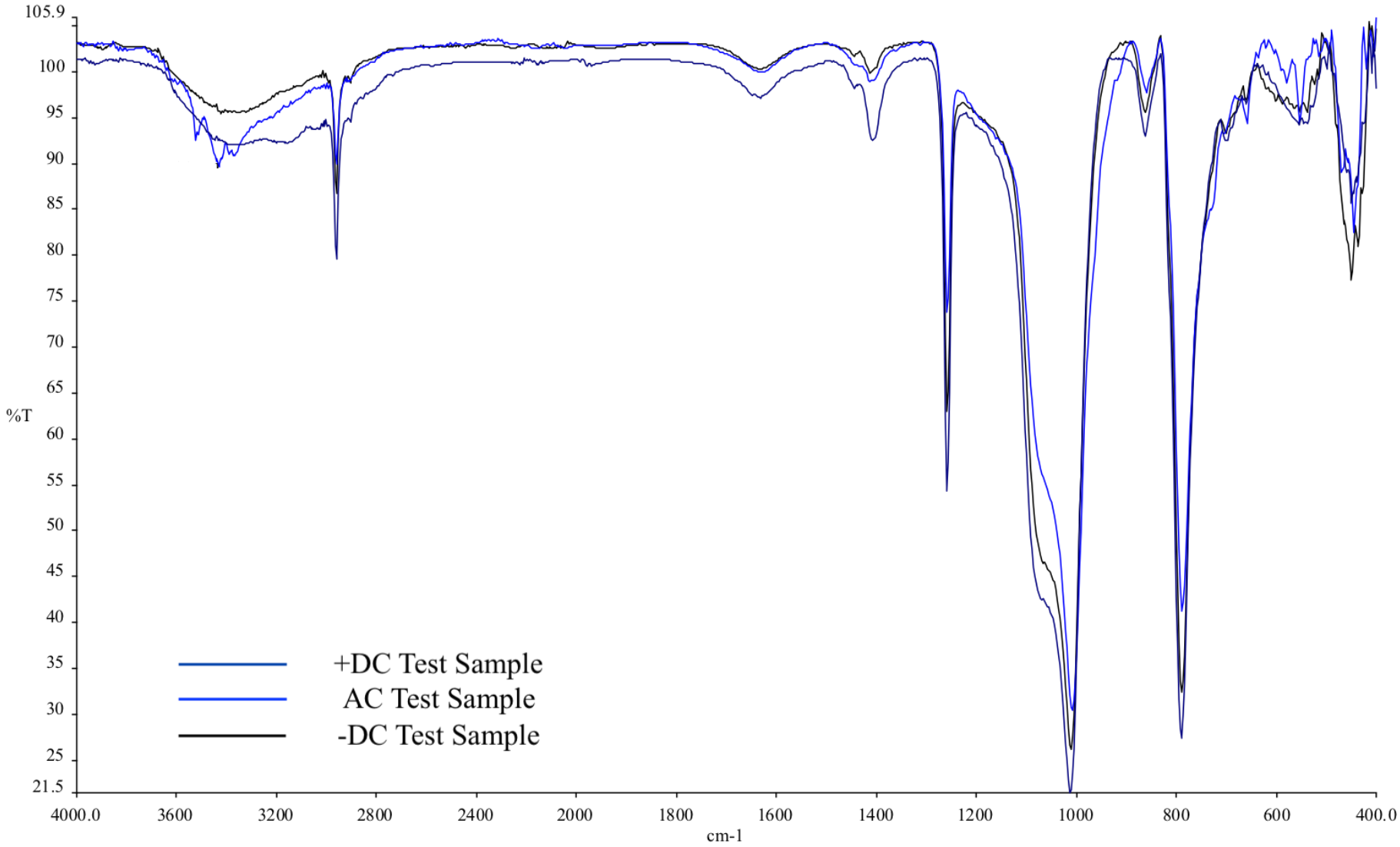

Figure 4-39: FTIR –+DC (navy),-DC (black) and AC (blue) test sample

The absorption bands characteristics shown in figure 4-38 the Si-O bonds is in the range of 1200 to 400 cm^{-1} under -DC. The peak at 2962 cm^{-1} is due to C – H stretching bond in CH_2 and CH_3. In figure 4-39 there is almost a similar pattern with the control sample. The peak at 1340 cm^{-1} is due to the deformation of CH in Si-CH_3. The assumption was that the silicone rubber lost moisture during testing because of the large amount of heat that was produced as suggested by Mahatho et al [33]. The relative intensities of Si-CH_3, Si $(\mathrm{CH}_3)_2$, C – H and Si-O-Si were found to diminish after recovery compared to the control sample.

Figure 4-39 shows the absorption spectrum of ±DC and AC test samples. The spectrum recorded showed little distinctive absorption peaks as compared to that of the control sample. The +DC test sample was more damaged as compared to the –DC and AC test samples. The dry band arcing for silicon rubber occurs when the hydrophobicity of the silicone is temporarily lost. The peaks in the range 1400 cm^{-1} to 400 cm^{-1} depict the damaged areas, as there are C-O and Si-CH_3 stretching which indicate a separation of the bonds. However, under polluted and wet conditions a conductive wet layer covers the insulation materials. The absorption peaks for +DC, –DC and AC test samples appear the same. This analysis confirms with Khaaiye et al [31] [45], as the waveforms bare similar characteristics. Khaaiye et al. showed that the chemical composition of silicone rubber samples under AC and DC tracking cause almost similar degradation, C-O and Si-CH_3 bonds stretching. The peak intensity of most of the bonds such as Si-C, Si-O, C-H and Si-O-Si were reported to be not much. Hence, there was no distinction in their absorption peaks between aged and un-aged samples. Mahatho et al [33] analysis also reported similar results that there were no visible differences from the control spectra comparing 4.5 kV, 6.3 kV positive and - DC tests.

4.4.1.1 **Summary**

FTIR analysis proved to be helpful in getting the understanding of the chemical properties of the samples and as well identifying the functional groups of the polymeric insulator silicon rubber. The samples particles collected for +DC, -DC and AC test were evaluated quantitatively. A control sample spectrum was used as a reference point by comparing deviations of attenuation of absorption peaks under +DC, -DC and AC. The spectrum showed distinct peaks in the range of 400 – 4000 cm^{-1}.

The width and intensity of the peaks produced in the spectrum are dependent on the material composition, shape, and size of molecules. Absorption peaks were obtained at 450, 795, 1000, 1350 and 2900 cm^{-1} for all samples +DC, -DC and AC. These vibrational peaks each corresponding to a particular bond. The sharp peak at 788 cm^{-1} is due to the stretching vibrations of Si $(\mathrm{CH}_3)_2$. The high peak seen on the spectra especially under +DC is a result of high temperatures of approximately 900 °C. It was noted that the peaks at 2800 cm^{-1} and 3100 cm^{-1} refer to CH stretching mode, caused much damage under +DC. Alkane's vibration stretch caused peaks at 1350 cm^{-1} causing discharges and damage of bonds due to leakage current. Overall, similar characteristics were depicted by +DC, -DC and AC silicone rubber samples in terms of their absorption peaks. The infrared spectra is an effective tool to use in determining absorption bands for polymeric insulating materials.

4.4.2 Scanning Electron Microscopy (SEM) with Energy Dispersive Spectroscopy Analysis

SEM images provide qualitative information of the type and extent of surface degradation. It helps to see the level of roughness due to the erosion and the micro-cracks created as a result of the discharges. The tested samples were firstly cleaned thoroughly with distilled water and centrifuge the samples to concentrate them. The electron microscope inspects topographies of test samples at very high magnification. The energy dispersive spectroscope (EDS) was part of the analysis, to show the elemental composition of the samples. Periodic elements were found in the fractured samples. The analysis was carried out for the +DC, -DC and AC test samples.

4.4.2.1 **Positive DC test Sample Analysis**

Figure 4-40 shows the scanning electron microscope microphotograph of +DC test sample. The overall magnitude of damage on the surface due to tracking can be seen below. The SIR sample appear to have a finer and smoother surface particles arrangement. The distribution of the sample surface seems to be evenly spaced. The surface became hard and brittle with a loss of its original colour. Larger cracks appear to be visible on the surface of the test sample.

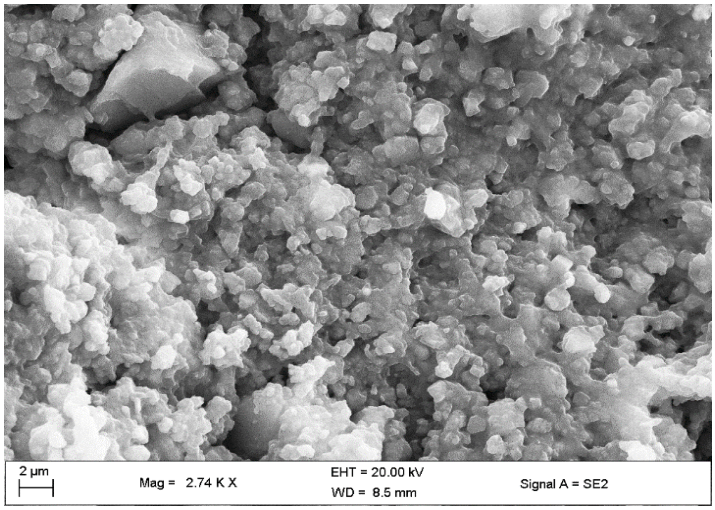

Figure 4-40 SEM – Positive DC test sample image showing the effect of tracking

Carbon (C), oxygen (O), chromium (Cr), aluminium (Al), magnesium (Mn), iron (Fe), and silicon (Si) are the elements that were detected on the sample surface by EDS. The Si and O detected in the X-ray counts originate from (Si-O-Si) backbone of the silicone polymer. The Al was detected due to the presence of alumina trihydrate (ATH). The composition of Al is seen to be higher than other elements. The Cl detected was obtained from the contaminant solution ammonium chloride ($\mathrm{NH_4CL}$) reaction. Electrode corrosion resulted in iron (Fe) elements present on the sample surface. The elemental compositions results are presented in Figure 4-41.

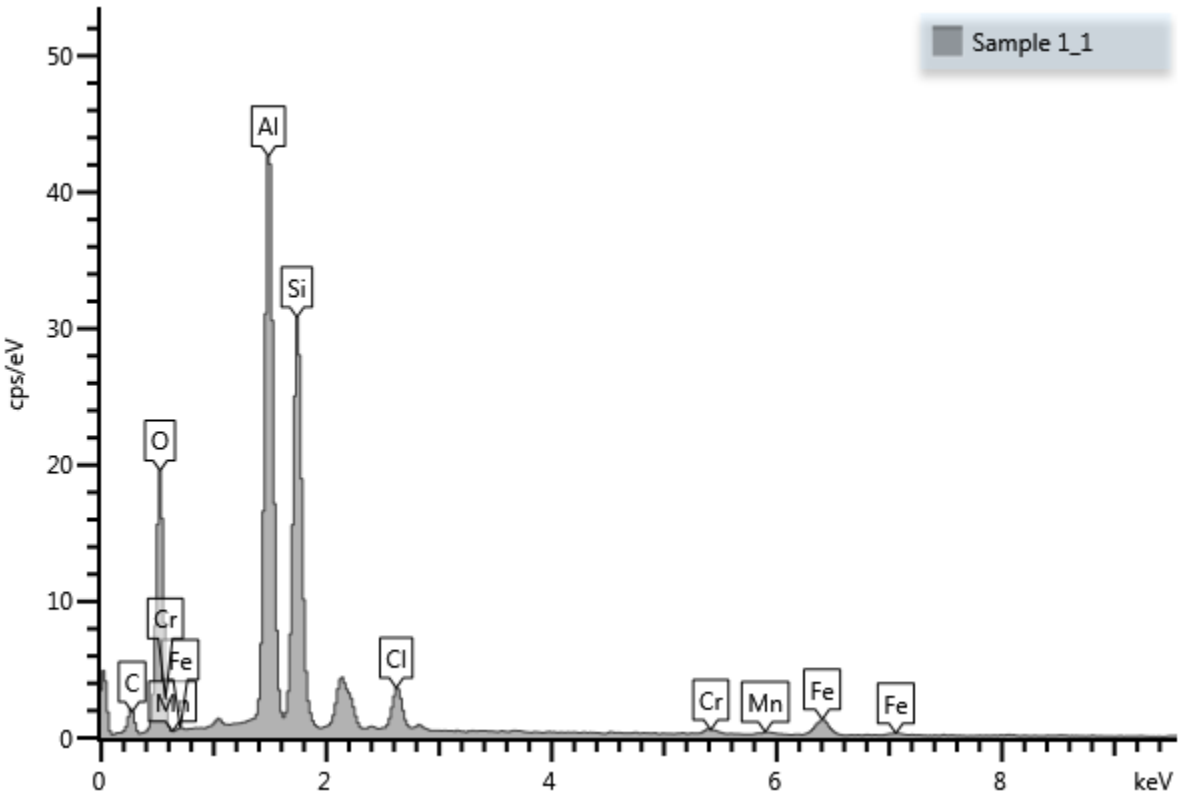

Figure 4-41: EDS – Positive DC test sample

4.4.2.2 **Negative DC test Sample Analysis**

It can be clearly seen in figure 4-42 that the surface shows more valleys and hills and it appear to be rough as compared to the +DC, AC samples. The morphology changes of the surface of silicone rubber samples due to tracking were evident from SEM images.

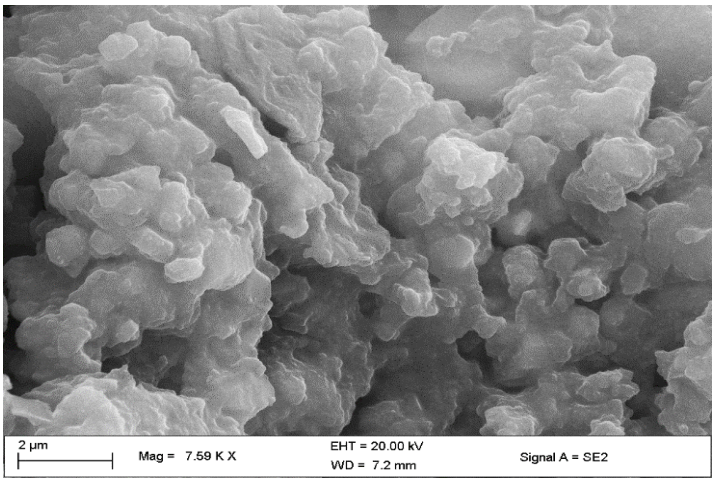

Figure 4-42: SEM – Negative DC test sample

The EDS detected similar elements as were found under +DC. Figure 4-43 shows the elemental compositions spectrum consisting of Si, Al, 0, C, Cr, Al and Fe. The spectra show lower intensity of Al and higher intensity of Si, which is not the case as compared under +DC, on the surface of the SIR sample.

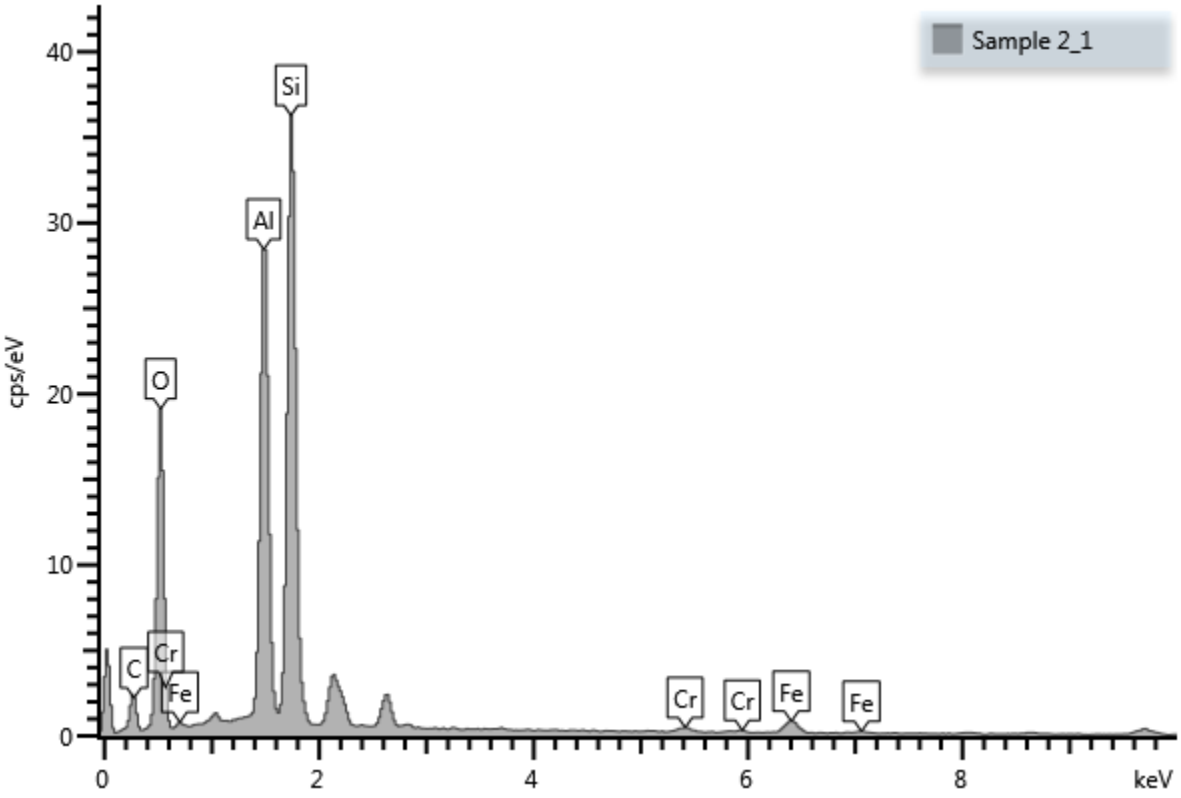

Figure 4-43 EDS – Negative DC test sample

4.4.2.3 **AC Test Sample Analysis**

It can be seen in figure 4-44 that the surface shows fewer valleys and hills and it is smoother than the +DC, -DC test samples. The eroded depth grooved in deeply. The even surface of the test sample helped in reducing the tracking depth.

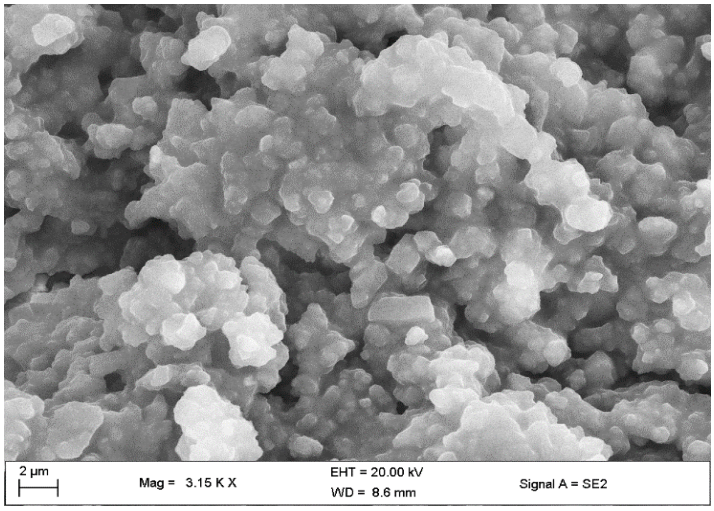

Figure 4-44: SEM – AC test sample

Figure 4-45 shows the elemental composition of the sample. The elements detected by EDS were the same as in +DC and –DC tests. A higher intensity of Al and Si are found as depicted by figure 4-43. Two additional small peaks of calcium (Ca) appeared only in the spectra, originated from traces in the contaminant solution. There is an increase of O from Si-O-Si.

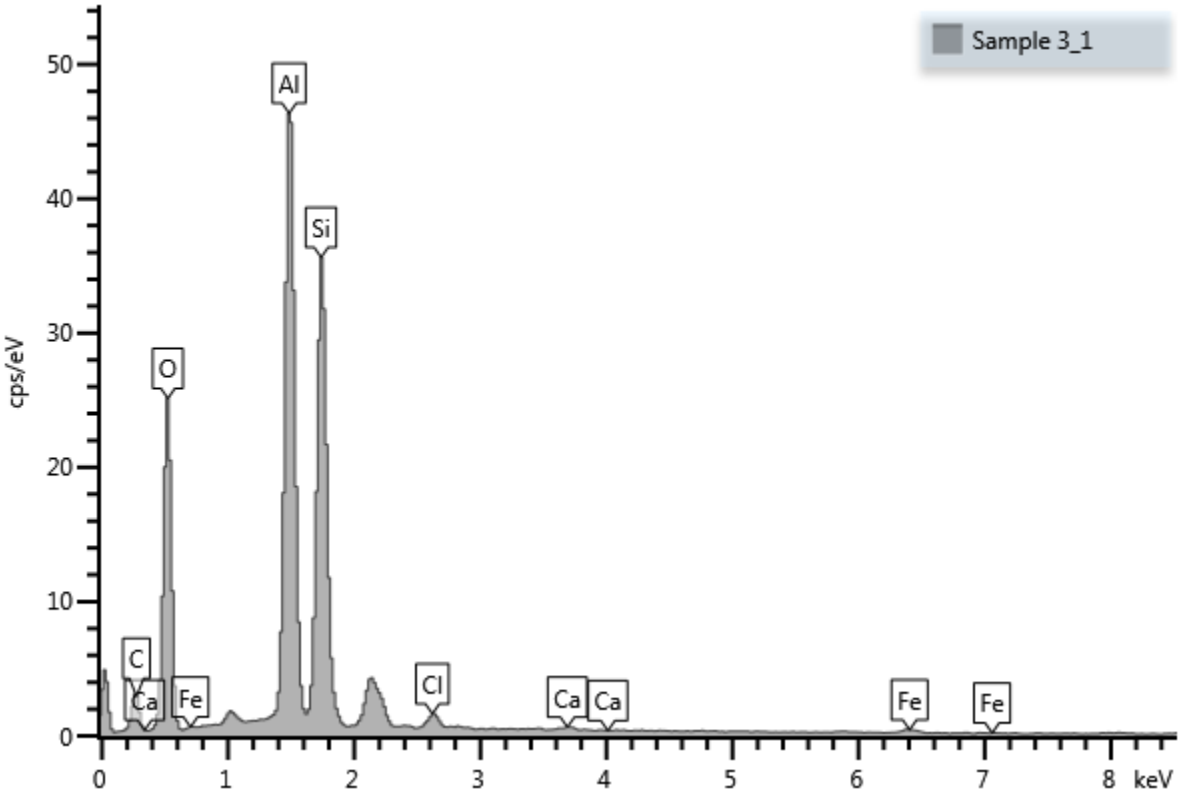

Figure 4-45: EDS – AC test sample

4.4.2.4 **Summary of SEM physiochemical analysis**

Table 4-6: EDS analysis comparison

Elements	Sample 1 – Positive DC		Sample 2 – Negative DC		Sample 3 - AC	
	Wt %	Wt % Sigma	Wt %	Wt % Sigma	Wt %	Wt % Sigma
C	19.75	0.72	22.46	0.66	22.64	0.62
O	40.27	0.45	42.45	0.45	44.04	0.42
Al	18.79	0.21	13.70	0.16	17.09	0.18
Si	15.78	0.19	19.22	0.22	14.98	0.16
Cl	2.09	0.06	-	-	0.61	0.03
Ca	-	-	-	-	0.14	0.03
Cr	0.54	0.06	0.45	0.06	-	-
Mn	0.26	0.06	-	-	-	-
Fe	2.52	0.09	1.72	0.08	0.49	0.06
Total	100.00		100.00		100.00	

It can be seen in Table 4-6 that for the +DC test sample there are higher presence of iron (Fe) with 2.54 % as compared to –DC test sample with 1.72 % and AC test sample with 0.49 %. The oxygen concentration reduced for all the samples and again +DC test sample lost most oxygen. The test sample under +DC have lower carbon, oxygen silicon concentration compared to –DC and AC test samples. +DC test sample show a higher concentration of aluminium compared to –DC and AC. The corrosion of the electrodes was highest in the +DC test thereby causing more iron content. There is a great severity of DC dry band arcing compared with AC, and it has been attributed to causing more corrosion of test electrodes. Electrode corrosion is seen to be the dominant factor according to the graphs as it shows an indication of the extent of test sample degradation. The decrease in oxygen concentration in +DC was due to high temperatures which resulted in ATH filler to dehydrate as suggested by Khaaiye et al [32] [45] [31]. FTIR results showed that the sample under AC retained its bond water, did not vaporise completely therefore traces of Ca were detected originating from water. The intensity of dry band arcing determines the extent of erosion depth of a test sample controlled by how high the leakage current is. SEM showed the magnitude of damage on the surface of the samples. +DC had larger cracks that were visible on the sample surface. –DC sample showed more valley and hills on the surface compared to +DC and AC samples. AC sample surface showed fewer valleys and hills, and appeared to be smoother compared to +DC and –DC samples. This is in agreement with EDS and FTIR results that +DC cause a higher tracking and erosion than –DC and AC. The morphological changes of the surface of silicone rubber insulation samples due to tracking were evident from the SEM images and EDS analysis.

4.4.3 Transmission electron microscope (TEM) Analysis

TEM is a powerful tool for directly imaging nanomaterials to determine particle size and shape. It is a quantitative measure of particle or grain size, size distribution and morphology as shown by the images for the +DC, –DC and AC test samples. The imaging has a higher resolution of a factor of about 1000. The images captured in this dissertation were zoomed approximately in the range of 200 nm to 500 nm. In order to obtain high-quality images, test samples were cleaned thoroughly with distilled water and were fractured through the damaged area using a razor blade. The fractured samples were mixed with ethanol in small tubes. They were allowed to cool at room temperature. The samples were mounted on stubs and analysed afterwards following conventional procedures. Images of particle sizes and size distribution were captured.

In this study TEM was used to characterize the dispersion of the particles within the silicone rubber composite material. The intent was to find information about each sample surface topography and composition for the tested samples. The electron microscope produces images of a particular sample by scanning it with a focused beam of electrons. TEM can achieve resolution better than 1 nm. This material analysis provides vast valuable information on SIR sample, which make it possible for comparison of the +DC, -DC and AC test samples composition. The TEM produced very high-resolution (200 nm to 500 nm) images of different sample surfaces.

4.4.3.1 **Positive DC Test Sample**

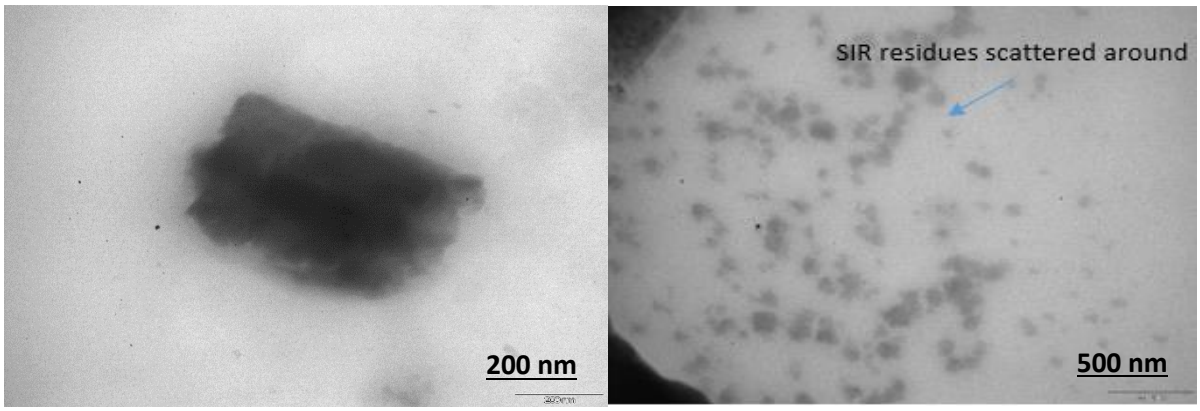

Figure 4-46: TEM – Positive DC test sample Images showing fractured particles (Resolution 200 nm to 500 nm)

TEM analysis in figure 4-46 shows the molecular structural changes on the surface of SIR insulator material. It shows the particles under high resolution to determine particle sizes and shape. It can be seen that the SIR particles are spread evenly around. Similar results were obtained by Lixian et al [43] showed that the particles sizes changed with time and the rubber matrix is influenced by vulcanization rate, which depend on the applied voltage. There are large agglomerates in the image suggesting that the SIR material eroded immensely. That is an indication that deterioration of the test sample has taken place. Aging of the sample revealed some physical changes on the surface.

4.4.3.2 **Negative DC Test Sample**

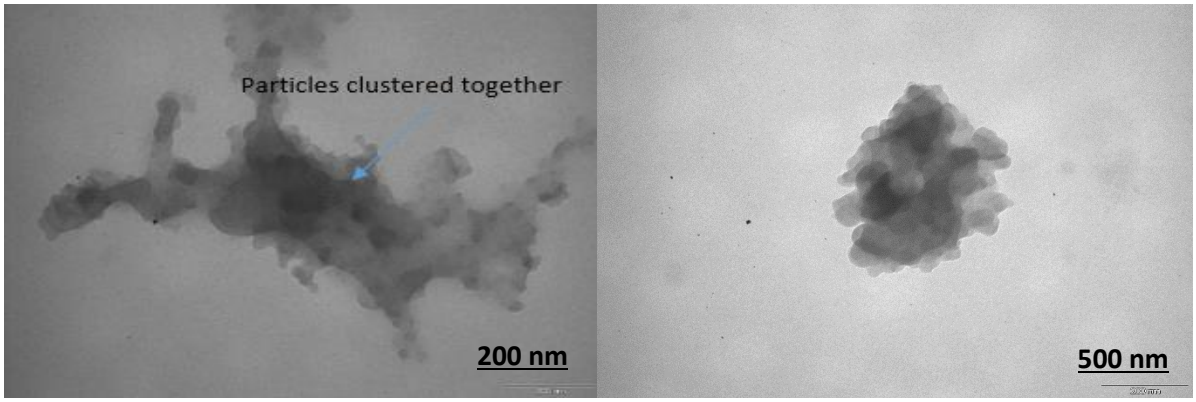

Figure 4-47: TEM – Negative DC test sample images (Resolution 200 nm to 500 nm)

Figure 4-47 shows the –DC test sample particles observation. The arrangements of the particles are seen to be more clustered together. Under –DC the erosion was not aggressive as compared to +DC. It was also observed that they appear to be transparent under a high-resolution microscope. This analyse the distribution of particle size under –DC and the dispersion is very important to see the consistent properties of the silicone rubber particles.

4.4.3.3 **AC Test Sample Analysis**

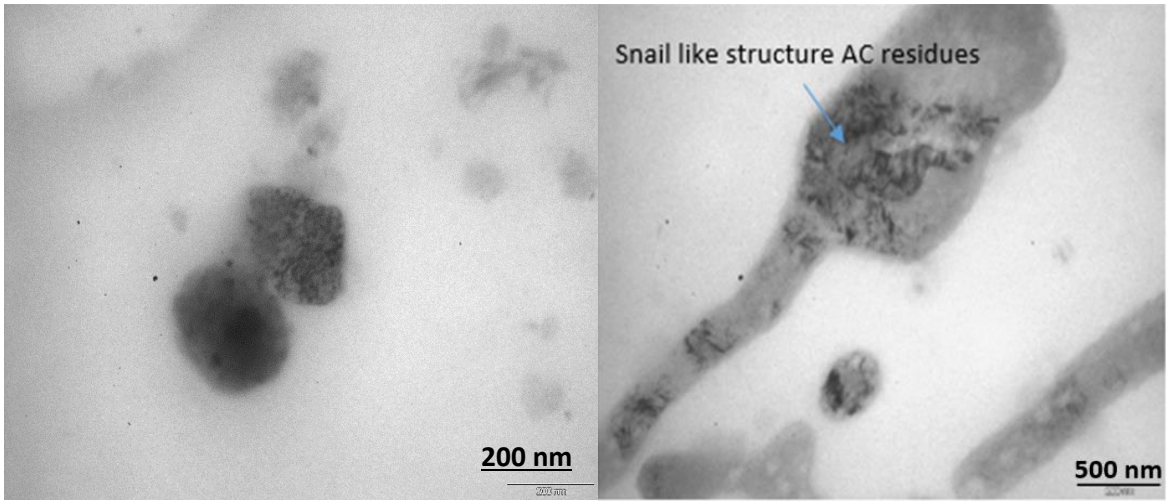

Figure 4-48: TEM – AC test sample (Resolution 200 nm to 500 nm)

The SIR particles appear to be snail like under the high-resolution microscope (200 nm) as shown in figure 4-48. The interfacial tension of the SIR particles is present. The analysis is providing information in real space, showing the spatial distribution of SIR residues. The silicon particles are composed of elements such as Si, O, C, H and N, detected by EDS in the previous section. Hence, they appear darker in bright-field images. The organic particles are seen to be particularly small and refined which indicated that they were less erosion under AC as compared to +DC and –DC test.

4.4.3.4 **Summary of TEM analysis**

From the above results, it was concluded that silicone rubber organic particles were uniformly dispersed in the rubber matrix. Under +DC individual silicone rubber surface particles were observed to be scattered around. Under –DC the particles are bound together and have an irregular shape. Furthermore, the silicone rubber surface residues appear to be snail-like under the high-resolution microscope under AC test voltage. The morphology of the silicon rubber interphase matrix was almost spherical.

The particles sizes were measured before the testing to be in the range of 6 nm to 26 nm, having an average size of around 18 nm. Under –DC the residues were almost transparent, very small with the size of 4 nm to 8 nm. Under +DC the particles sizes were measured to be between 5 nm to 9 nm. Under AC test voltage the particles were in the range from 2 nm to 5 nm. The extent of erosion was compared by looking at the particles sizes and shape. Bhat et al. [42] investigated the use of red mud as a reinforcing material in the polymer matrix and they found similar characteristics of particles showing agglomeration in some parts of the composite films. They showed that the average particles sizes decreased which suggested evidence of material damage. It can be concluded that the erosion seemed to be more aggressive under +DC because of how scattered the particles looked. The erosion was moderate under –DC test and AC test.

4.5 Conclusion of the Results

There were significant differences in the performance of silicone rubber under +DC, -DC and AC tests voltages. In all the test carried out, tracking was evident. Visual tests showed that HTV silicone rubber deteriorated after the 6 – hour inclined plane test. The +DC test sample appeared to be the most degraded followed by – DC test sample and least AC test sample. A higher mass loss reduction erosion of 0.84 g was obtained under +DC test samples. A better performance of silicone rubber was obtained under the – DC test sample. Impressive performance under AC test sample were observed with a lower mass loss of 0.45 g. The leakage current did not correlate with the visual test results due to the measurement system configuration. The leakage current results showed a lower magnitude of 9.40 mA under +DC voltage, compared to 11.90 mA under AC voltage. The leakage current of 8.92 mA was recorded under – DC voltage which was less than +DC voltage. The +DC voltage would be expected to have a higher leakage current because of the severity of material damage concurred. Post aging analysis showed the changes of HTV silicone rubber matrix morphology and surface roughness after the voltage application. FTIR graphs showed little distinction of absorption peaks between the aged and un-aged samples. The damaged areas where depicted to have C-O and Si-CH_3 functional groups stretching which indicated a separation of the bonds. The peak intensities of bonds such as Si-C, Si-O, C-H and Si-O-Si were almost similar under all the tests voltages. SEM together with EDS analysis showed that there was severe tracking and erosion under +DC test samples as compared to – DC and AC test samples, and it correlates with the visual tests. SEM micrographs showed rough surfaces with larger cracks under +DC test sample. – DC test sample showed what appeared to be valleys and hills on the silicone rubber surface. AC test sample surface showed fewer valleys and hills, and had smoother surface. EDS showed a higher presence of iron under +DC test voltage. The higher iron content was due to the excessive corrosion of electrodes which occurred under +DC voltage application. TEM analysis showed that the particles under +DC test sample were more scattered around as compared to – DC and AC test samples, which suggested severe material damage after the tests.

CHAPTER 5: CONCLUSION

5.1 Conclusions

The objective of this research was to evaluate and analyse the relative performance of polymeric SIR insulator material. The inclined plane test was used to compare and contrast HTV silicone rubber insulator material resistance to tracking and erosion under HVDC and HVAC. IEC 60587 standard was used to conduct the work as the guideline. Some contradictions were raised and a critical analysis was presented based on the available literature. A quantitative analysis was also presented in a systematic manner, elaborating the silicone rubber morphology after undergoing incline plane conditions.

- IEC-60587: 2007 standard recommends testing of one sample at a time as this reduces the voltage drop during the entire period of the test as was observed. Under AC, the leakage current was captured to be higher resulting in aggressive, audible and frequent arcing, it was observed to cause little physical damage. The plotted graph for AC showed that the average leakage current of 11.90 mA increased gradually.

- DC leakage current was seen to be slightly lower than that of AC under the same applied voltage of 4.5 kV. The plotted graph again showed that there was a steady increase in the average leakage current with time for +DC. This implies that the surface resistances of silicon rubber test sample gradually decreased. The steady trend also meant that aggressive tracking and erosion was taking place. It was observed that the inclined plane test under +DC voltage at some point became an open circuit immediately after the test sample stopped arcing.

- Comparatively, Minimal erosion was observed in –DC voltage testing with associated longer discharges activities as compared to +DC and AC. The –DC discharges were elongated towards the high voltage electrode and become more randomly scattered.

- During the tests carried out different temperatures were recorded, hence it was observed that the performance of silicon rubber was affected. The maximum temperature was measured to be more than 250 °C using a FLIR camera. Silicon rubber materials perform better not just because they are more resistant to discharges, but because of the change of nature of moisture flow due to varying temperatures. The highest hydrophobicity loss was experienced in all the test voltages. It was observed that after washing the test samples hydrophobicity was recovered, but during the test, it was lost. It was noted that an un-energised sample recovered hydrophobicity if left for a longer time under test.

- The same comparable results were also found under quantitative analysis. The physiochemical results confirmed with the visual observations results that the +DC voltage causes a greater material damage than AC. The characteristics of HTV silicon rubber under +DC, -DC and AC were compared looking at the functional group's absorption peaks with FTIR analysis. FTIR data showed little distinction between the aged and un-aged samples. EDS showed the elemental composition of the samples. SEM showed test samples having more cracks and a rough surface under +DC than in AC and -DC where smooth surfaces where observed. TEM analysis showed notable differences between DC and AC voltage, by characterizing the

dispersion of the particles within the silicone rubber composite material. The texture of the test samples was observed to be finer in +DC as compared to –DC and AC.

5.2 Recommendations for Future Studies

They are some unidentified uncontrollable variables responsible for the scattering of the results in the inclined plane test. Listed below are improvements which can be done in future;

- The liquid ammonium chloride contaminant flow sometimes deviates from the centre of the test sample, causing it to flow at the edge of the surface sample. This affect the tracking and erosion as the degradation will concentrate at one spot along the edge. An infrared laser can be applied as an alternative procedure.

- A great number of SIR test samples could be used when conducting a statistical analysis in future when expanding on outdoor polymeric insulation materials in order to obtain credible results.

- In every test, it can be proposed to use new a set of electrodes. They tend to wear out due to electrolysis later polluting the liquid contaminant solution. When manufacturing electrodes for IPT water jet cutting or laser cutting can be used as alternatives methods.

- An optical instrument can be used to measure the erosion depth precisely rather than mechanical methods prescribed in the work.

- It was observed and concluded that SIR supports an applied 4.5 kV tracking voltage with low erosion levels. Precise conclusions can be obtained if additional analysis on the mechanical, physical and chemical are carried out such as design failure analysis, hydrophobicity and aging tests. They can be of paramount importance in the electrical insulation of power systems.

CHAPTER 6: REFERENCES

[1] IEC-60587, “Electrical Insulating Materials Used Under Severe Ambient Conditions,” in *Test Methods for Evaluating Resistance to Tracking and Erosion*, 5, 2007.

[2] R. A. Ghunem, S. H. Jayaram and E. A. Cherney, “Inclined plane initial tracking voltage for AC,+ DC and-DC,” in *Electrical Insulation (ISEI), Conference Record of the 2012 IEEE International Symposium on Electrical Insulation*, San Juan, PR, USA, 2012.

[3] Du, B. X., L. Yang, J. W. Zhang and Y.Gao, “Dynamic behavior of space charge in epoxy/metal-oxide nano-composite,” in *Electrical Insulating Materials (ISEIM), Proceedings of 2011 International Conference on Electrical Insulating Materials*, Kyoto, Japan , 2011.

[4] G. Arshad , M. Momen and A. Nekahi, “Properties and applications of superhydrophobic coatings in high voltage outdoor insulation,” *IEEE Transactions on Dielectrics and Electrical Insulation,* vol. 24, no. 6, pp. 3630 - 3646, 2017.

[5] Buontempo, Rodolfo Cardoso and Dellallibera, Adriano A and Costa, Eduardo C Marques and Pissolato, Darcy Ramalho and Mei and Lucia Helena Innocentini, “Electrical assessment of commercial 6.0-kV HTV silicone rubber for power insulation,” *Measurement,* vol. 89, pp. 114--119, 2016.

[6] K. Papailiou and F. Schmuck, “Silicone composite insulators: materials, design, applications,” in *Power Systems*, Switzerland, Springer Science & Business Media, 2012, pp. 2--24.

[7] M. Amin, . M. Akbar and M. Salman, “Composite insulators and their aging: An overview,” *Science in China Series E: Technological Sciences,* vol. 50, no. 6, pp. 697--713, 2007.

[8] M. Ali and R. Hackam, “Recovery of hydrophobicity of HTV silicone rubber after accelerated aging in saline solutions,” *IEEE Transactions on Dielectrics and Electrical Insulation,* vol. 16, no. 3, pp. 842--852, 2009.

[9] J. Reynders, I. Jandrell and S. Reynders, “Review of aging and recovery of silicone rubber insulation for outdoor use,” *IEEE Transactions on Dielectrics and Electrical Insulation,* vol. 6, no. 5, pp. 620--631, 1999.

[10] R. Sarathi and S. Chandrasekar, “Diagnostic study of the surface condition of the insulation structure using wavelet transform and neural networks,” *Electric Power Systems Research,* vol. 68, no. 2, pp. 137--147, 2004.

[11] W.-Y. Zhou, . S.-H. Qi, H.-Z. Zhao and N.-L. Liu, “Thermally conductive silicone rubber reinforced with boron nitride particle,” *Polymer composites,* vol. 28, no. 1, pp. 23--28, 2007.

[12] J. Looms, “Insulators for high voltages,” in *IET Power and Energy Series*, London, United Kingdom, Institution of Engineering and Technology, 2006, pp. 20 - 31.

[13] M. G. Danikas, “Polymer outdoor insulators,” *Acta Electrotehnica Napocensis,* vol. 40, no. 1, pp. 3--10, 1999.

[14] M. Ehsani, H. Borsi, E. Gockenbach, J. Morshedian and G. Bakhshandeh, “An investigation of dynamic mechanical, thermal, and electrical properties of housing materials for outdoor polymeric insulators,” *European polymer journal,* vol. 40, no. 11, pp. 2495--2503, 2004.

[15] ASTM-D2303, “Standard Test Methods for Liquid-Contaminant,” *Inclined Plane Tracking and Erosion of Insulating Materials..*

[16] S. Kühnel, S. Kornhuber, R. Bärsch and J. Lambrecht, “On the arc-resistance when tested with DC- and AC-stress by the example of silicone elastomers,” in *2016 IEEE Conference on Electrical Insulation and Dielectric Phenomena (CEIDP)*, Toronto, 2016.

[17] R. Gorus, E. Cherney and R. Hackam, “The AC and DC performance of polymeric insulating materials under accelerated aging in a fog chamber,” *IEEE Transactions on Power Delivery,* vol. 3, no. 4, pp. 1892--1902, 1988.

[18] B. Limbo, “Insulator Aging Tests with HVAC and HVDC Excitation using the Tracking Wheel Tester,” in *MSc Dissertation, University of Stellenbosch*, 2009.

[19] CIGRE-D1.27, “Feasibility Study for a DC Tracking and Erosion Test,” International Council On Large Electric Systems, March 2015.

[20] Y. Yin, X. Liang, Y. Zhou and X. Li, “Study of tracking wheel test method under DC voltage,” *Properties and Applications of Dielectric Materials, 2003. Proceedings of the 7th International Conference,* vol. 1, pp. 439--442, 2003.

[21] T. Kuroyagi, H. Homma, T. Takahashi and K. Izumi, “A fundamental study on the surface degradation of polymer insulation material in DC applications,” *IEEE Transactions on Electrical Insulation and Dielectric Phenomena ,* vol. 2, pp. 682 - 685 , 1998.

[22] M. Salama, M. Sallam and R. Bartnikas, “Effect of wheel speed on the tracking time in a rotating wheel-spray tracking test,” *IEEE transactions on power delivery,* vol. 9, no. 3, pp. 1217--1221, 1994.

[23] A. Gazzola, “Tracking wheel test for dc polymeric insulators,” in *UNIVERSITÀ DEGLI STUDI DI PADOVA*, 2011.

[24] G. P. Bruce, S. Rowland and A. Krivda, “Performance of silicone rubber in DC inclined plane tracking tests,” *IEEE Transactions on Dielectrics and Electrical Insulation,* vol. 17, no. 2, pp. 521 - 532, 2010.

[25] R. A. Ghunem, S. H. Jayaram and E. Cherney, “The DC inclined-plane tracking and erosion test and the role of inorganic fillers in silicone rubber for DC insulation,” *IEEE Electrical Insulation Magazine,* vol. 31, no. 1, pp. 12--21, 2015.

[26] M. Izadi, M. A. Rahman and M. Ab Kadir, “On the voltage and electric field distribution along polymer insulator,” in *Power Engineering and Optimization Conference (PEOCO), 2014 IEEE 8th International Power Engineering and Optimization Conference (PEOCO2014)*, Langkawi, Malaysia , 2014.

[27] G. P. Bruce, G. a. Rowland and A. SM and Krivda, “DC inclined-plane testing of silicone rubber formulations,” in *Electrical Insulation and Dielectric Phenomena, 2008. CEIDP 2008. Annual Report Conference on Electrical Insulation and Dielectric Phenomena*, Quebec, QC, Canada, 2008.

[28] J. V. Vas, B. Venkatesulu and M. J. Thomas, “Tracking and erosion of silicone rubber nanocomposites under DC voltages of both polarities,” *IEEE Transactions on Dielectrics and Electrical Insulation,* vol. 19, no. 1, pp. 91 - 98, 2012.

[29] J. Knauel, A. Wagner and R. Puffer, “DEVELOPMENT OF A MODIFIED INCLINED PLANE TEST FOR THE INVESTIGATION OF THE TRACKING AND EROSION BEHAVIOR UNDER DC STRESS,” in *19th International Symposium on High Voltage Engineering, Pilsen, Czech Republic*, 2015.

[30] G. Heger, . H. Vermeulen, J. Holtzhausen and W. Vosloo, “A comparative study of insulator materials exposed to high voltage AC and DC surface discharges,” *IEEE Transactions on Dielectrics and Electrical Insulation,* vol. 17, no. 2, pp. 513 - 520, 2010.

[31] S. F. Kaaiye and . C. Nyamupangedengu, “Comparative study of AC and DC inclined plane tests on silicone rubber (SiR) insulation,” *High Voltage,* vol. 2, no. 2, pp. 119--128, 2017.

[32] S. Khaaiye, “A COMPARATIVE STUDY OF DC AND AC INCLINED PLANE TESTS ON SIR MICRO-COMPOSITE INSULATORS,” *MSc Disseration, University of the Witwatersrand,* 2016.

[33] N. Mahatho, I. Jandrell, T. Govender and N. Parus, “Ageing of silicone rubber insulators under high voltage direct current: results of inclined plane testing and material analysis,” in *Proc. of the 18th Int. Symp. on High Voltage Engineering (ISH)*, Seoul, Korea, 2013.

[34] P. Ashitha and S. Ganga, “A STUDY ON TRACKING AND EROSION RESISTANCE OF SILICONE RUBBER DURING DC INCLINED PLANE TRACKING WITH UV RADIATIONS SUPER IMPOSED,” in *The 20th International Symposium on High Voltage Engineering*, Buenos Aires, Argentina, 2017.

[35] P. Biswas, S. Ganga, M. Naskar and M. G. Veena, “RESISTANCE TO DC TRACKING AND EROSION OF UV AGED SILICONE RUBBER INSULATOR,” in *International Conference on High Voltage Engineering and Technology (ICHVET-2015)*, 2015.

[36] . J.-Y. Heo, H.-G. Cho and L.-Y. Soon, “A Comparison of AC and DC surface discharges characteristics for silicone rubber,” in *Condition Monitoring and Diagnosis (CMD), 2012 International Conference on Condition Monitoring and Diagnosis*, Bali, Indonesia, 2012.

[37] . R. Gorur, E. Cherney, C. De Tourreil, D. Dumora and R. Hackam, “Round robin testing of RTV silicone rubber coatings for outdoor insulation,” *IEEE Transactions on Power Delivery,* vol. 11, no. 4, pp. 1881--1887, 1996.

[38] I. Ramirez-Vazquez and R. Nava, “Application of nano particles for the modification of high voltage insulators,” *IEEE Transactions on Dielectrics and Electrical Insulation,* vol. 6, no. 20, pp. 2262--2269, 2013.

[39] B. Reddy, A. Verma and D. Prasad, “Surface Erosion Studies on Polymer Insulators Used for High Voltage Transmission,” *International Journal of Plasma Environmental Science & Technology,* vol. 10, no. 2, pp. 121-124, 2016.

[40] S. Chandrasekar, R. Sarathi and M. Danikas, “Analysis of surface degradation of silicone rubber insulation due to tracking under different voltage profiles,” *Electrical Engineering,* vol. 89, no. 6, pp. 489--501, 2007.

[41] I. Gunes, “Examination of Surface Tracking on Polyurethane Foam Insulators,” *Procedia-Social and Behavioral Sciences,* vol. 195, pp. 2629--2633, 2015.

[42] A. Bhat, H. Khalil and A. Banthia, “Dielectric and material properties of poly (vinyl alcohol): Based modified red mud polymer nanocomposites,” *Journal of Polymers and the Environment,* vol. 20, no. 2, pp. 395--403, 2012.

[43] S. Lixian , L. Zhanhong, Z. Hanmei and L. Ai, “The effect of bound rubber on vulcanization kinetics in silica filled silicone rubber,” *State Key Laboratory Cultivation Base for Nonmetal Composites and Functional Materials, Southwest University of Science and Technology,* vol. 6, no. 103, pp. 101470--101476, 2016.

[44] K. Chrzan, “INCLINED PLANE TEST, INFLUENCE OF TRANSFORMER POWER,” in *Proceedings of the 16th International Symposium on High Voltage Engineering*, 2009.

[45] S. Kaaiye, C. Nyamupangedengu and I. Jandrell., “A COMPARATIVE STUDY OF DC AND AC INCLINED PLANE TESTS ON SILICONE MICRO-COMPOSITE INSULATORS,” in *The 19th International Symposium on High Voltage Engineering,*, Pilsen, Czech Republic, 2015.

[46] Pico Technology, PicoLog CM3 CURRENT DATA LOGGER Datasheet, Pico Technology Ltd, 2017.

[47] P. Sarkar, A. Haddad, R. Waters, H. Griffiths, N. Harid and P. Charalampidis, “Inclined-plane tests of textured silicone rubber Samples,” in *High Voltage Engineering and Application (ICHVE), 2010 International Conference on High Voltage Engineering and Application*, New Orleans, LA, USA, 2010.

[48] R. A. Ghunem, “Using the inclined-plane test to evaluate the resistance of outdoor polymer insulating materials to electrical tracking and erosion,” *IEEE Electrical Insulation Magazine,* vol. 31, no. 5, pp. 16--22, 2015.

[49] M. Ehsani, H. Borsi, E. Gockenbach, G. Bakhshandeh and J. Morshedian, “Modified silicone rubber for use as high voltage outdoor insulators,” *Advances in Polymer Technology: Journal of the Polymer Processing Institute,* vol. 24, no. 1, pp. 51--61, 2005.

[50] K. Haji, Y. Zhu, M. Otsubo and C. Honda, “Surface modification of silicone rubber after corona exposure,” *Plasma Processes and Polymers,* vol. 4, no. 1, pp. 1075--1080, 2007.

[51] G. P. Bruce, “Ageing of Outdoor Polymeric Insulation under HVDC,” in *Ph.D Thesis, School of Electrical and Electronic Engineering*, University of Manchester, U.K, 2009.

[52] H. Chakerwarti, A. Agarwal, P. Kumar and N. Gupta, “Study of Silicone Rubber Based Composites with Nanosized Fillers,” in *Materials Science Forum*, Ann Arbor, MI, USA , 2015.

[53] K. Papailiou and F. Schmuck, “Silicone composite insulators: materials, design, applications,” in *Power Systems*, Switzerland, Springer Science & Business Media, 2012, pp. 2--24.

APPENDIX A: Measuring Equipment and Test Methodology

This section describes additional methods and techniques used for the testing and analysis of the silicone rubber samples.

A.1 Test Setup

The experiment to conduct the IPT was setup as follows. A single step-up autotransformer 250 V 25 A 3-phase feed the 32 kVA, 230 V / 19 kV high voltage transformer. For AC tests, the high voltage transformer is connected straight to IPT high voltage electrode via 22.5 kΩ resistors to smoothen the voltage ripples. For DC test setup, a 34.7 µF capacitor is connected through a diode in series with 450 MΩ resistors. The capacitor makes it possible to discharges the voltage fast when rearranging the equipment. The capacitor is also used for protection of the circuit. A half wave rectifier circuit for negative DC test is constructed by reversing the direction of the diode.

A supply voltage of 4.5 kV was used for all the test. As per the IEC-60587 standard a constant tracking voltage method was implemented. A steady flow of liquid contaminant is maintained for about 5 minutes before the voltage application to wet the entire filter paper. Visual observations and recordings were conducted.

A.2 Electrode type used

According to the IEC 60587 standard, it outlines that stainless steel is to be used for constructing the inclined plane test. Two kinds of stainless steel were selected as electrode materials namely austenitic steel (widely used steel) and AISI 316L austenitic steel type (used in the design because of its anti-pitting characteristics) [47].

Stainless steel electrodes were employed for this wok. At the high voltage electrode, a pad of eight layers of filter paper is fitted under it. The filter paper smoothens out the flow of contaminant solution. The top electrode quill tip edges should contact the sample face evenly. The filter paper must be behind electrode and not protrude as to prevent contact of electrode to the sample. The filter paper edges are folded back behind the electrode to prevent contaminant squirting out of the sides. The clip must not pinch contaminant hose so hard as to cause hose to plastically collapse. The hose end must not be inserted so deep as to be pinched between electrode and test sample.